THE AMERICAN JOURNAL OF PATHOLOGY

VOLUME XXXVI MARCH, 1960 NUMBER 3

POSTHEPATITIC, POSTNECROTIC, AND NUTRITIONAL CIRRHOSIS

A PATHOLOGIC ANALYSIS

EDWARD A. GALL, M.D.

From the Department of Pathology, College of Medicine, University of Cincinnati, and the Cincinnati General Hospital, Cincinnati, Ohio

In the course of a survey of hepatic cirrhosis as observed at necropsy at the Cincinnati General Hospital, it became apparent that conventional criteria for classification of this condition were not sufficiently clearly drawn to permit ready inclusion of many examples encountered. Certain definitive, albeit uncommon conditions, such as postnecrotic,[1] obstructive,[2] congestive (cardiac) [3,4] and pigmentary (hemochromatosis) cirrhosis, were easily distinguished by reason of special, universally appreciated properties. All of these, however, comprised only 35 per cent of the cases of cirrhosis. It was the remaining 65 per cent which appeared to require clarification.

The term "cirrhosis" itself is the subject of some disagreement. All investigators appear to predicate the existence of hepatic fibrosis with wide distribution. Most authors, following the dictates of Rössle, also incorporate such requirements as parenchymal cell destruction and regeneration, with the implication that the former constitutes an essential precipitating factor.[5,6] In some instances architectural distortion or a progressive nature of the lesion are considered prerequisites.[7-9] Thus, in composite, cirrhosis is considered to be a chronic, continuing disorder, stemming from low grade or recurrent necrosis, characterized by inflammation, nodular regeneration and diffuse connective tissue proliferation.[10] By some, those forms of fibrosis which follow single episodes

This investigation was supported in part by the John R. Stark Memorial Research Fund.

Received for publication, July 9, 1959.

of necrosis are excluded.[11,12] Others question whether the residual fibrosis in postnecrotic cirrhosis is real (proliferative) or apparent (condensation of pre-existing stroma).[13,14] A definition which would embrace all requirements would be cumbersome, equivocal, and something of a semantic monstrosity. The comparatively simple delineation "a widely distributed hepatic fibrosis stemming from parenchymal necrosis or persisting inflammation" permits the inclusion of all of the commonly accepted forms of cirrhosis, recognizes the existence of multiple causes and mechanisms, and excludes such focal and spotty lesions as hepar lobatum and cicatrization following localized necrosis (infarction, abscess, etc.).

The welter of subdivisions is in even greater need of simplification. Such labels as Laennec's, Hanot's, portal, primary biliary, cholangiolitic, trabecular, septal, micronodular, coarsely nodular, alcoholic, fatty and nutritional cirrhosis undoubtedly have limited local usefulness.[15–18] For broad interchange, however, the variations in interpretation are of such order as to restrict greatly the value of such nomenclature. Essential to the interpretation of this terminology is a clear recognition and understanding of structural features.

The present report represents a critical evaluation of the anatomic patterns in two forms of cirrhosis which do not appear to have been sharply distinguished from each other. In this paper these are designated as nutritional and posthepatitic cirrhosis, terms which have the benefit of fairly general usage.[19,20] A contrast is also drawn between these two and postnecrotic cirrhosis.[1,21,22] The latter is chosen as a base line since there is little controversy as to its mechanism of development which, indeed, is reproducible experimentally.[12,23,24] Moreover, there is some evidence that this lesion has not been as sharply defined as its characteristics should warrant.[25–27]

In addition to the essentially descriptive portrayals, an effort is made to introduce considerations of pathogenesis in respect to each category. The large number of specimens examined, and the developmental stages encountered would appear to justify this procedure despite the obvious need for presumption.

Material

During the 25-year period (1931 to 1955) selected for investigation, 16,332 necropsy examinations were carried out at the Cincinnati General Hospital. The annual procurement rate averaged 46 per cent of deaths. A significant number of the patients, however, were in early infancy (2,485); an additional 1,590 were less than 21 years of age. The incidence of primary hepatic lesions in infancy, childhood and youth was

exceedingly low. Among the 12,257 adults, on the other hand, cirrhosis was encountered in 755 (Table I), an incidence of 6 per cent.

Gross descriptions as given in the protocols were carefully analyzed and the features cited and tabulated. Specimens, often from multiple

TABLE I

HEPATIC CIRRHOSIS
NECROPSY CASES, CINCINNATI GENERAL HOSPITAL (1930 TO 1955)

Type of cirrhosis	No. of cases
Posthepatitic cirrhosis	262
Nutritional cirrhosis	231
Mixed cirrhosis	72
Obstructive (biliary) cirrhosis	67
Postnecrotic cirrhosis	61
Congestive (cardiac) cirrhosis	34
Pigmentary cirrhosis (hemochromatosis)	28
Total	755

sites, were of tissue fixed in formalin or Zenker-acetic acid and embedded in paraffin; sections were stained with hematoxylin and eosin. Paraffin blocks were available in almost all instances and wet formalin tissue in many. Additional sections were stained for elastic tissue, reticulin, connective tissue by the Masson trichrome method, and for fat as desired.

OBSERVATIONS

Six distinctive patterns of cirrhosis were identified (Table I). The names applied to these (postnecrotic, nutritional, posthepatitic, obstructive, pigmentary, and congestive cirrhosis) have general recognition although varying connotations. A seventh category, mixed cirrhosis, exhibited the features of two or more forms, each to a degree sufficient to permit detection. In the other categories minor differences in structure were commonplace, but the essential nature of the underlying condition was readily appreciated. Of pertinence were the gradations attributable to intensity and duration which permitted the formation of a developmental sequence of pathogenetic events.

The prototypes of the 2 most common forms, nutritional and posthepatitic cirrhosis and, for the reason given above, postnecrotic cirrhosis are described in detail and contrasted with each other. In each case an effort is made to trace the mechanism of development from tissues available in earlier stages of the particular disorder.

Postnecrotic Cirrhosis

(Subacute or healed yellow atrophy; toxic cirrhosis; coarsely nodular cirrhosis)

Gross Features. This form of cirrhosis is characterized by a misshapen liver which is heavy but often reduced in bulk. In advanced stages the organ may be inordinately shrunken. Residual parenchyma has a relatively normal or pallid brown color which may be altered (bright yellow, green) by activity of necrosis or regeneration.

Broad scarring and not coarse nodulation constitutes the characteristic feature here (Table II). Major portions (indeed, an entire lobe) of the liver may be replaced by homogeneous cicatrization. More often, however, broad scars course irregularly among islands of surviving parenchyma (Figs. 4 and 7). The collagenized zones are relatively

TABLE II

DIFFERENTIAL DIAGNOSIS OF CIRRHOSIS

Diagnostic features	Postnecrotic	Nutritional	Posthepatitic
Macroscopic			
Size	Normal or reduced	Enlarged	Normal or reduced
Color	Gray-brown	Yellow	Reddish brown
Texture	Tough +++	Tough ++, greasy	Tough ++
Scarring:			
Type	Coarse	Fine	Trabecular
Distribution	Irregular	Uniform	Uniform
Breadth	0.1–5.0 cm.	0.01–0.1 cm.	0.1–0.3 cm.
Nodule:			
Size	Fleck–7 cm.	0.2–0.3 cm.	0.5–1.5 cm.
Uniformity	Irregular	Uniform	Uniform
Microscopic			
Intact lobule	±	o	+++
Pseudolobulation	++	+++	±
Fat	±	+++	±
Pseudoductule	+++	+	+
Hemosiderin	±	+	o
Bile stasis	+	+	o
Central veins	+	o	+++

smooth, tough, pale (grayish white to greenish brown) and depressed. Nodules are embedded in this matrix and project above it.

The nodular component represents persisting parenchyma, and the range in size is from barely perceptible, fleck-like foci to coarse, irregular masses 5 to 7 cm. in diameter. These may be widely dispersed

in the smooth background of collagen (Fig. 1) or may be in relatively close proximity (Fig. 4) with an irregular "cobblestone" construction. Even in the latter circumstance, however, coarse scars intervene. On occasion, terminal events lead to softening of certain nodules, causing them to differ from the remainder and to simulate the appearance of hepatoma.

Microscopic Features. Here, too, the lesion is highlighted by scarring. Cicatrization of unequal but generally coarse nature proceeds in irregular manner throughout. Strands are both fibrillar and densely collagenized. There is little uniformity as to stromal breadth or its content. Fibroblasts, inflammatory cells, vascular channels and duct-like structures are manifest in variable proportions. Inflammatory cells are predominantly lymphocytes but may be accompanied by other forms of leukocytes. Histiocytes and entrapped single parenchymal cells are often indistinguishable. In recently induced lesions, fibroblast nuclei assume a vesicular, youthful appearance, but only an occasional mitotic figure is detected. Vascularity is abundant in the fresh process; it is reduced but never sparse in the older lesions.

Despite persistence in some large areas of parenchyma, complete retention of normal architecture is exceptional (Fig. 10). In most instances, actually, the distortion is of high order, and such landmarks as are detected (central veins, portal areas) are displaced and disarranged. The great preponderance of elements comprise regenerative nodules in which the residual pattern of the liver cell cords (plates) [28] is completely lost (Fig. 13). The cords are broadened, two or more cells in breadth, and exhibit diverse polarity; they border upon contorted sinusoids with essentially unremarkable Kupffer cell content. The latter are phagocytic of bile pigment or particulate debris in the event of recent hepatic necrosis.

Agonal complications introduce a heterogeneity of hepatic cell alterations. Fatty vacuolation rarely constitutes a prominent feature; on the other hand, evidence of patchy "fall out," regenerative proliferations of different durations, or terminal massive necrobiosis are common. The latter is a frequent fatal concomitant of exsanguination from bleeding varices.

Pathogenesis. Submassive hepatic necrosis of such order as to permit survival and healing but not restoration of the liver constitutes the basis for postnecrotic cirrhosis. Diffuse massive necrosis (acute yellow atrophy) with parenchymal destruction to an extent incompatible with life represents one extreme of this process, and transitory focal or zonal necrosis from which complete structural recovery is possible is the other.[29,30] In all instances a wide variety of causes may be operative;

these are infectious, dietary, toxic, and circulatory. The ultimate lesion induced, except in the instance of zonal necrosis, is indistinguishable as to cause.

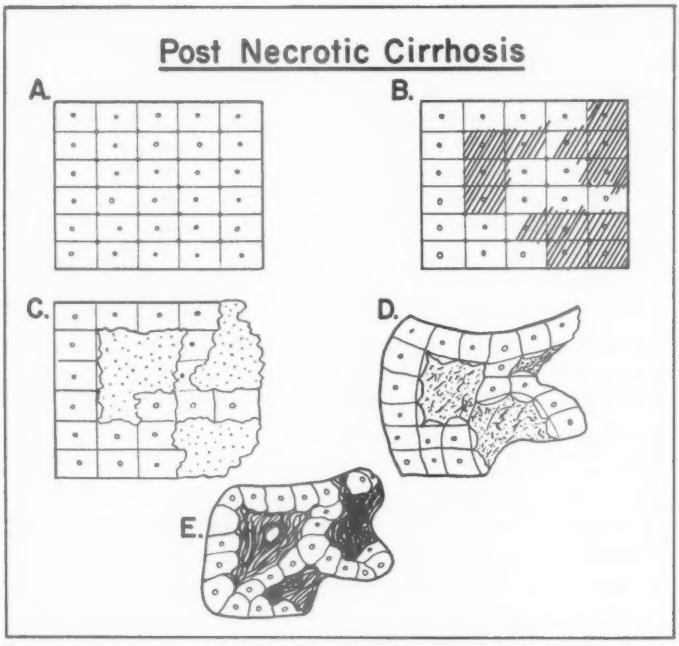

TEXT-FIGURE 1. Schema for pathogenesis of postnecrotic cirrhosis.

A. Normal liver. Lobules are shown as squares; small centrally placed circles represent centrilobular veins. Circles at cross angles denote location of portal areas.
B. Large crosshatched regions represent areas of submassive necrosis.
C. Dotted spaces indicate "fall out" of parenchyma in necrotic areas.
D. Areas of necrosis undergo collapse of stromal framework with distortion of residual parenchyma. The latter is the seat of regenerative proliferation.
E. Darkened wavy areas represent collagenization and broad scarring of stromal collapse zones. Remaining lobules are enlarged and distorted.

In massive necrosis the liver is smooth, congested or bile stained, and flabby. Microscopically, one observes almost total loss of parenchymal elements; only portal areas, congested sinusoids, the reticular framework, inflammatory cells, and particulate debris (intra-and extracellular) remain. In many instances minute fleck-like islands, solitary cells, or narrow fringes of deformed surviving elements about the portal areas may be encountered in fatal cases.

In the surviving individual, life is maintained in precarious fashion by the remaining parenchymal elements. Subsequently, two phenomena occur simultaneously (Text-fig. 1). In the regions devoid of parenchyma, collapse of the pre-existing reticulin framework and relatively unaf-

fected portal areas occurs.[31,32] The structures which are condensed in this manner vary in extent with the breadth of necrosis. Falling together, thus, are the sinusoids, perisinusoidal reticulin, surviving single or small clusters of hepatic cells, and portal tracts. There results a loosely fibrillar, highly vascularized stroma, containing inflammatory cells in rich abundance, displaced interlobular ductules, and minute groups of liver cells. In due course, collagenization occurs, and with its development there is reduction in both vascular and inflammatory components. Ductules and residual parenchymal cells are compressed and attenuated in the thickening stroma.

Simultaneously, persisting parenchyma of sufficient amount resists collapse although the contiguous stroma is draped about the periphery in capsule-like fashion. The appearance of encapsulation becomes more striking as regenerative proliferation occurs in these islands. As they enlarge and abut upon the condensed stroma, a roughly spherical configuration is induced and mutual compression supervenes. The nodulations may vary in proximity and in diameter, depending upon initial size and dispersion. The intrinsic architecture is much perverted, and regular lobular arrangement is inapparent although portal tracts and centrilobular veins are distributed at random.

Enmeshed in the stroma are epithelial structures with cord or ductular aspect; these are of especial interest (Fig. 10). They are more abundant in earlier lesions. Some of them undoubtedly represent preexisting interlobular biliary ductules displaced and brought together by loss of parenchymal substance. Most of them, however, appear to be freshly formed.

There has been much debate as to the origin of these structures.[33] Some contend their derivation by proliferation of pre-existing bile ducts; others consider that they represent abortive efforts of regeneration of small isolated groups of parenchymal cells trapped within the connective tissue; still others consider them to be inactive remnants of displaced parenchyma in process of compression atrophy.[34] The lack of orderly supporting elements, elastica[35] in particular, the frequent appearance of the phenomenon in all forms of liver cell disturbance, and the prominence of similar duct-like structures in the centrilobular regions in congestive cirrhosis[36] (a portion of the lobule where preexisting ducts cannot be said to contribute) lead one to the conclusion that this pattern does not reflect proliferation of true ducts.[37,38] Since origin from parenchymal elements appears likely, the designations pseudoductule or pseudotubule are preferable.[38] True ductular proliferation occurs almost exclusively in association with obstruction. This is the case in obstructive (biliary) cirrhosis but may, in a minor

way, reflect focal obstruction by scar in other forms of hepatic fibrosis. That abnormality of "cholangioles" lies at the root of pseudoductule formation is considered highly doubtful.[39]

Nutritional Cirrhosis
(Alcoholic, fatty, micronodular, Laennec's cirrhosis)

Gross Features. The liver here is characteristically heavy and much enlarged, often extending well below the costal margin. It frequently exceeds normal weight by at least 25 per cent, and increases of 100 per cent (3,000 to 4,000 gm.) are not unusual (Table II). The organ is golden yellow, with gradations attributable to dietary correction or agonal necrosis (brown to green). The free surface is pebbled by fine uniform nodulations, approximating 2 to 3 mm. in diameter, separated by a network of narrow, slightly depressed scars (Figs. 2 and 5). How much this deserves the appellation "hobnail" liver, in this era of unfamiliarity with hobnails, is open to serious question. Characterized by toughness, the sectioned surface is yellow and greasy, and maintains the uniform, fine nodularity and a delicate tracery of intervening fibrosis (Fig. 8). On occasion, nodulations are of such minuteness as to afford an appearance not unlike that of tanned pigskin.

Microscopic Features. Parenchymal cells are disarranged, swollen and, as a rule, uniformly coarsely vacuolated (Figs. 11 and 14). Lipid content may be released to form intercellular pools surrounded by the remnants of depleted cells.[40] Sinusoids are narrowed or inapparent, and cell columns lack radial structure. Indeed, centrilobular veins are detected only rarely.

Nodules are roughly the size of lobules but are devoid of lobular landmarks. Delicate fibrillar tongues interconnect stellate portal areas and join with similar strands arising from the central vein region (Figs. 17 and 18). The lobule is not only encompassed but is segmented as well. It is this phenomenon which is styled pseudolobulation.[28]

Connective tissue strands do not exceed a thickness of one mm. and are usually of the order of 100 to 500 μ. Interlobular ductules remain unaffected, but a rich production of pseudoductules is common (Fig. 17). Portal areas and their extensions may be surrounded by fringes of minute truncated epithelial cords with Medusa head appearance.[41] These, of course, are not peculiar to this, or any other, form of cirrhosis.

Pseudolobules seldom exceed one mm. in diameter and are comparatively uniform; they obviously do not represent the grossly visualized nodules which usually measure 2 to 3 mm. (Figs. 3, 5 and 18).

The overall microscopic pattern thus consists of fatty micronodules which lack central veins and other histologic landmarks and about which

is interspersed a fine fibrous network. In the latter are found pre-existing portal area structures, inflammatory cells and newly formed pseudoductules.

Pathogenesis. Nutritional cirrhosis stems from the excessively fatty liver, characteristically but by no means exclusively encountered in the neglected alcohol addict. Almost all parenchymal cells are gorged with lipid, and the liver, in consequence, is enlarged, smooth and buttery in appearance. Disruption of overstuffed cells is common, and lipid aggregates gather with intercellular location; this phenomenon appears to be bland and is not accompanied by either inflammatory reaction or detectable desmoplasia.[42] A contribution to stromal tension may contrive in some way to initiate fibrosis, but this is equivocal.

Of somewhat more provocative nature are episodes of noninfectious (toxic) hepatitis, characterized by a transformation of the customary coarse, smoothly outlined lipid vacuoles (Fig. 16). These assume a microvacuolar, foamy character, with blurring and fuzziness of outline and, in the event of formalin fixation, a deposit of "formalin pigment."[43] Serious cellular injury is manifested by eosinophilia and swelling of mitochondria (Mallory's alcoholic hyalin), necrosis of single or grouped cells with accompanying neutrophil exudate, and extensive intercellular (intracanalicular) inspissation of bile. Which factor or factors serve to precipitate episodes of this nature are unknown; undoubtedly they are many and varied. In many respects the alterations are similar to those observed in the lesion termed "florid cirrhosis" by Popper.[6,44]

During recurrent periods of this character, with parenchymal unrest and necrosis, and probably the result of them, there is portal space edema and the appearance of a variable amount of leukocytic exudate; neutrophils and lymphocytes have varying prominence in relation to the degree of intralobular necrosis. Kupffer cells, other phagocytes, and even hepatic epithelium contain significant amounts of hemosiderin during this period, and bile plug formation (canalicular) is a common concomitant.

In due course, an increase of fibrillar connective tissue results in further portal area enlargement and the assumption of a stellate silhouette, as delicate fibrils emerge in "creeping" manner (Text-fig. 2). Simultaneously, but to a lesser degree, edema, inflammation and stromal fibrillation may be observed in the narrow connective tissue collar supporting the centrilobular vein. From both peripheral and central locations fine fibrillar prongs emerge; some terminate abruptly. In the case of the portal areas, some connect with twigs arising from nearby portal regions, and others, in highly characteristic manner, insert themselves into the lobules, ultimately joining with the fronds arising in the centrilobular region.

This slowly progressive process ("creeping fibrosis") leads to division of the lobule in segmental fashion, resulting in "pseudolobules," minute circumscribed nodules comprised of fat-filled liver cells without radial

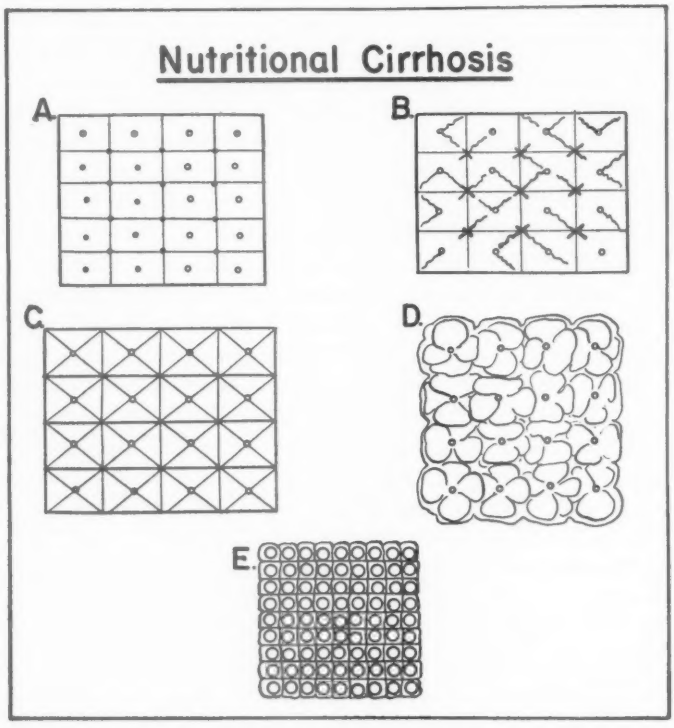

TEXT-FIGURE 2. Schema for pathogenesis of nutritional cirrhosis.

A. Normal liver. Details are as given in Text-figure 1.

B. Fatty alteration is not shown. Portal areas are enlarged, stellate, and narrow tongues of connective tissue ("creeping fibrosis") are seen to emerge from both portal tracts and central veins.

C. Fibrillar tongues interconnect and cause both circumscription and segmentation of hepatic lobules (pseudolobule formation).

D. Contraction of stroma and fatty engorgement of parenchyma lead to enlargement and spherical configuration of pseudolobules.

E. Contraction has resulted in a uniform, fine nodulation. The latter represents pseudolobules lacking in central veins and normal lobular architecture.

structure. The participation of the perivenous stroma in the centrilobular region leads to the apparent loss of this landmark, which is now embraced by the newly formed trabeculations.

The ultimate pattern is thus a series of relatively equal-sized, spherical fatty nodules of approximately lobule volume. These are surrounded by

delicate connective tissue septums containing the remnants of portal area structure and centrilobular veins and, in varying proportions, newly formed pseudoductules and inflammatory cells.

Posthepatitic Cirrhosis

(Coarsely nodular, trabecular, septal, portal, Laennec's cirrhosis)

Gross Features. Of normal or slightly reduced bulk, the liver here has a reddish-brown, essentially normal coloration. As in the case of nutritional cirrhosis, nodulation is relatively uniform, but it is significantly coarser, the nodules measuring 0.5 to 1.5 cm. (Figs. 3 and 6). Fibrosis, too, is narrow and trabecular, the strands forming a meshwork surrounding the nodules in regular fashion. The fine trabecular tracery is especially noteworthy on the sectioned surface (Fig. 9). Neither the greasy texture of nutritional cirrhosis nor the coarse scarring of postnecrotic cirrhosis are manifest (Table II).

Microscopic Features. Narrow bands of fibrous tissue traverse the parenchyma, extending from portal area to portal area with unilobular disposition, or more commonly, with multilobular pattern, enclosing 2 to 5 lobules (Fig. 15). One or the other arrangement prevails in a given case. The fibrous septums measure 0.1 to 0.3 cm. in breadth and appear as prolongations of portal area stroma. There is relatively little intralobular intrusion, and the central veins notably remain unaffected (Fig. 15). Varying numbers of lymphocytes appear in the stroma, occasionally with condensation about biliary ductules (pericholangitis) which are otherwise unaffected. This feature has no recognizable functional implication. As in nutritional cirrhosis, pseudoductule formation is a frequent occurrence.

Parenchymal cells contain little or no lipid; indeed, they usually exhibit an essentially normal lobular, radial pattern. Central veins maintain their anatomic position, and pseudolobulation is not a feature (Figs. 12 and 15). Recurrent inflammatory activity is characterized by patchy, nonzonal, individual cell degeneration and necrosis. Small satellite clusters of lymphocytes pinpoint the sites of parenchymal disorder.

Pathogenesis. It is implicit in the designation, posthepatitic cirrhosis, that this condition is considered a sequela of an underlying smoldering inflammation. Whether this is necessarily of infectious (viral) nature is not entirely clear.

There is ample evidence that the populace maintains a reservoir of subclinical viral hepatitis, composed of individuals who have never exhibited clinical manifestations and of those who have seemingly recovered from the disease.[45] It is this group, of course, which provides the omnipresent hazard of homologous serum jaundice. In a recent survey

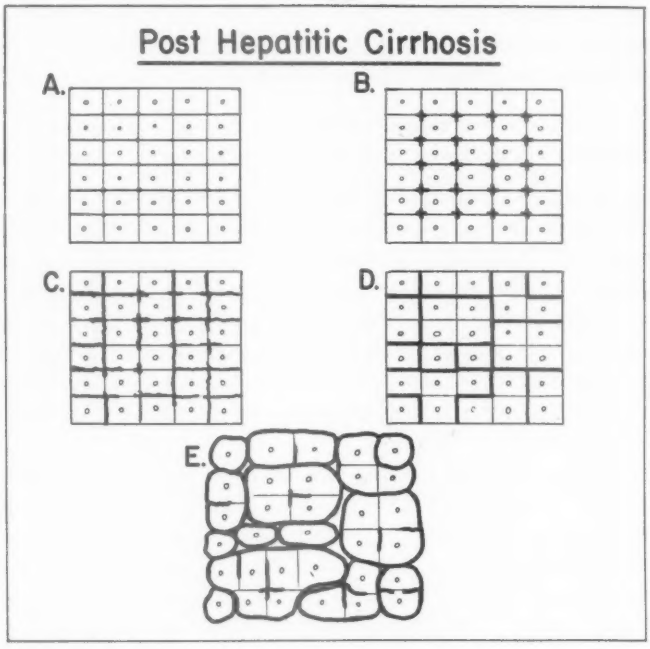

TEXT-FIGURE 3. Schema for pathogenesis of posthepatitic cirrhosis.

A. Normal liver. Details are as given in Text-figure 1.

B. "Universal triadal inflammation" of chronic hepatitis is characterized by enlargement and stellate configuration of all portal areas.

C. Delicate fibrous strands emerge from portal areas and extend in perilobular fashion. These approach and interconnect with similar processes arising in adjacent portal tracts.

D. Interconnections provide a trabecular pattern embracing single lobules or small groups of lobules which have otherwise retained architectural integrity.

E. Trabecular contraction has resulted in spherical nodule formation. Enclosed lobules exhibit unimpaired structure.

unrelated to the present investigation, the liver sections in over 3,000 patients examined at necropsy at the Cincinnati General Hospital during the 5-year period 1953 to 1957 were re-examined. There were approximately 1,000 instances in which the liver had been considered unaffected by significant abnormality of either intrinsic or extrinsic character by the initial examiner. Sections from these livers were scrutinized with a single criterion in view—the existence of chronic (lymphocytic) inflammatory exudates in every portal area ("universal triadal inflammation"). Although this phenomenon is not necessarily pathognomonic of viral hepatitis, it does represent a lesion which invariably accompanies this disorder in its various phases.[46,47] Among the 1,000 specimens, there were approximately 5 per cent which exhibited this process. In these, the

portal areas were enlarged, edematous and heavily populated with lymphoid cells (Fig. 12). It is postulated that in certain instances post-hepatitic cirrhosis arises in such a milieu.

In its earliest phases the lesion here differs from that of smoldering hepatitis only by the appearance of mild desmoplasia. As in the case of nutritional cirrhosis, delicate fibrils of connective tissue appear to emerge, affording a stellate outline to the interlobular tract. There is only mild and inconspicuous parenchymal cell alteration without specific location, and centrilobular veins remain unaffected.

The minute fibrillar tongues continue to extend, as in "creeping fibrosis," and in milder lesions terminate without interconnection or encirclement of the lobule. There is only negligible intralobular intrusion and, thus, an absence of pseudolobulation (Text-fig. 3). In the more advanced stages, fusion of strands from adjacent or even distal portal areas eventuates, and the liver evinces a septate architecture. Unilobular encirclement may occur, but a multilobular pattern is usual. In the latter instance nodules may contain the components of several lobules, central veins are readily detected, and there are often essentially normal portal tracts distributed within the nodule.

Discussion

At the Sixth Josiah Macy, Jr., Foundation Conference on Liver Injury (1947) a confusion of terminology and appreciation of cirrhosis was disturbingly manifest.[48] It is clear from the published proceedings of this meeting that 8 distinguished pathologists found themselves in complete agreement as to designation in only 19 of 106 microscopic sections. The sections had been considered by each of the submitting participants to be representative of a variety of liver disorders. It is little wonder that pathologists with more casual interest and with less authority approach consideration of hepatic cirrhosis in gingerly fashion. An uncertainty as to morphologic criteria for recognition has permitted the development of a number of clinical labels improperly assumed to have pathologic justification. The use of stereotyped terms (portal, Hanot's and Laennec's cirrhosis)[6,49] and the implication that clinical syndromes necessarily have a consistent pathologic background (chronic alcoholism,[50] primary biliary,[17,51,52] xanthomatous, or cholangiolitic cirrhosis[53,54]) have led to distressing divergencies of meaning.

Many forms of cirrhosis are well defined and more or less generally appreciated, if not as to form, certainly as to significance. There appears to be reasonable clinical, morphologic, and pathogenetic basis for the distinction of obstructive, congestive, parasitic, pigmentary, and post-necrotic varieties. A number of other forms with varying cause and pat-

tern are attributable, as in the case of pigmentary cirrhosis (hemochromatosis), to genetic metabolic defects (Wilson's disease, galactosemia, mucoviscidosis,[55] etc.). The two forms, nutritional and posthepatitic cirrhosis, which comprised 65 per cent of the cases encountered in the present survey, though clearly distinguishable from each other, have been variously classified, confusingly described, and, at least in the case of the posthepatitic variety, not too well separated from postnecrotic cirrhosis. There seems some purpose, therefore, in specifying their qualities in sharp descriptive fashion.

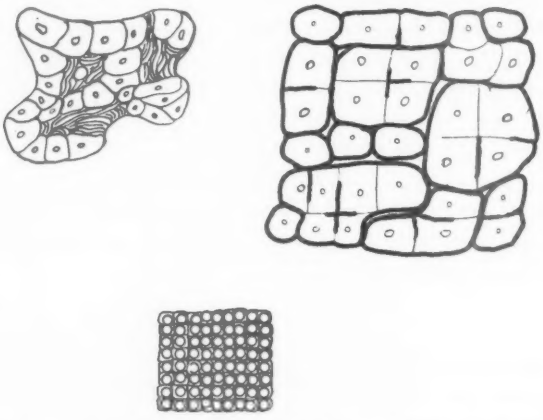

TEXT-FIGURE 4. Differential features in postnecrotic, posthepatitic and nutritional cirrhosis.

Upper left: Postnecrotic cirrhosis. Broad, irregularly distributed scars separate and surround the disarranged residuum of parenchyma. The latter is composed of nodules of varied (often large) size.

Upper right: Posthepatitic cirrhosis. Scarring has a narrow trabecular pattern. Fibrous septums enclose single lobules or groups of lobules, the architectural integrity of which have been maintained.

Bottom: Nutritional cirrhosis. Minute nodules are relatively uniform in size and configuration. These are enclosed within a delicate tracery of connective tissue. Nodules are pseudolobules and lack normal lobular landmarks.

The speculations as to mechanism of development and underlying cause are justifiably subject to censure. In no instance has a single causative factor been unequivocally demonstrated. The combination of stages as encountered in different cases for the purpose of establishing pathogenetic schemes constitutes a presumption subject to criticism. The lack of serial biopsy specimens as a basis for interpretation, however, leaves no alternative. At least this method provides a basis for a working evaluation and certainly cannot reflect upon the validity of the distinctive structural alterations observed in the advanced lesions (Text-fig. 4).

Although it is true that in the full-blown lesion, complete consistency of pattern is not a regular occurrence, variations imposed by complications occurring during a terminal illness are ordinarily recognizable as such.[56] This is also the case in respect to those disorders which may affect the lesion earlier in its course. A damaged liver is known to be vulnerable to noxae which under ordinary circumstances might have little effect upon it. This undoubtedly accounts for the group of cases classified as "mixed cirrhosis." In such instances a liver which is the seat of one form of cirrhosis may have superimposed upon it the recognizable features of another variety. Thus, one finds postnecrotic cirrhosis with its focalized scarring accompanying one or another form of hepatic fibrosis. This in no way lessens the need for recognition of prototypes. It is reasonable to expect that clear definition of pathologic entities will ultimately permit clinical pathologic correlations not possible in the present uncertain state.

Summary

A survey of necropsy specimens of liver obtained at the Cincinnati General Hospital during the 25-year period (1931 to 1955) has provided 755 examples of cirrhosis for analysis.

These have been classified as posthepatitic, nutritional, obstructive, postnecrotic, congestive, pigmentary, and mixed forms of cirrhosis.

Three types, posthepatitic, nutritional, and postnecrotic cirrhosis, have been singled out for detailed appraisal of their gross and microscopic characteristics and for speculation as to mechanisms of development.

Methods for differentiation of the 3 entities are outlined.

References

1. Karsner, H. T. Morphology and pathogenesis of hepatic cirrhosis. *Am. J. Clin. Path.*, 1943, 13, 569–606.
2. Judd, E. S., and Counseller, V. S. The effects of obstructive lesions of the common duct on the liver. *J.A.M.A.*, 1927, 89, 1751–1756.
3. Boland, E. W., and Willius, F. A. Changes in the liver produced by chronic passive congestion; with special reference to the problem of cardiac cirrhosis. *Arch. Int. Med.*, 1938, 62, 723–739.
4. Sherlock, S. The liver in heart failure; relation of anatomical, functional and circulatory changes. *Brit. Heart J.*, 1951, 13, 273–293.
5. Mallory, G. K. The Liver and Biliary Tract. In: Textbook of Pathology with Clinical Applications. Robbins, S. L. (ed.). W. B. Saunders Co., Philadelphia, 1957, Chapt. XXII, pp. 812–865.
6. Popper, H., and Schaffner, F. Liver: Structure and Function. The Blakiston Division, McGraw-Hill Book Co., Inc., New York, 1957, 777 pp.
7. Karsner, H. T. Human Pathology. J. B. Lippincott Co., Philadelphia, 1955, ed. 8, 960 pp.
8. Davidson, C. S. Cirrhosis of the liver. *Am. J. Med.*, 1954, 16, 863–873.

9. KLATSKIN, G., and RAPPAPORT, E. M. Late residuals in presumably cured acute infectious hepatitis. *Ann. Int. Med.*, 1947, **26**, 13–26.

10. HERBUT, P. A. Pathology. Lea & Febiger, Philadelphia, 1959, 1516 pp.

11. HIMSWORTH, H. P., and GLYNN, L. E. Toxipathic and trophopathic hepatitis. *Lancet*, 1944, **1**, 457–461.

12. HIMSWORTH, H. P. Lectures on the Liver and Its Diseases. Harvard University Press, Cambridge, Mass., 1950, ed. 2, 222 pp.

13. MOORE, R. A. A Textbook of Pathology. Pathologic Anatomy in Relation to the Causes, Pathogenesis and Clinical Manifestations of Disease. W. B. Saunders Co., Philadelphia, 1951, ed. 2, 1048 pp.

14. MALLORY, F. B. Cirrhosis of the liver; five different types of lesions from which it may arise. *Bull. Johns Hopkins Hosp.*, 1911, **22**, 69–75.

15. HART, J. F., and LISA, J. R. Histogenesis of Laennec's cirrhosis. *New York J. Med.*, 1937, **37**, 1619–1626.

16. HOWARD, R., and WATSON, C. J. Antecedent jaundice in cirrhosis of the liver. *Arch. Int. Med.*, 1947, **80**, 1–10.

17. KUNKEL, H. G. Biliary Cirrhosis. In: Diseases of the Liver. Schiff, L. (ed.). J. B. Lippincott Co., Philadelphia, 1956, pp. 467–488.

18. RATNOFF, O. D., and PATEK, A. J., JR. The natural history of Laennec's cirrhosis of the liver. An analysis of 386 cases. *Medicine*, 1942, **21**, 207–268.

19. BAGGENSTOSS, A. H., and STAUFFER, M. H. Posthepatitic and alcoholic cirrhosis: clinicopathologic study of 43 cases of each. *Gastroenterology*, 1952, **22**, 157–180.

20. SHERLOCK, S. Post-hepatitis cirrhosis. *Lancet*, 1948, **1**, 817–822.

21. BEAVER, D. C., and ROBERTSON, H. E. The specific character of toxic cirrhosis as observed in cinchophen poisoning. A review of five fatal cases. *Am. J. Path.*, 1931, **7**, 237–258.

22. LUCKÉ, B. The pathology of fatal epidemic hepatitis. *Am. J. Path.*, 1944, **20**, 471–593.

23. CAMERON, G. R.; KARUNARATNE, W. A. E., and THOMAS, J. C. Massive necrosis ("toxic infarction") of the liver following intra-portal administration of poisons. *J. Path. & Bact.*, 1937, **44**, 297–303.

24. POPPER, H. Liver disease—morphologic considerations. *Am. J. Med.*, 1954, **16**, 98–117.

25. SMETANA, H. Pathology of Hepatitis. In: Diseases of the Liver. Schiff, L. (ed.). J. B. Lippincott Co., Philadelphia, 1956, Chapt. 10, pp. 258–301.

26. KELSALL, A. R.; STEWART, A., and WITTS, L. J. Subacute and chronic hepatitis. *Lancet*, 1947, **2**, 195–198.

27. KUNKEL, H. G., and LABBY, D. H. Chronic liver disease following infectious hepatitis. II. Cirrhosis of the liver. *Ann. Int. Med.*, 1950, **32**, 433–450.

28. POPPER, H., and ELIAS, H. Histogenesis of hepatic cirrhosis studied by the three dimensional approach. *Am. J. Path.*, 1955, **31**, 405–441.

29. PRATT, J. H., and STENGEL, A. Toxic cirrhosis resulting from acute liver atrophy. *Am. J. M. Sc.*, 1927, **173**, 1–11.

30. WILSON, J. D., and GOODPASTURE, E. W. Yellow atrophy of the liver. Acute, subacute and healed. *Arch. Int. Med.*, 1927, **40**, 377–385.

31. MARCHAND, F. Ueber Ausgang der acuten Leberatrophie in multiple knotige Hyperplasie. *Beitr. path. Anat.*, 1895, **17**, 206–219.

32. BJORNEBOE, M., and RAASCHOU, F. Pathology of subchronic atrophy of the liver. Comparison with Laennec's cirrhosis. *Arch. Int. Med.*, 1949, **84**, 933–957.

33. MILNE, L. S. The histology of liver tissue regeneration. *J. Path. & Bact.*, 1909, **13**, 127–160.

34. BAEHR, G., and KLEMPERER, P. Degenerative and diffuse inflammatory diseases of the liver. The correlation of pathology and clinical medicine as illustrated by cases from the clinical pathological conferences of the Mt. Sinai Hospital, N.Y. *Internat. Clin.*, 1929, II (39th series), 107–148.

35. FLEXNER, S. Nature and distribution of the new tissue in cirrhosis of the liver. *Univ. M. Mag.*, Philadelphia, 1900–1901, **13**, 613–620.

36. MOSCHCOWITZ, E. The morphology and pathogenesis of cardiac fibrosis of the liver. *Ann. Int. Med.*, 1952, **36**, 933–955.

37. DOEHLERT, C. A., JR.; BAGGENSTOSS, A. H., and CAIN, J. C. Obstructive biliary cirrhosis and alcoholic cirrhosis. Comparison of clinical and pathologic features. *Am. J. Clin. Path.*, 1955, **25**, 902–914.

38. ROLLESTON, H. D., and MCNEE, J. W. Diseases of the Liver, Gall-Bladder and Bile-Ducts. Macmillan & Co., Ltd., London, 1929, 884 pp.

39. GIBSON, W. R., and ROBERTSON, H. E. So-called biliary cirrhosis. *Arch. Path.*, 1939, **28**, 37–48.

40. HARTROFT, W. S. The sequence of pathologic events in the development of experimental fatty liver and cirrhosis. *Ann. New York Acad. Sc.*, 1954, **57**, 633–645.

41. GALL, E. A., and BRAUNSTEIN, H. Hepatitis with manifestations simulating bile duct obstruction (so-called "cholangiolitic hepatitis"). *Am. J. Clin. Path.*, 1955, **25**, 1113–1127.

42. HARTROFT, W. S. The Locus of the Beginning of Dietary Cirrhosis. In: Liver Injury. Transactions of the Eighth Conference, Josiah Macy, Jr., Foundation, New York, April 28–29, 1949, pp. 126–164.

43. GALL, E. A. The Diagnosis of Hepatitis by Needle Biopsy. In: Hepatitis Frontiers. Henry Ford Hospital International Symposium. Little Brown & Co., Boston, 1957, pp. 475–498.

44. POPPER, H.; SZANTO, P. B., and PARTHASARATHY, M. Florid cirrhosis. A review of 35 cases. *Am. J. Clin. Path.*, 1955, **25**, 889–901.

45. STOKES, J., JR.; BERK, J. E.; MALAMUT, L. L.; DRAKE, M. E.; BARONDESS, J. A.; BASHE, W. J.; WOLMAN, I. J.; FARQUHAR, J. D.; BEVAN, B.; DRUMMOND, R. J.; MAYCOCK, W. D.; CAPPS, R. B.; and BENNETT, A. M. The carrier state in viral hepatitis. *J.A.M.A.*, 1954, **154**, 1059–1065.

46. WEISBROD, F. G.; SCHIFF, L.; GALL, E. A.; CLEVELAND, F. P., and BERMAN, J. R. Needle biopsy of the liver. III. Experiences in the differential diagnosis of jaundice. *Gastroenterology*, 1950, **14**, 56–72.

47. DIBLE, J. H.; MCMICHAEL, J., and SHERLOCK, S. P. V. Pathology of acute hepatitis. Aspiration biopsy studies of epidemic, arsenotherapy, and serum jaundice. *Lancet*, 1943, **2**, 402–408.

48. Liver Injury. Transactions of the Sixth Conference, Josiah Macy, Jr., Foundation, New York, May 1–2, 1947.

49. POPPER, H., and SCHAFFNER, F. Nutritional hepatic injury. *A.M.A. Arch. Int. Med.*, 1954, **94**, 785–800.

50. HALL, E. M., and MORGAN, W. A. Progressive alcoholic cirrhosis. A clinical and pathologic study of sixty-eight cases. *Arch. Path.*, 1939, **27**, 672–690.

51. AHRENS, E. H., JR.; PAYNE, M. A.; KUNKEL, H. G.; EISENMENGER, W. J., and BLONDHEIM, S. H. Primary biliary cirrhosis. *Medicine*, 1950, **29**, 299–364.
52. EVANS, P. R. Biliary cirrhosis. *Arch. Dis. Child.*, 1939, **14**, 89–108.
53. RICKETTS, W. E., and WISSLER, R. W. Cholangiolitic biliary cirrhosis (primary biliary cirrhosis). *Ann. Int. Med.*, 1952, **36**, 1241–1277.
54. WATSON, C. J., and HOFFBAUER, F. W. The problem of prolonged hepatitis with particular reference to the cholangiolitic type and to the development of cholangiolitic cirrhosis of the liver. *Ann. Int. Med.*, 1946, **25**, 195–227.
55. GALL, E. A., and LANDING, B. H. Hepatic cirrhosis and hereditary disorders of metabolism. *Am. J. Clin. Path.*, 1956, **26**, 1398–1426.
56. DIBLE, J. H. Degeneration, necrosis, and fibrosis in the liver. *Brit. M. J.*, 1951, **1**, 833–841.

Drs. Thomas E. Gaffney and Edwin E. Fisher aided in the compilation of data. Mrs. M. M. Cook prepared the text-figures.

LEGENDS FOR FIGURES

Figures 1 to 3 illustrate the gross external appearance of the liver in 3 forms of cirrhosis. Reduction is approximately equal in each specimen.

FIG. 1. Postnecrotic cirrhosis. Nodules with irregular configuration and varied size project above the background of depressed, pallid scarring.

FIG. 2. Nutritional cirrhosis. The pale yellow surface is characterized by small, granular nodulations. Scarring is comparatively fine and uniform in distribution.

FIG. 3. Posthepatitic cirrhosis. Nodulations are coarser than those observed in nutritional cirrhosis; smaller and more uniform than those in postnecrotic cirrhosis.

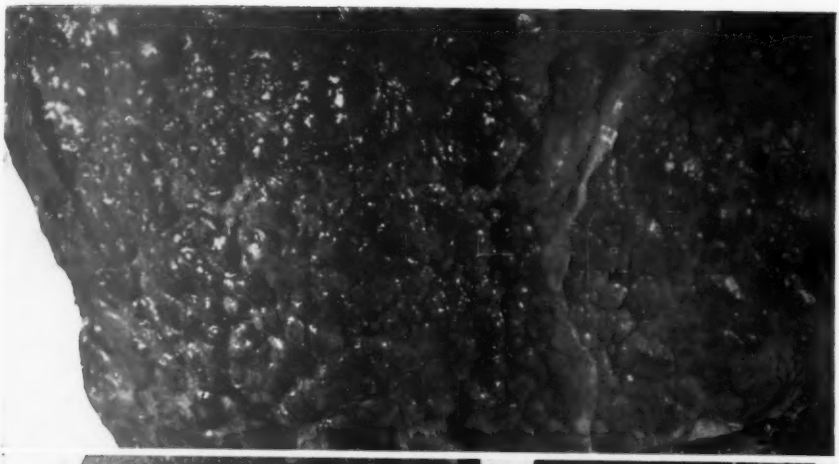

1

2

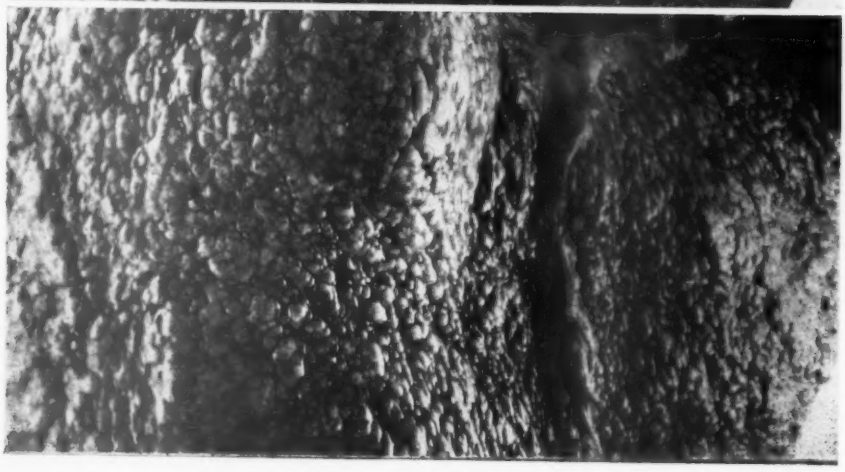

3

Figures 4 to 6 illustrate the gross appearance of the sectioned liver in cirrhosis. Reduction is approximately equal in each specimen.

FIG. 4. Postnecrotic cirrhosis. Coarse, irregular scarring outlines large, heterogeneous nodulations. Note the bumpy appearance of the external surface viewed in silhouette.

FIG. 5. Nutritional cirrhosis. Nodulations are small and uniform. Fine scarring affords the appearance of pigskin.

FIG. 6. Posthepatitic cirrhosis. Uniform but relatively large nodules are separated by a fine trabecular network.

4

5

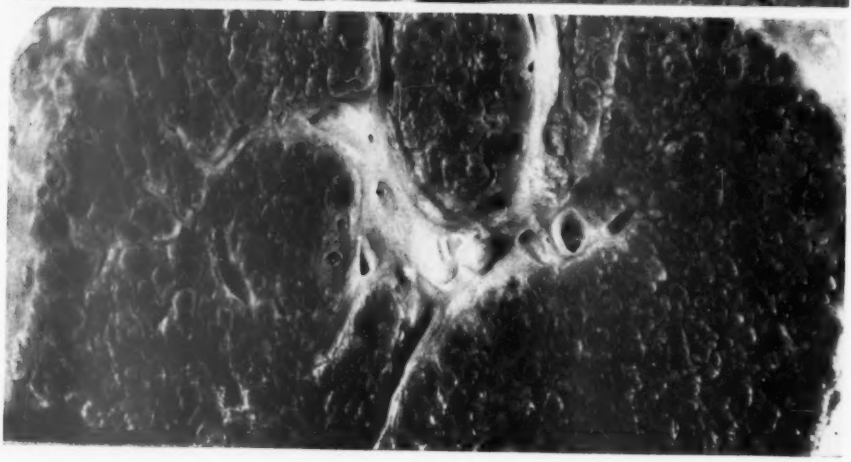

6

Figures 7 to 9 illustrate the sectioned surface of the liver in cirrhosis; a close-up view. Magnification is identical in each specimen.

FIG. 7. Postnecrotic cirrhosis. As in Figure 4, the pattern is highlighted by nodules of irregular bulk set in a coarse fibrous framework.

FIG. 8. Nutritional cirrhosis. Both the external and sectioned surfaces are shown. Fine (0.2 cm.), uniform nodularity is clearly manifest.

FIG. 9. Posthepatitic cirrhosis. Scarring is trabecular and nodules are relatively uniform in size (0.5 to 1.5 cm.) and shape.

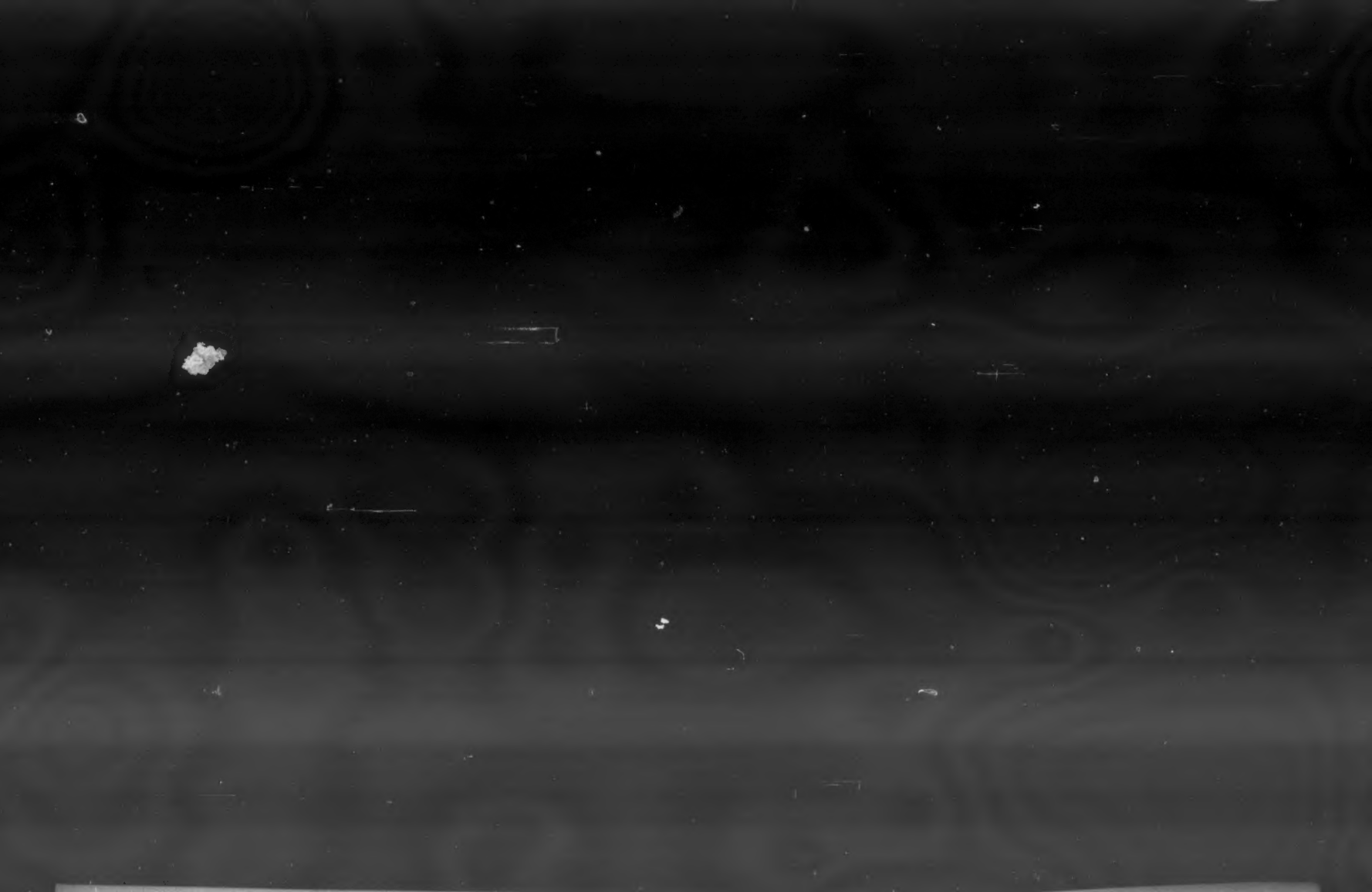

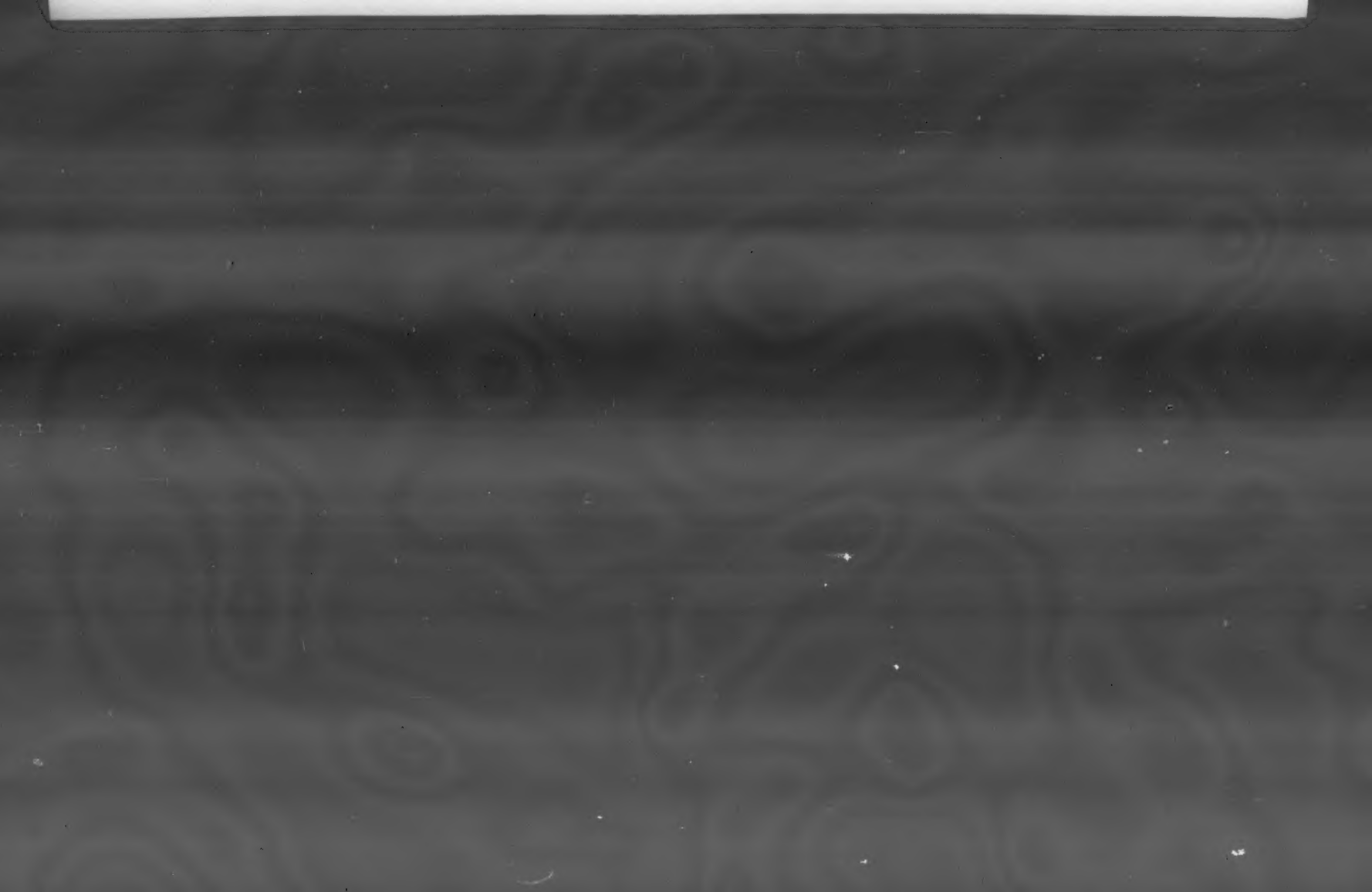

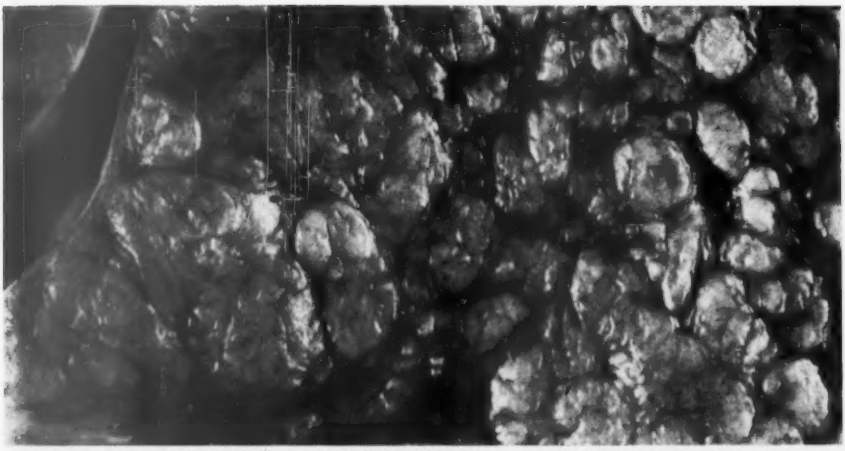

7

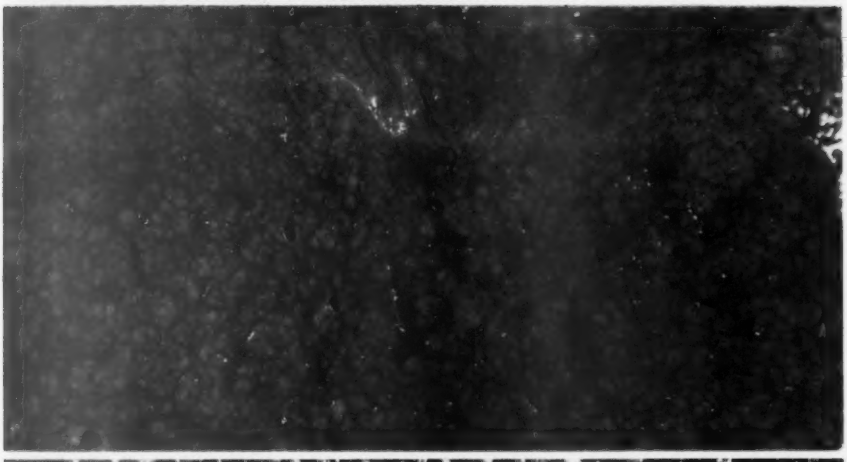

8

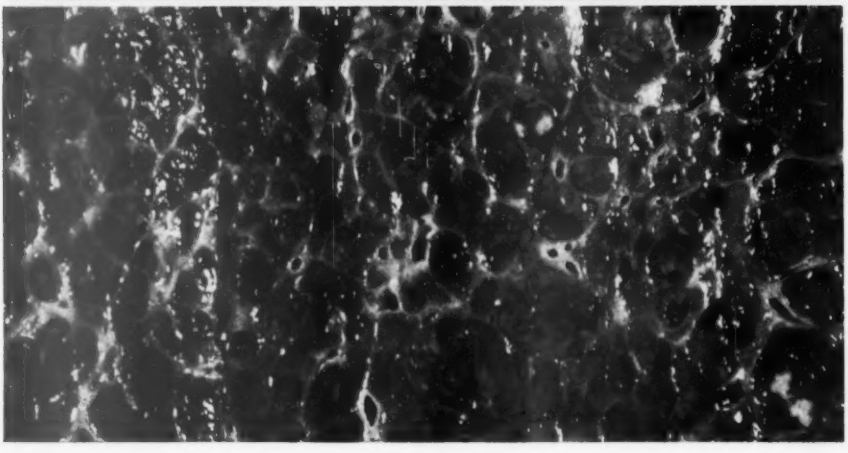

9

Figures 10 to 12 are photomicrographs illustrating early stages in the development of hepatic cirrhosis. These and all remaining sections were stained with hematoxylin and eosin.

FIG. 10. Submassive hepatic necrosis, exhibiting early regeneration of parenchyma. Broad zones of stromal collapse contain pre-existing portal areas, reticulin and entrapped ductules. Some of the latter are interlobular ducts; others are pseudoductules. In the upper portion of the photograph, islands of residual parenchyma are in process of regeneration. × 60.

FIG. 11. Fatty liver with early portal area fibrosis. The lesion is probably reversible at this stage. Stellate portal regions are highlighted on a background of fatty parenchyma. × 60.

FIG. 12. Chronic active hepatitis (viral?). Parenchymal relations are undisturbed. Portal regions are enlarged, barely stellate, finely fibrotic, and contain a heavy sprinkling of lymphocytes. Nodulation has not been induced. × 60.

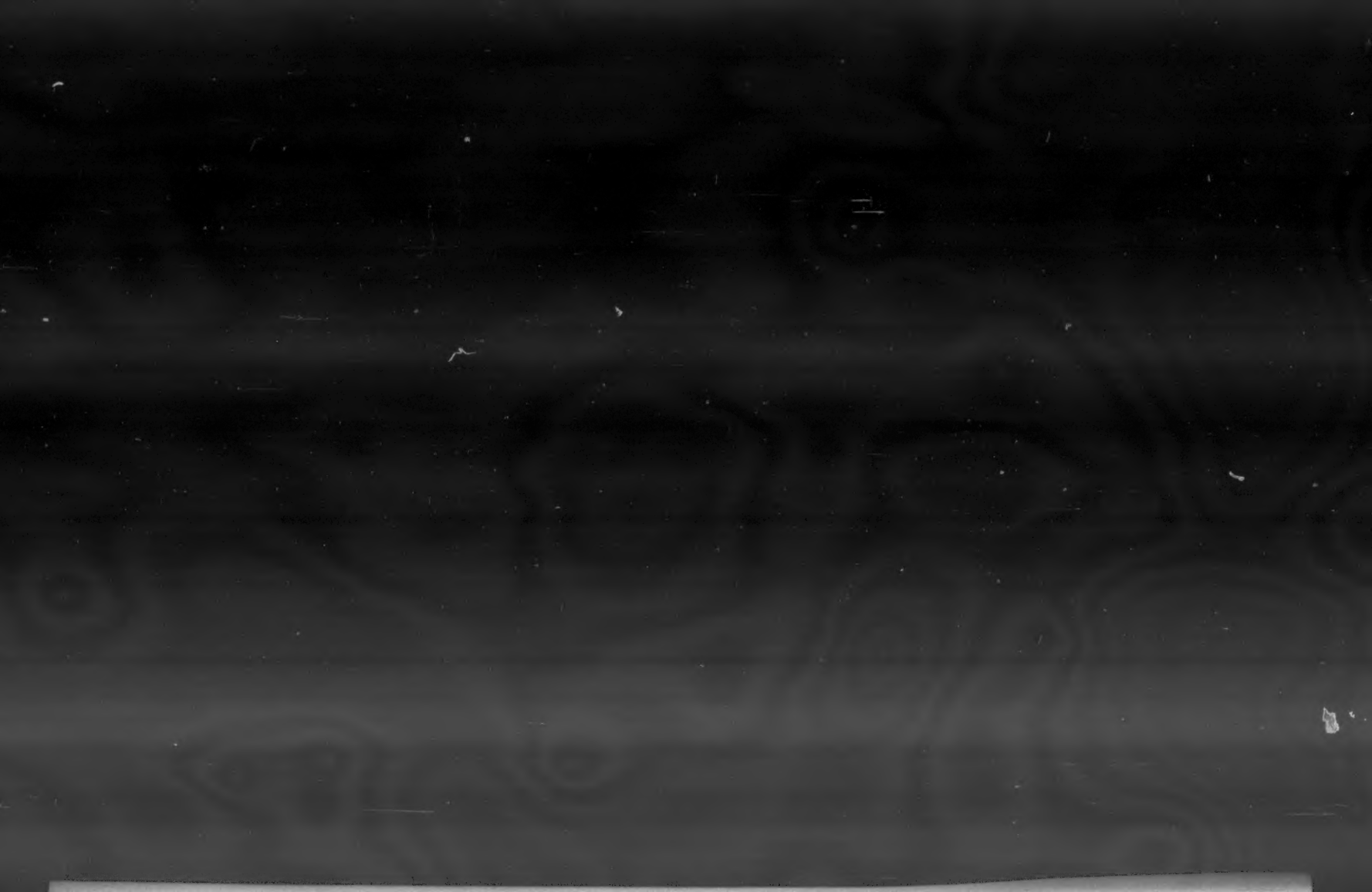

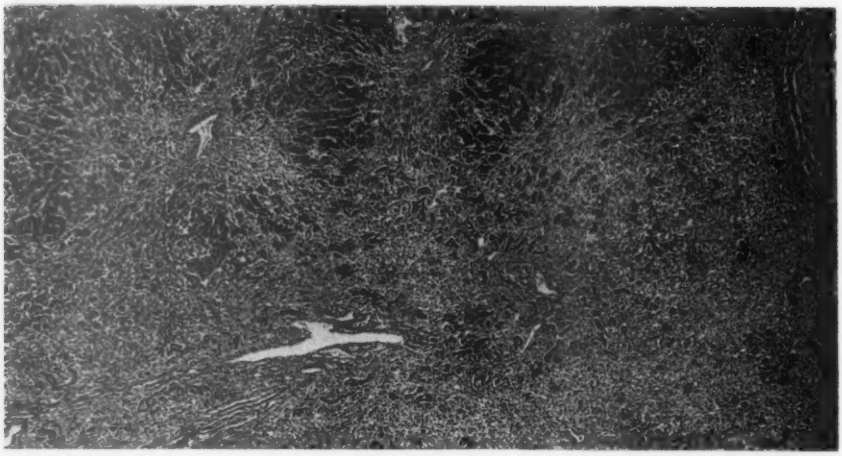

10

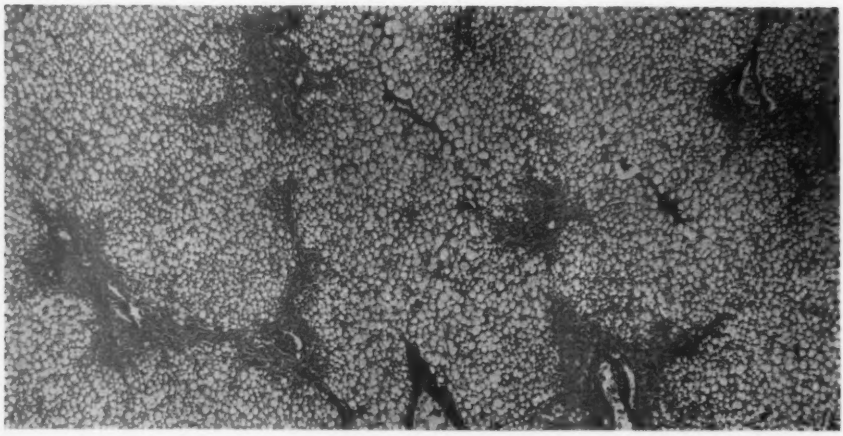

11

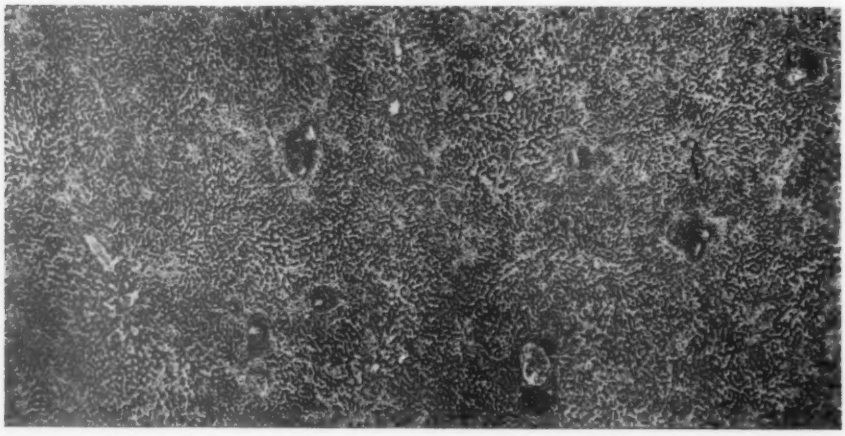

12

Figures 13 to 15 are photomicrographs illustrating advanced stages of hepatic cirrhosis.

FIG. 13. Postnecrotic cirrhosis. Embedded in a broad background matrix of collagen are regenerated parenchymal nodules lacking in regular conformation. × 60.

FIG. 14. Nutritional cirrhosis. Small, fatty pseudolobules are enclosed by delicate fibrous strands obscuring both portal islands and central veins. × 60.

FIG. 15. Posthepatitic cirrhosis. Trabeculations surround nodules containing components of several lobules (portal areas, central veins). × 60.

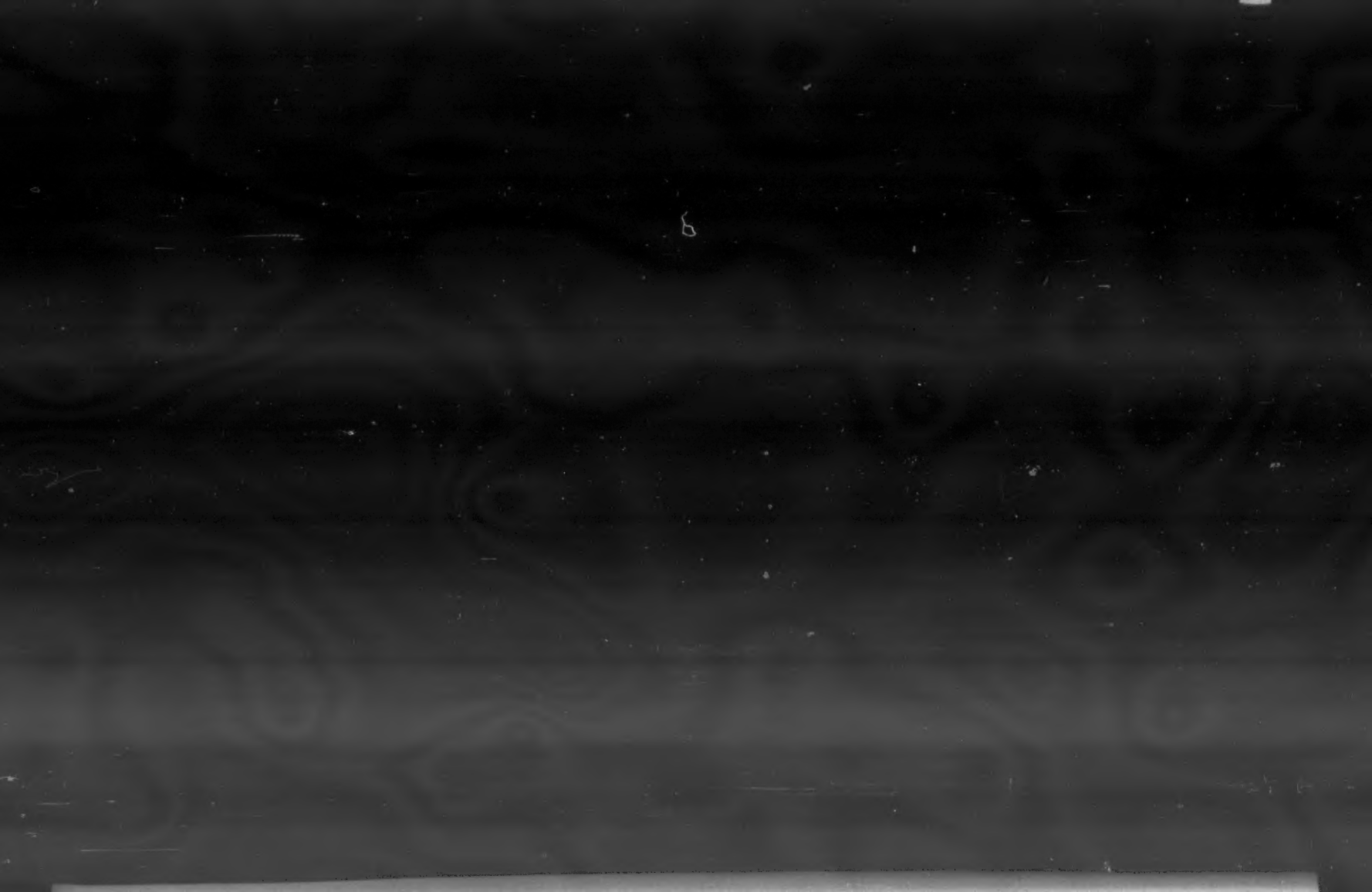

13

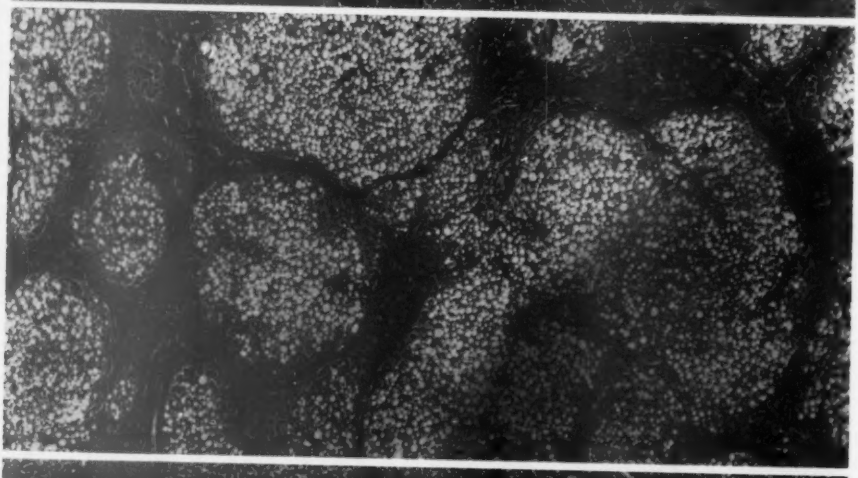

14

15

FIG. 16. Toxic hepatitis. Coarse vacuoles exhibit fuzzy margins. Most cells are filled with fine, foamy, lipid vacuoles. Kupffer cells and parenchymal elements are heavily bile stained, and there is an eosinophilic hyaline network in many of the liver cells. × 500.

FIG. 17. Nutritional cirrhosis. "Creeping fibrosis" characterized by interconnection of fibrillar tongues emerging from portal and central vein sheaths. Pseudolobule formation is induced by segmentation of the fatty parenchymal lobule. There is marked pseudoductule formation. × 500.

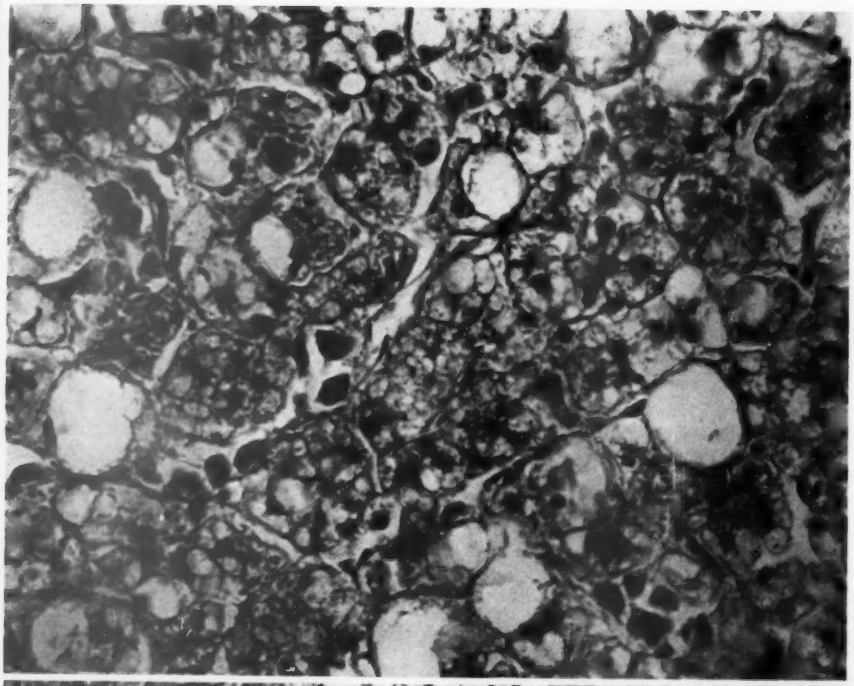

16

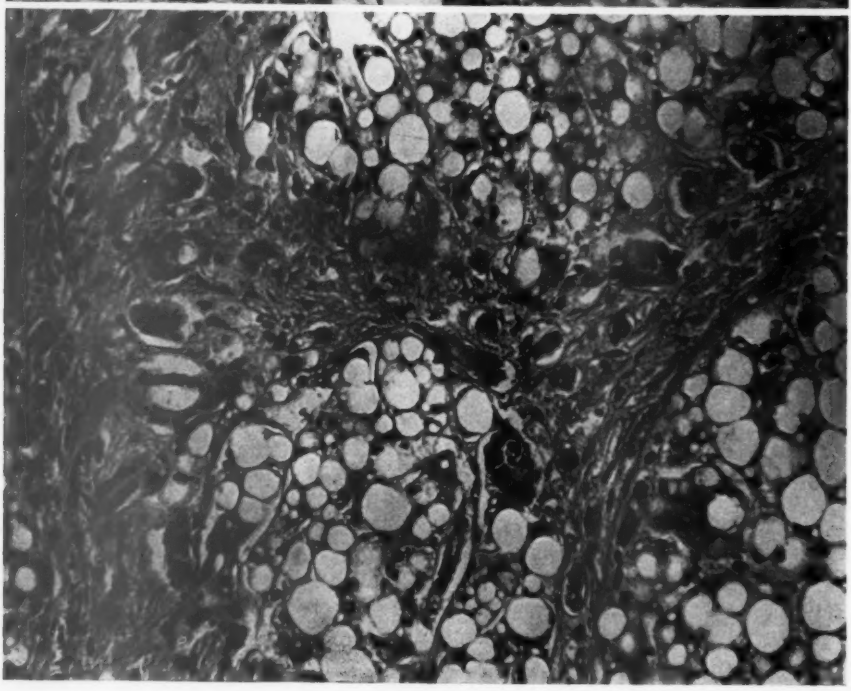

17

FIG. 18. A pseudolobule in nutritional cirrhosis. Spherical nodule of fat-filled parenchyma is lacking in radial pattern or lobular landmarks. Nodule is outlined by a delicate frond of connective tissue. × 500.

FIG. 19. Posthepatitic cirrhosis. From a stellate portal area, the seat of chronic inflammation, narrow fibrous trabeculae extend to adjacent portal areas (not in the photograph). × 500.

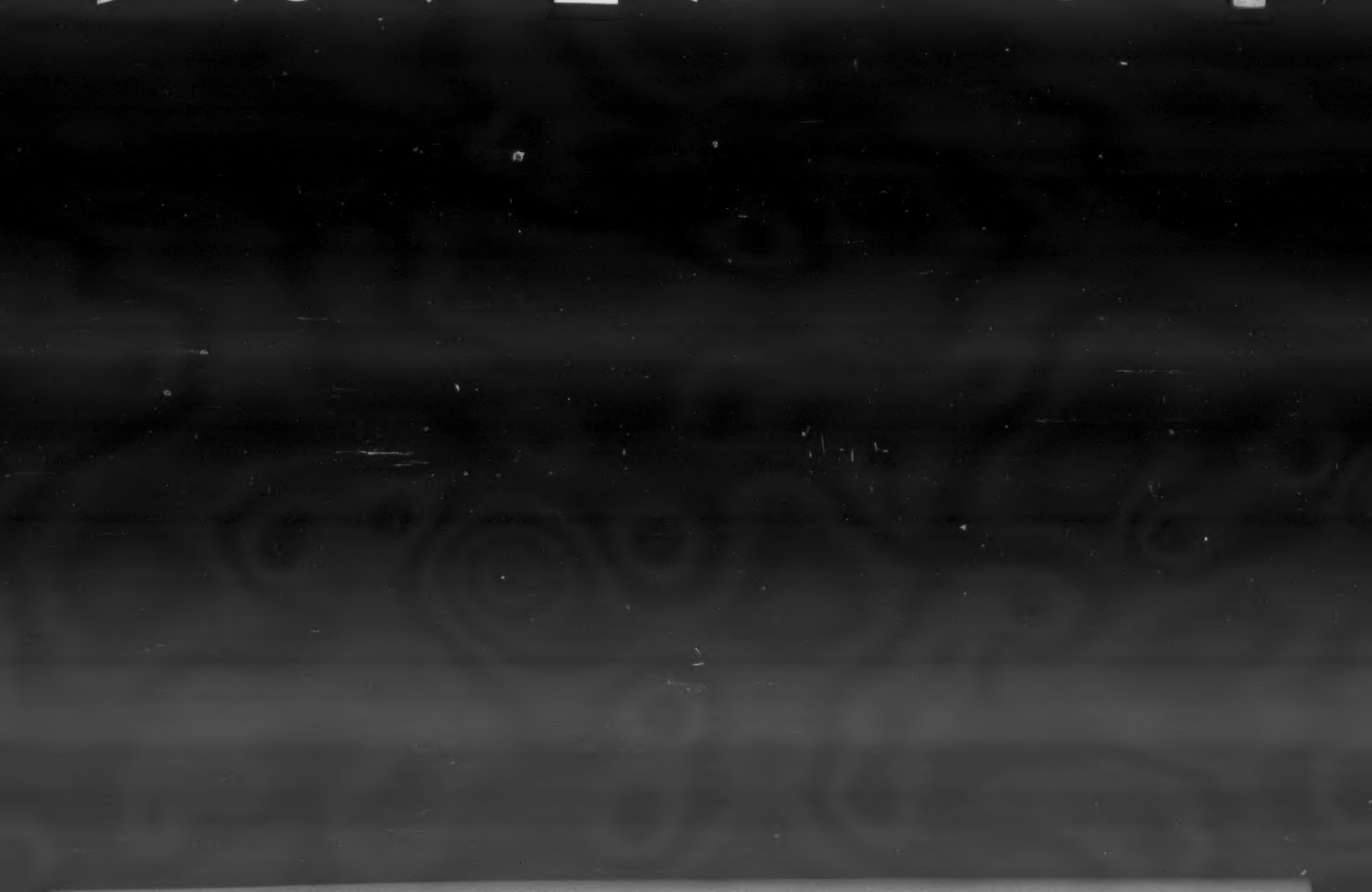

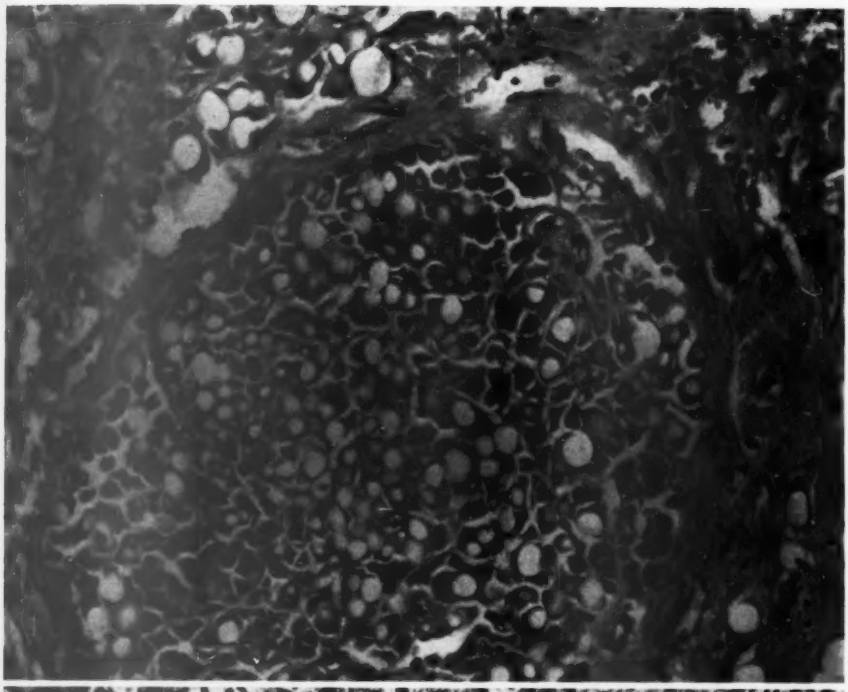

18

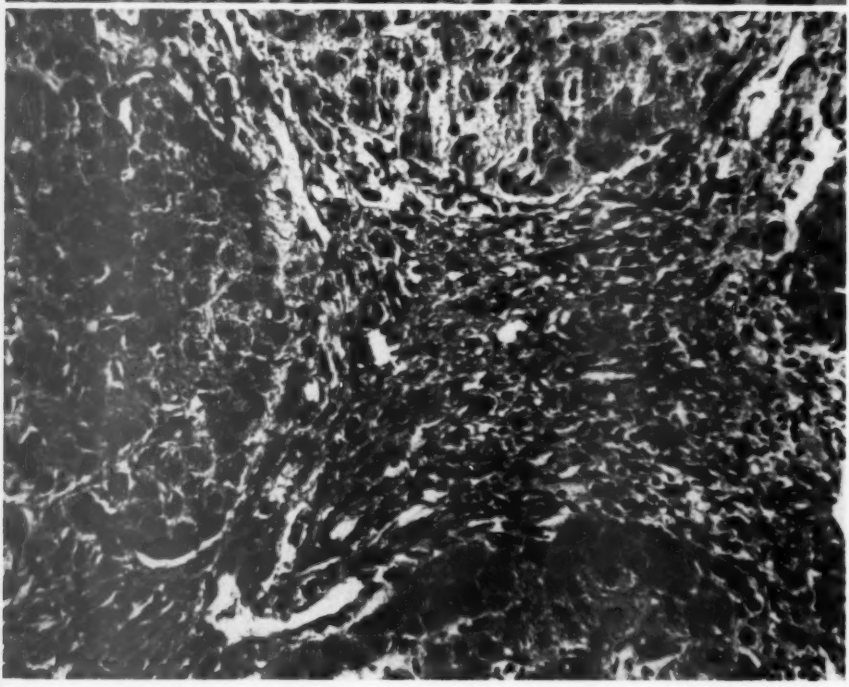

19

In Memoriam

On November 12, 1959, Miss Lillian M. Leavitt died in Brookline, Massachusetts, at the age of 69 years. During the period from 1923 to 1940, Miss Leavitt acted as editorial assistant to Dr. Frank B. Mallory when he was Editor-in Chief, first of *The Journal of Medical Research* and, from 1925 on, *The American Journal of Pathology*. Her very careful and meticulous proofreading set the standard for the high degree of accuracy maintained in The Journal subsequent to this period. The pattern and caliber of The Journal reflect Miss Leavitt's great devotion.

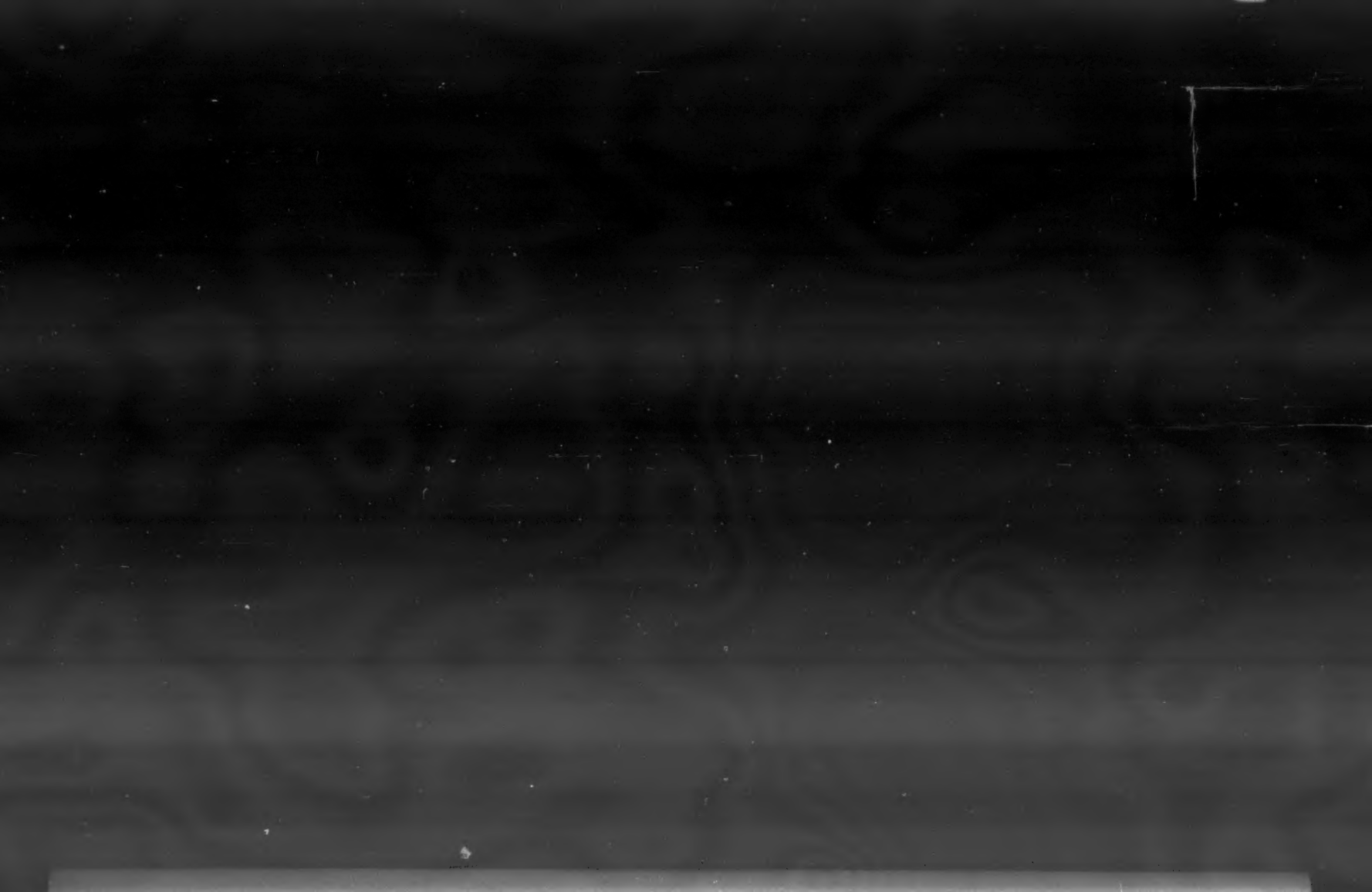

THE FINE STRUCTURE OF CEREBRAL FLUID ACCUMULATION

II. Swelling Produced by Triethyl Tin Poisoning and Its Comparison with That in the Human Brain

Richard M. Torack, M.D.; Robert D. Terry, M.D., and H. M. Zimmerman, M.D.

From the Lucy and Henry Moses Research Laboratories of the Laboratory Division, Montefiore Hospital, New York, N.Y.

The first part of this investigation [1] concerned the localized, mild cerebral swelling secondary to experimental cold injury of the mouse brain. Electron microscopy revealed that the fluid accumulated solely within glial cytoplasm. In view of this strict localization, it seemed desirable to study other types of cerebral fluid accumulation. The purpose was to learn whether different causative agents, different rates of onset and different degrees of severity altered the location of the fluid.

The ingestion of alkyl tin compounds has been demonstrated to cause lethal cerebral swelling in human beings and in experimental animals.[2,3] The brain is apparently the only organ affected, and is said to be diffusely and severely edematous. Magee, Stoner and Barnes [3] described the morphologic alterations as seen with the light microscope; they maintained that the fluid was interstitial in location. However, previous studies of brain tissue with the electron microscope have shown the intercellular space to be very small both in the normal brain [4,5] and under conditions of swelling.[1,6,7] Therefore, the electron microscope was utilized to determine the site of the fluid accumulation in alkyl tin poisoning.

The fine structure of human cerebral swelling was compared with the experimental swelling in animals. The cerebral tissue surrounding some intracranial neoplasms in man has been described as being swollen.[8,9] Under such conditions the brain is enlarged, rather dry, and soft. It is considered on the basis of light microscopy that the accumulated fluid is at least in part intracellular.

Material and Methods

Triethyl tin sulfate (obtained through the courtesy of H. van der Kirk of Utrecht, The Netherlands) and triethyl tin hydroxide (Metal and

This work was supported by a grant (B-1944) from the National Institute of Neurological Diseases and Blindness of the National Institutes of Health. Publication was aided by the Sandy Schneider Memorial Fund.

Received for publication, June 25, 1959.

Thermit Corporation, Rahway, New Jersey) were used to prepare a 0.2 per cent aqueous solution. The former was preferred since it proved to be more soluble in water. This solution was added to a mixture of powdered Rockland Mouse Diet and water to make concentrations of the triethyl tin which varied from 12 to 32 parts per million. These mixtures and water *ad libitum* constituted the sole diet for the young adult C_3H mice used in the experiment. Initially, the animals became irritable and developed roughened coats. Muscle weakness was prominent, especially in the hind limbs. The mice next reached a stage which was marked by diminished activity and virtual paralysis of the hind limbs. Terminally, there was increasing generalized rigidity with shallow respiration. The animals were sacrificed at different stages of involvement.

Tissues from 25 animals were examined by light microscopy. The tissue was fixed in neutral 10 per cent formalin and stained with hematoxylin and eosin, and by the periodic acid-Schiff (PAS) technique. Specimens from 18 animals were investigated with the electron microscope. For this purpose the tissue was fixed for 90 minutes in 2 per cent osmium tetroxide buffered with veronal acetate.[10] Following rapid dehydration, the tissue blocks were embedded in methacrylate resin. They were sectioned with a Porter-Blum (Servall) microtome and mounted on formvar carbon-coated copper grids. RCA electron microscopes of the EMU-3A and EMU-3D series were used.

Human brain tissue was obtained during neurosurgical procedures. The tissue was removed from the swollen area surrounding intracranial neoplasms. The tumors consisted of a metastatic carcinoma (primary site, carcinoma of the kidney), an astrocytoma, an ependymoblastoma, two mixed malignant gliomas and a glioblastoma multiforme. The human specimens were processed in the same fashion as the experimental tissue.

Results

Hematoxylin and eosin stained preparations of the mouse cerebrum revealed severe loosening of cerebral structure in the myelinated areas of the brain (Figs. 1 and 2). This change was diffuse, and appeared to be much more severe than the swelling which occurred following cold injury.[1] There were dilatation of the perivascular clear spaces and swelling of glial cell bodies. Apart from the glial enlargement, the exact location of fluid accumulation could not be determined. Periodic acid-Schiff stained preparations did not demonstrate a significant amount of PAS-positive material.

Electron microscopic examination revealed the most important morphologic alteration to consist of enlargement of glial cell processes. In the less severe lesions these processes contained relatively normal mitochon-

dria and endoplasmic reticulum, and were surrounded by intact cell membranes (Fig. 3). The affected cells appeared to be of the same type as the clear glial cells which were implicated in the response to cold injury. The other glial cell types were not significantly altered. The degree of enlargement of the clear glial cells was considerably greater than that found in cold injury. There was no apparent fluid accumulation except within these cell processes.

In the more advanced stages, endothelial cells were swollen so that their cytoplasm appeared less dense. The mitochondria of the clear glial elements were enlarged. There also appeared to be an increased number of microglia throughout the edematous areas. A striking feature was characterized by focal rupture of clear glial cell membranes (Fig. 4), but even in the immediate vicinity of these broken membranes there was no significant dissection of fluid into the intercellular space (Fig. 5). Adjacent cell membranes maintained their normal 10 to 30 mμ spacing.

One ml. of one per cent trypan blue was injected subcutaneously into several mice manifesting various degrees of alkyl tin intoxication. In no case did the vital dye penetrate the blood-brain barrier to stain the cerebrum. This substantiated the observations of Magee and co-workers.[3]

Electron microscopic examination of the human tissue revealed anatomic alterations similar to those due to triethyl tin. Enlarged clear glial cell processes were again identified (Fig. 6). In many regions the cell processes were intact, and there was little alteration of endothelium and mitochondria. Other areas appeared more severely affected, and exhibited edema of the endothelium, swelling of mitochondria, and prominent microglia. In addition, rupture of clear glial cell membranes, similar to that found in severe tin poisoning, was noted (Fig. 7). Again, there was no extracellular fluid accumulation.

Discussion

The cerebral fluid disturbance produced by the oral ingestion of alkyl tin compounds appeared to be fundamentally similar to that found in experimental cold injury.[1] In those experiments, a 30-second application of carbon dioxide ice to the cerebrum of the mouse produced local swelling of the brain. Examination of the tissue by electron microscopy revealed enlargement of the cell bodies and of the cytoplasmic extensions of the clear glial cells. The same clear glial cells and their processes were similarly affected in the animals poisoned with the tin compounds. There was no evidence to indicate the existence of an intermediary phase with intercellular fluid accumulation in response to either type of injury. The relatively minor differences in structural alteration could probably be related to the difference in severity of the conditions. However, it must

be stated that the mode of action of the alkyl tin compounds is largely unknown. Thus, the ruptured membranes, the endothelial swelling and the mitochondrial enlargement may conceivably be due to tin toxicity directly, rather than to a secondary effect attributable to excessive fluid accumulation.

Some of the animals were killed at a stage when only mild symptoms of tin intoxication were present; others were allowed to continue until the disease was very severe. In some of the experimental groups the clinical indications of nervous system disorder came on suddenly, but in others there was a gradual onset. None of these differences could be correlated with a change in the location of the swelling as seen with the electron microscope.

In the case of cold injury, the blood-brain barrier was broken down so that subcutaneously injected trypan blue stained the swollen cerebral hemisphere. The swelling produced by the ingestion of triethyl tin, however, was not accompanied by an alteration of this barrier as tested by trypan blue. Its competence, therefore, did not determine the location of the fluid accumulation any more than did the degree of severity or rate of onset.

The swollen human brain revealed lesions which were remarkably similar to those in the experimentally altered mouse brain. Again, there was dilatation of the clear cells without enlargement of the intercellular spaces. Ruptured plasma membranes were reminiscent of triethyl tin poisoning. With regard to the location of the excess fluid in human tissue, the electron microscope confirmed the data gained by light microscopy. By both methods the excess fluid appeared to be wholly intracellular. This emphasizes the disparity between the observations with the light microscope and with electron microscopy with regard to the site of fluid localization in tin poisoning.

Cerebral edema, as contrasted to cerebral swelling and as defined by Spatz,[8] is characterized by an enlarged, soft, wet brain. With the light microscope, the excessive fluid seems to occupy an intercellular position. This type of human wet brain has not yet become available for investigation with the electron microscope. The fluid accumulation which results from alkyl tin intoxication had been previously classified as interstitial,[3] and this lesion has, therefore, been categorized as cerebral edema. However, the electron microscope reveals an anatomic change which is similar to the intracellular swelling due to cold injury. The data obtained from these experiments and from the work of Gerschenfeld, Wald, Zadunaisky and de Robertis[6] and Luse[7] do not reveal a fundamental difference between cerebral swelling and cerebral edema. This tends to confirm the opinion of Perret and Kernohan[11] that cerebral edema is a more severe

phase of fluid surcharge. As described above, with increasing severity of swelling, there are increasing numbers of broken cell membranes. It is possible that with more severe swelling, a stage may be reached where a significant proportion of glia have ruptured membranes. This morphologic change is probably accompanied by a lessened rigidity of the cytoplasmic gel which is seen in the electron micrograph as dilution and decreased density of the cytoplasm. Under such circumstances the brain may appear wet and assume the picture of edema.

In the first part of this investigation, it was shown that the normally minute cerebral intercellular space does not enlarge in response to the increased fluid accumulation due to cold injury. On this evidence it was suggested that this very small intercellular space had little or no functional significance in fluid transport. The present experiments again reveal the essentially inert and unresponsive nature of the cerebral extracellular area. This implies that another mechanism is required to carry on the process of fluid transport in the brain. Lumsden [12] postulated that this was an intracellular function and that the astrocyte was the cell which is involved. He cited the length of the cells of this type, their pulsatile motility, and the presence of protoplasmic currents as evidence for this hypothesis. In our investigations, the clear glial cells were the units affected in abnormal fluid accumulation. These, then, are apparently the cells which carry on the function of fluid transport.

Summary

1. Alkyl tin compounds in small amounts (12 to 32 parts per million) in the food of mice caused diffuse swelling of the brain.

2. With the light microscope the excess fluid appeared to be interstitial in location, but the electron microscope revealed severe swelling of the clear glial cells without an increase in prominence of the minute intercellular space.

3. Human cerebral tissue from the swollen area surrounding brain tumors also showed an increase in the cytoplasmic volume for clear glial cells without enlargement of the intercellular space.

4. The presence of numerous ruptured glial cell membranes distinguished these types of cerebral swelling from that previously reported in experimental cold injury. The significance of these ruptures is discussed.

5. It is suggested that the clear glial cell plays an important role in cerebral fluid transport.

References

1. Torack, R. M.; Terry, R. D., and Zimmerman, H. M. The fine structure of cerebral fluid accumulation. I. Swelling secondary to cold injury. *Am. J. Path.*, 1959, **35**, 1135–1147.
2. Stoner, H. B.; Barnes, J. M., and Duff, J. I. Studies on the toxicity of alkyl tin compounds. *Brit. J. Pharmacol.*, 1955, **10**, 16–25.
3. Magee, P. M.; Stoner, H. B., and Barnes, J. M. The experimental production of oedema in the central nervous system of the rat by triethyltin compounds. *J. Path. & Bact.*, 1957, **73**, 107–124.
4. Farquhar, M. G., and Hartmann, J. F. Neuroglial structure and relationships as revealed by electron microscopy. *J. Neuropath. & Exper. Neurol.*, 1957, **16**, 18–39.
5. Schultz, R. L.; Maynard, E. A., and Pease, D. C. Electron microscopy of neurons and neuroglia of cerebral cortex and corpus callosum. *Am. J. Anat.*, 1957, **100**, 369–407.
6. Gerschenfeld, H. M.; Wald, F.; Zadunaisky, J. A., and de Robertis, E. P. D. Function of astroglia in the water-ion metabolism of the central nervous system. *Neurol.*, 1959, **9**, 412–425.
7. Luse, S. A., and Harris, B. Electron microscopy of the brain in experimental edema. (Abstract) *Anat. Rec.*, 1959, **133**, 305.
8. Spatz, H. Die Bedeutung der "symptomatischen" Hirnschwellung für die Hirntumoren und für andere raumbeengende Prozesse in der Schädelgrube. In: Wanderversammlung der südwestdeutschen Neurologen und Psychiater am 1. und 2. Juni 1929 in Baden-Baden. *Arch. Psychiat.*, 1929, **88**, 790–794.
9. Greenfield, J. G. The histology of cerebral oedema associated with intracranial tumours (with special reference to changes in the nerve fibers of the centrum ovale). *Brain*, 1939, **62**, 129–152.
10. Palade, G. E. A study of fixation for electron microscopy. *J. Exper. Med.*, 1952, **95**, 285–299.
11. Perret, G. E., and Kernohan, J. M. Histopathologic changes of the brain caused by intracranial tumors (so-called edema or swelling of the brain). *J. Neuropath. & Exper. Neurol.*, 1943, **2**, 341–352.
12. Lumsden, C. E. The Cytology and Cell Physiology of the Neuroglia and of the Connective Tissue in the Brain with Reference to the Blood-brain Barrier. Proceedings, Second International Congress on Neuropathology, London. Excerpta Medica Foundation, Amsterdam, 1955, pp. 373–376.

[*Illustrations follow*]

Legends for Figures

Fig. 1. Intact mouse cerebrum, showing the normal compact structure of the corpus callosum (CC), fimbria (F) and internal capsule (IC). Hematoxylin and eosin stain. × 100.

Fig. 2. Mouse cerebrum in chronic triethyl tin poisoning. There is loosening of the fibers of the corpus callosum (CC), fimbria (F) and internal capsule (IC). Hematoxylin and eosin stain. × 100.

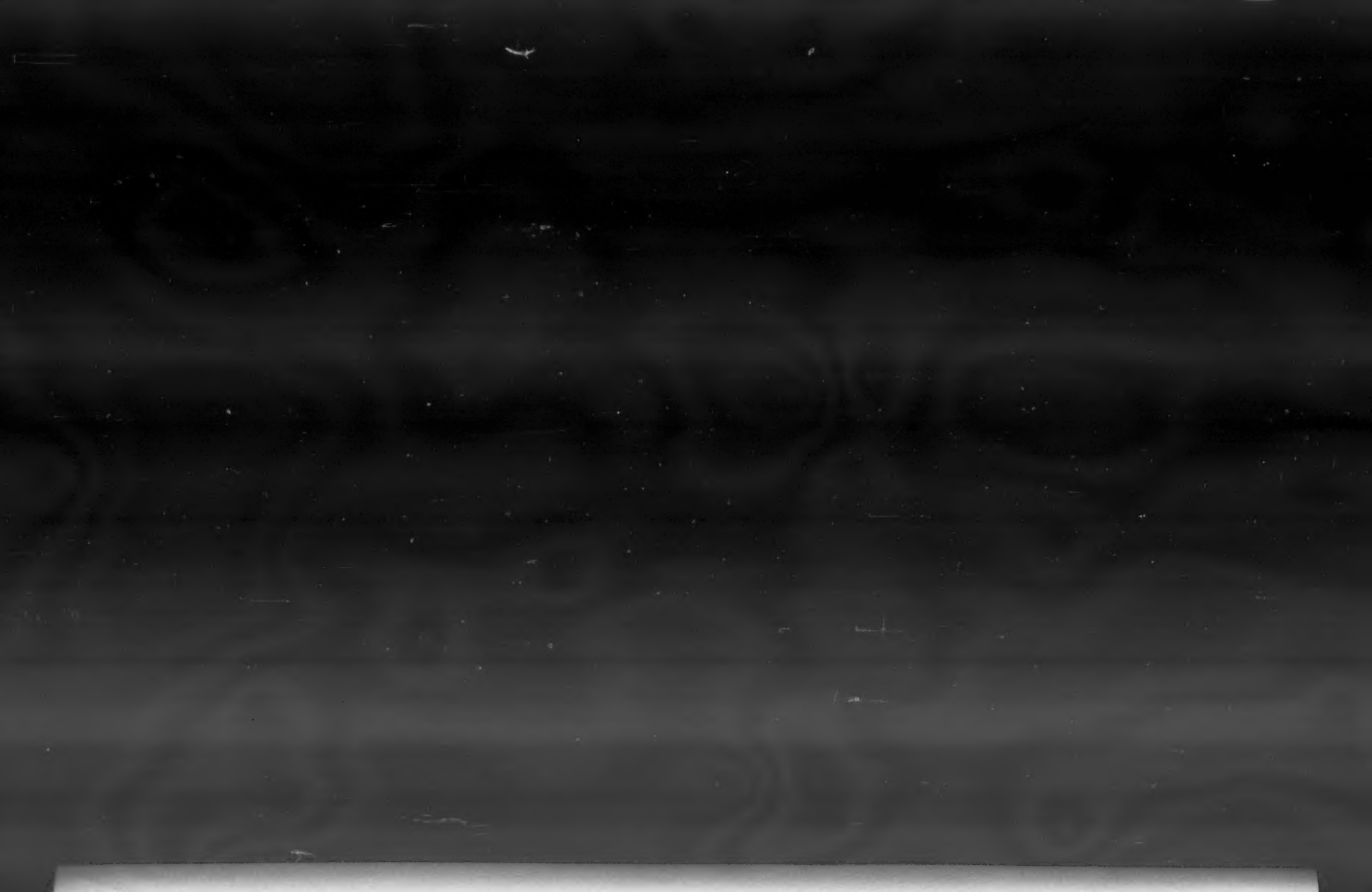

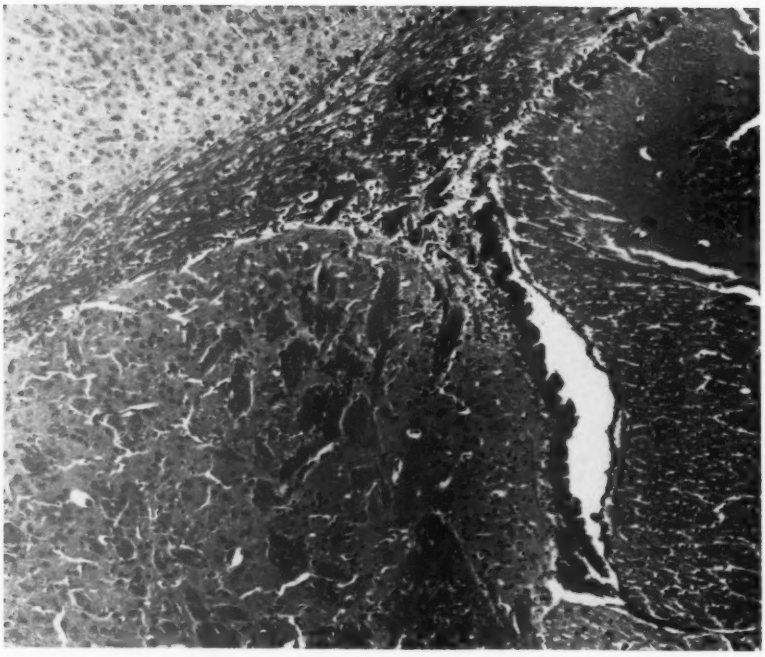

1

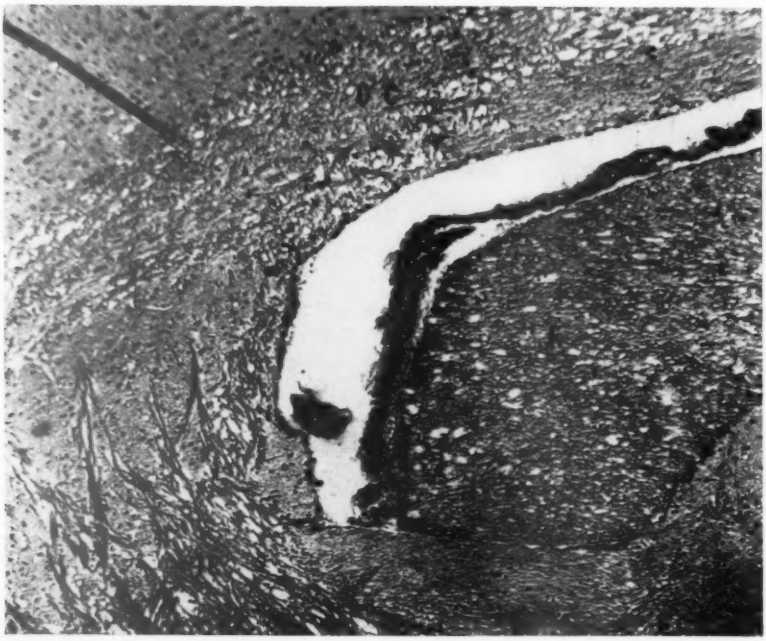

2

FIG. 3. Moderate glial swelling in tin intoxication. BV, blood vessel; M, mitochondrion; MNF, myelinated nerve fiber; ER, endoplasmic reticulum; GP, process of clear glial cell. × 10,600.

FIG. 4. Swollen glial processes with ruptured membranes (RGM) in tin poisoning. ECN, endothelial cell nucleus; M, mitochondrion. × 10,300.

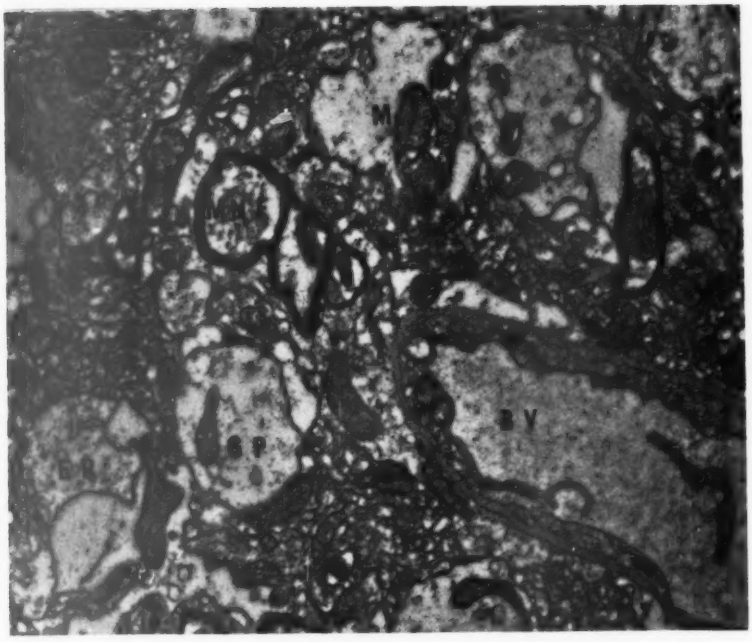

3

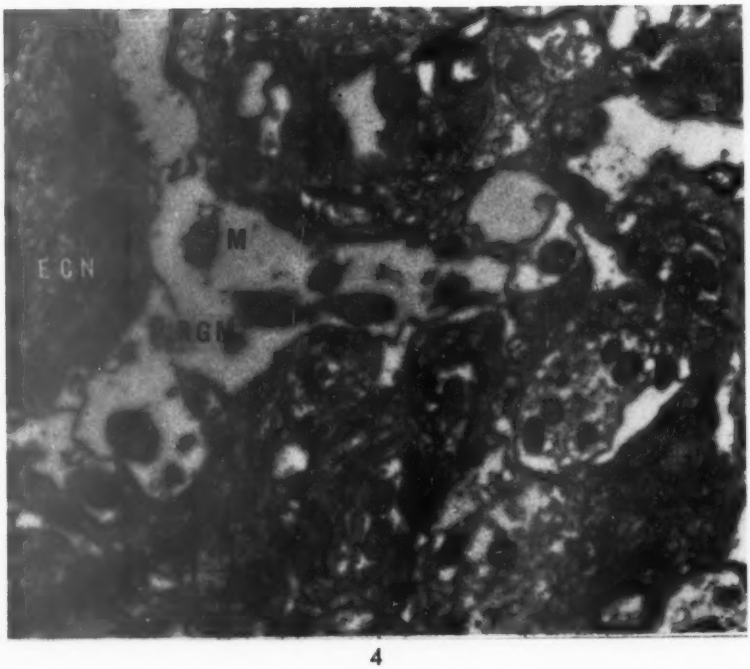

4

FIG. 5. Higher magnification of the broken plasma membranes (RGM) of enlarged clear glial cell processes (GP). × 25,800.

FIG. 6. Mild swelling of human cerebrum in an area adjacent to an astrocytoma. GP, process of clear glial cell; ER, endoplasmic reticulum; M, mitochondrion; MNF, myelinated nerve fiber. × 10,300.

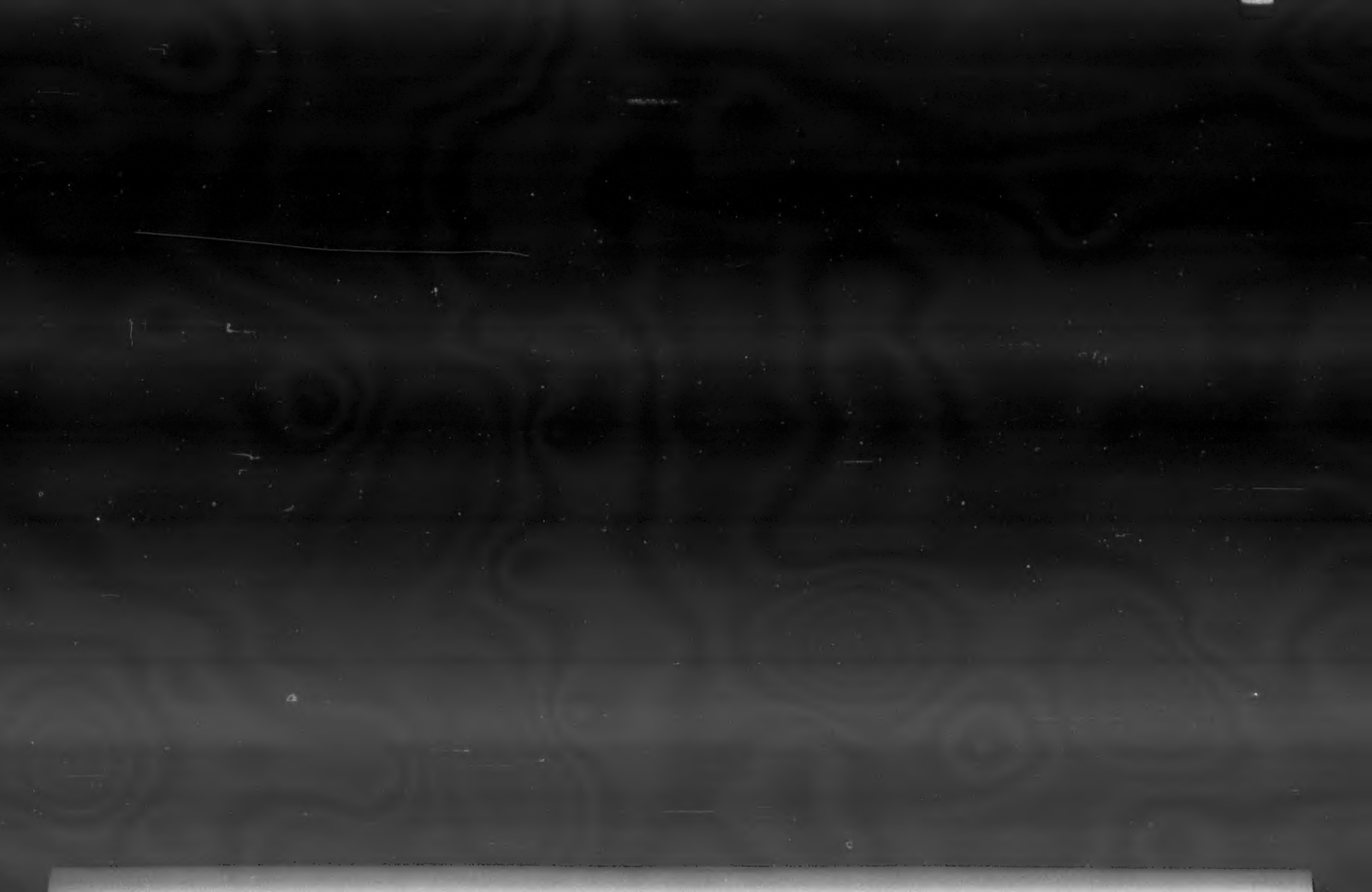

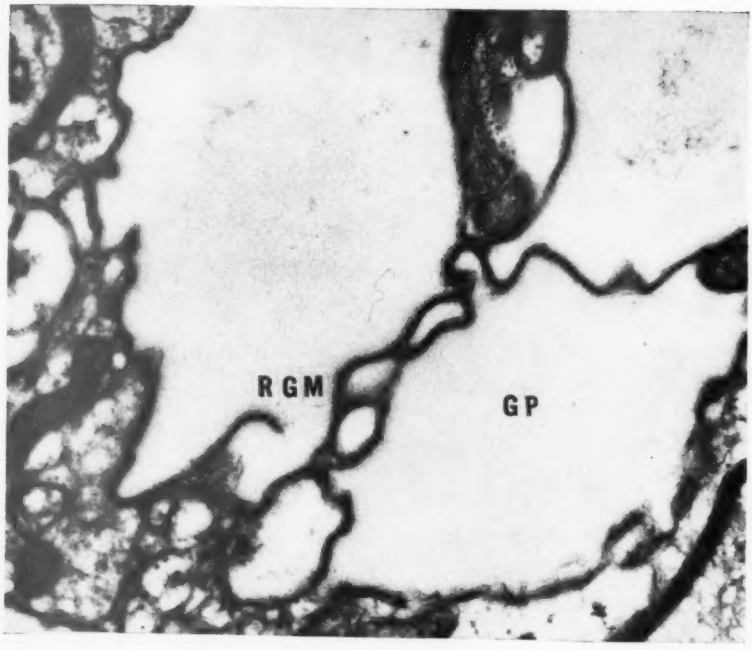

5

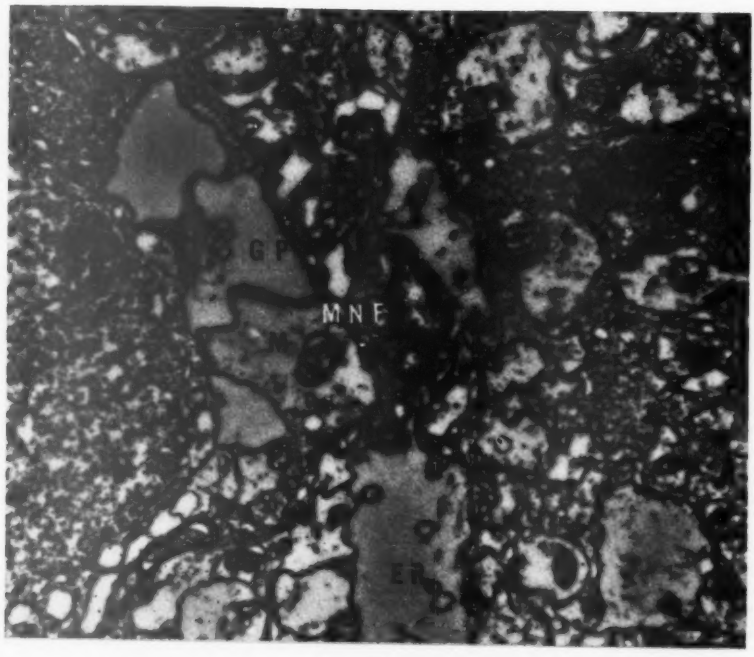

6

FIG. 7. Severe swelling of perivascular processes of clear glial cells (GP). Human cerebrum adjacent to metastatic carcinoma. RGM, ruptured plasma membranes; EC, endothelial cell cytoplasm; LI, lipid inclusions; ER, endoplasmic reticulum. × 10,300.

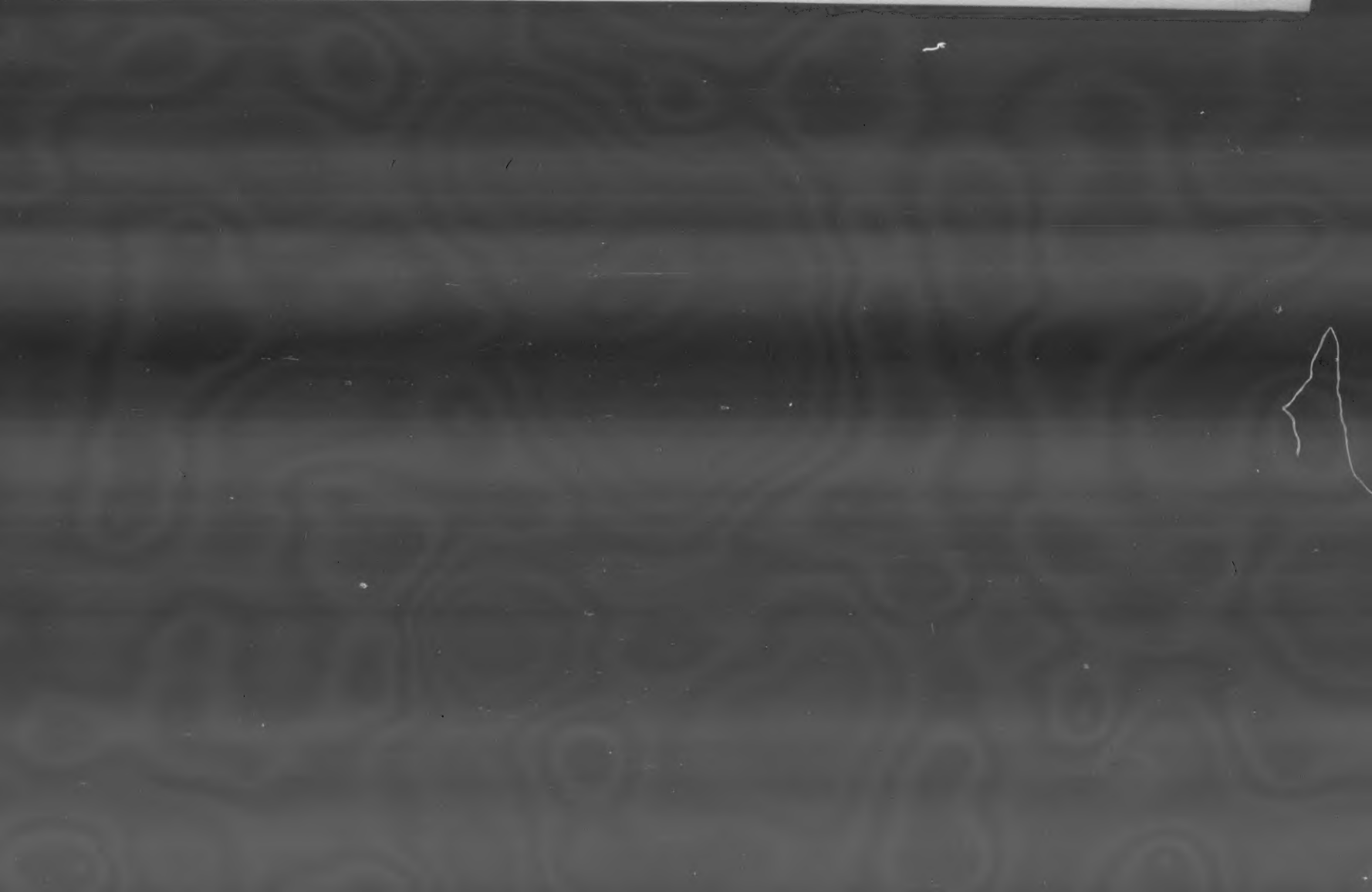

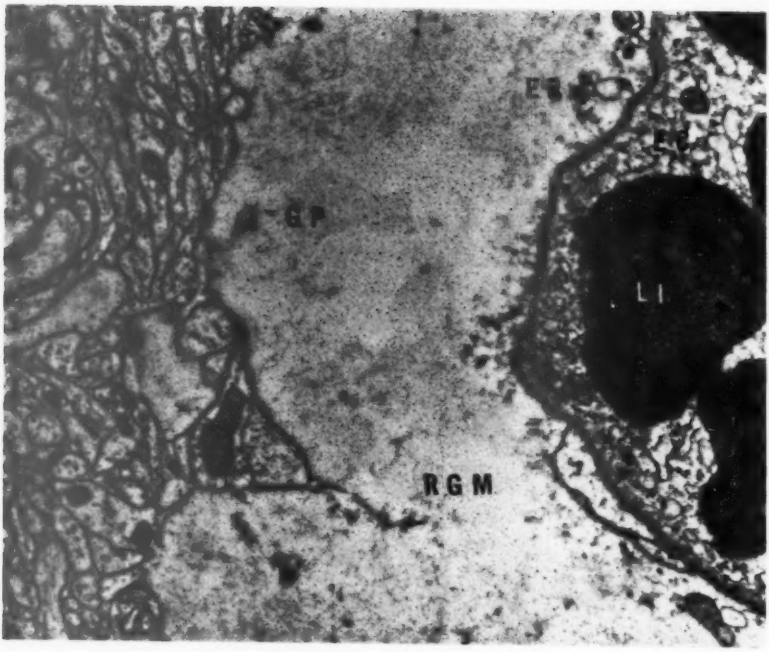

7

FOCAL INTIMAL PROLIFERATION IN THE CEREBRAL ARTERIES

W. E. Stehbens, M.B., B.S.

From the Department of Pathology, University of Sydney, Sydney, Australia

In investigating the pathogenesis of atherosclerosis, it is important to start with the earliest possible stage of the lesion, which as yet has not been carefully defined. Areas of intimal proliferation have been described in the aorta [1,2] and about the orifices of the large distributing arteries [3–5] in early life, but the cerebral arteries have not previously been examined in detail from this point of view. This intimal proliferation may be related to atherosclerosis, as Wilens [1] suggested. In the present work, serial sections of the cerebral arteries were made, rather than random sections as used by other workers. By this means, a more accurate localization of the thickenings in relation to the forks and a more thorough histologic study were made possible.

Material and Methods

The material consisted of 93 cerebral arterial forks from 22 human subjects, ranging in age from a fetus of 28 weeks to an infant of 8 months. All but 4 forks were bifurcations of the internal carotid and middle cerebral arteries. The tissues were fixed in 10 per cent formalin and embedded in paraffin. Serial sections were cut at 7 μ, in such a plane as to obtain Y- or T-shaped sections. From 5 to 9 consecutive sections were mounted on each slide. Toluidine blue, Mallory's phosphotungstic acid-hematoxylin (PTAH) or the McManus periodic acid-Schiff (PAS) technique were used to stain 2 nonconsecutive slides from near the center of the fork. All other slides were stained with Verhoeff's elastic tissue stain and counterstained with eosin.

The terminology used to define anatomic sites about the forks is the same as that used in a preceding paper.[6] The apex of the fork (Text-fig. 1) is the point at which the axial column of blood impinges on the vessel wall at the bifurcation. The apical angle is the angle between the two branches, and the lateral angles are those between the parent stem and each of the daughter branches. The face is the area on the uppermost part of the stem near the fork and between the entrances to the branches. The back (or dorsum) is the corresponding area on the under surface.

Received for publication, June 10, 1959.

Results

For the most part, the intima of the cerebral arteries of all sizes consisted of an endothelial layer and an internal elastic lamina, with no intermediate layer. The internal elastic lamina, when appropriately stained, appeared in transverse section as a darkly staining, frequently

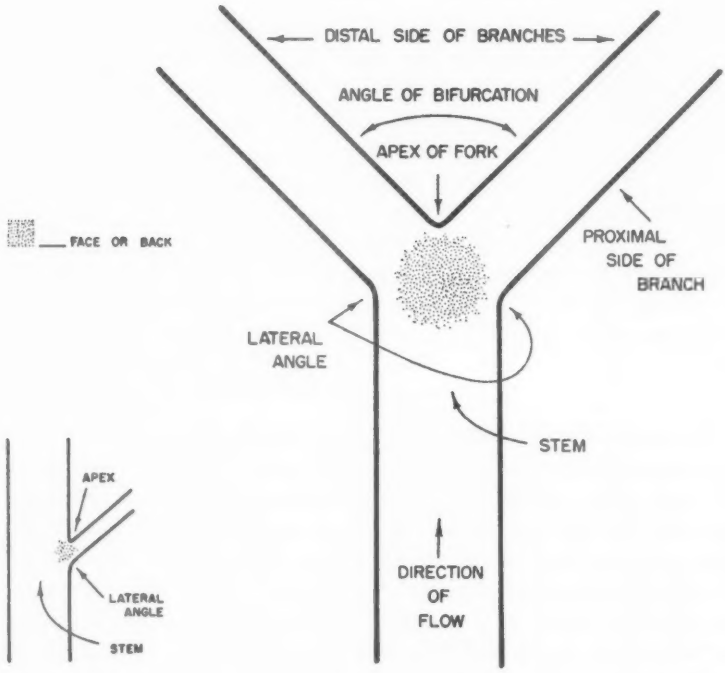

Text-figure 1. Diagram illustrating the terminology used for anatomic sites about the forks of vessels. (Reproduced from Stehbens [6] with permission of the publisher.)

wavy layer with sharply defined edges and of relatively uniform thickness. In tangential section it was a fenestrated membrane (Fig. 1). The fenestrae were mostly 2 to 3 μ in size, but varied from about 1 to 8 μ and were round or oval. They were fairly evenly distributed, though it was not uncommon for two to be very close together. The membrane, apart from the fenestrae, was fairly homogeneous. Variations from this structure occurred only in relation to the intimal thickenings or in those sites at which the thickenings were commonly found. Such changes took place in a regular sequence, both in location and in time, beginning in fetal life, even as early as 28 weeks.

Sequence of Development of Intimal Pads

Intimal thickenings were found only in relation to the sites of branching of the arterial tree. The intimal proliferation did not occur diffusely about each fork but occurred as separate pads which later coalesced. They were named apical, facial, dorsal, and lateral pads (Figs. 2 and 3) according to their position. The facial and dorsal pads were the earliest to be seen and the lateral pads next, while the apex was the last site to be affected. The sequence of the development and localization of these intimal pads was found to be constant. Lateral angle pads were never seen in the absence of facial and dorsal pads. It was only when facial, dorsal and lateral pads had enlarged and begun to coalesce (Fig. 2) that changes were found at the apex. Eventually, all these pads became continuous with one another. Without exception, the changes in all forks conformed to this pattern. Lateral pads occurred immediately beyond the site where the lateral wall began to curve into the proximal side of the daughter branch (Fig. 3). The extent of the alterations increased with increasing age of the subject and increasing size of the vessel. When there was considerable difference in the size of the two branches, there was only one lateral angle pad, as in Figure 3, on the side of the trunk from which the smaller branch took origin. Whatever the angle at which branches left the main stem, the position of the pads was the same, but the lateral pads were not always equal in size and extent on the two sides. At the bifurcation of the internal carotid artery, the lateral angle pad on the side of the anterior cerebral artery and elastic changes at the apex were sometimes found to develop earlier than the lateral angle pad on the side of the middle cerebral artery. There was also intimal proliferation at the orifices of smaller branches, but this was always less extensive.

Early Elastic Tissue Changes

Elastic tissue alterations were detected in the region of the face, dorsum, lateral angles and apex before the appearance of intimal proliferation. All intimal pads were associated with such changes, which were usually most prominent at the thickest portion or center of the pad but occasionally were seen beyond its edges. Sometimes the pad seemed to be slightly more extensive than the visible elastic tissue changes.

The changes in the elastic lamina consisted of loss in the depth and uniformity of staining which was associated with the lace-like and fibrillary appearances seen in Figure 4. In cross section, the lamina was often relatively straight and thin, or at times granular, segmented, or fuzzy (Fig. 5). Beading or a tendency to segmentation of the elastic lamina was also seen about the fork with or without some intimal thickening. The lamina, in places, failed to stain at all (Fig. 6).

Facial, Dorsal, and Lateral Pads

The earliest intimal pads found consisted primarily of smooth muscle fibers and some very fine elastic fibrils. In general, the smooth muscle fibers were less dense than in the media and were longitudinally arranged. In sections stained by PTAH, there appeared to be more intercellular matrix than in the media (Fig. 7), but with Verhoeff's stain (Figs. 8 and 9) the intercellular matrix appeared to consist of numerous elastic fibrils. The wavy elastic fibrils ran longitudinally in the pads and were probably thin laminas. These early pads were not areas of endothelial proliferation, for the endothelial cells were quite distinct from the underlying plain muscle fibers. Staining with toluidine blue and PAS revealed no metachromatic ground substance.

Larger and older pads had similar features. They were occasionally more than 200 μ in length, and often thicker than the media (Fig. 7). The underlying elastic lamina showed the changes (Fig. 4) described above. In addition, a new elastic lamina formed immediately beneath the surface (Fig. 10). This newly formed elastic lamina was usually most noticeable at the edge of the pad (Fig. 10), but it did often extend over the surface. The new lamina was thin, palely staining and very fibrillary (Fig. 11), though in older pads it was sometimes denser (Fig. 12). The lamina thus formed fused to the original lamina at the edges of the pad, and this gave the appearance of splitting of the original lamina. It seemed, however, that the duplication was caused not by splitting but by the formation of new elastic tissue beneath the endothelium. In Figure 12 the new lamina appears beaded in places, and near the arrow it is pale and lacy. Newly formed elastic laminas always showed these changes to some extent. In still more advanced plaques, musculo-elastic proliferation had proceeded on top of the second lamina (Fig. 13). The pad then appeared to consist of two strata, separated by a layer of elastic tissue. Other small laminas or fibrils in these pads were pale or indistinct.

These advanced pads with prominent accessory elastic laminas were found only in the forks of older subjects in which pads occurred at all areas about the fork.

Apical Pads

Apical pads occasionally projected well into the lumen, but usually were considerably thinner than those encountered elsewhere. The internal elastic lamina showed the same sort of alterations observed in other situations (Figs. 14 to 16). Apical pads also consisted mainly of muscle and elastic tissue. New elastic tissue tended to form beneath the endothelium, giving the elastic lamina a frayed or split appearance (Figs. 14

and 16). The pads sometimes appeared to be a part of the media, but elastic tissue stains revealed remnants of the original elastic lamina, distinguishing intima from media (Fig. 16). The outstanding feature of the apical pads was the general tendency for little intimal proliferation to take place, even in the presence of a fragmented or deficient elastic lamina. The apical pads were usually continuous with the facial and dorsal pads, and therefore might be merely the extension of the neighboring intimal thickenings.

Frequency and Severity of the Intimal Changes with Age

Grading the severity of the intimal lesions was technically difficult because the pads were cut in different planes of section, and the vessels varied considerably in size and angle of bifurcation. However, some indication of the frequency and severity of the alterations may be gained by dividing the specimens roughly into 3 groups. The first group consisted of 9 forks from 2 fetuses of 28 weeks' gestation. Changes in the elastic lamina with or without intimal proliferation were found in the facial and dorsal areas of 5 of these forks. The second group, consisting of 46 forks from fetuses of 36 weeks to infants of one month, revealed facial and dorsal pads in all cases. Some forks had lateral pads, but the apical regions were usually unaffected. A few of the pads contained two prominent elastic laminas. The remaining 38 forks from infants of 6 weeks to 8 months formed the third group. In these there were facial and dorsal pads in all cases and usually lateral and apical pads. These pads were generally larger and thicker than those of the other groups, and many of them contained 2 or 3 prominent elastic laminas.

Thus, the most marked alterations were observed in those instances in which there were pads at all sites about the fork; the least marked changes were observed in those in which there were only facial and dorsal pads.

Discussion

The nature of the intimal proliferation in the arteries of infants is unknown. There has been much speculation, and in general it has been assumed to be a normal structural component of an artery. Some authors,[1,7] however, have considered it to be the early stage or an integral part of atherosclerosis. The nature of the elastic tissue changes which preceded and were associated with intimal thickening is debatable, but they appeared to be steps leading to the eventual disappearance of the elastic lamina. Hass [8] said that the early stage of atrophy of elastica was characterized by the partial or complete loss of specific staining qualities, and the elastic tissue changes described here are probably degenerative.

In a recent study of intimal proliferation in the aorta,[2] atrophy of muscle and elastica was noted both in the intima and in the adjacent media.

If the elastic tissue alterations are degenerative, as it would appear, it follows that even at this early age there is some damaging factor at play. The intimal proliferation of the pads may be compensatory in nature because of the loss in tensile strength consequent upon the changes in the elastica. The pads continue to be associated with elastic tissue changes, and the new laminas also show similar features, suggesting that the hypothetical damaging factor persists. Recent evidence[9] suggests that turbulence may occur at the bifurcations and branchings of the cerebral arteries, and it may therefore be significant that the lateral and apical pads occur at stagnation points where the eddy currents are likely to occur. The facial and dorsal pads are not so easily related to flow patterns.

Summary

Intimal pads around bifurcations of the cerebral arteries of fetuses and infants were preceded by and associated with prominent elastic tissue changes, which might well be degenerative in nature. The pads appeared in a regular sequence. Facial and dorsal pads preceded the lateral angle pads. These had extended and had begun to coalesce before the apex was affected.

The pads consisted of musculo-elastic tissue. The apical pads were usually thinner than those at other sites, despite prominent changes in the elastic lamina. Successive laminas of elastica were formed, giving the intimal pads a stratified appearance.

References

1. Wilens, S. L. The nature of diffuse intimal thickening of arteries. *Am. J. Path.*, 1951, **27**, 825–839.
2. Movat, H. Z.; More, R. H., and Haust, M. D. The diffuse intimal thickening of the human aorta with aging. *Am. J. Path.*, 1958, **34**, 1023–1031.
3. Dock, W. The predilection of atherosclerosis for the coronary arteries. *J.A.M.A.*, 1946, **131**, 875–878.
4. Moon, H. D., and Rinehart, J. F. Histogenesis of coronary arteriosclerosis. *Circulation*, 1952, **6**, 481–488.
5. Levene, C. I. The early lesions of atheroma in the coronary arteries. *J. Path. & Bact.*, 1956, **72**, 79–82.
6. Stehbens, W. E. Medial defects of the cerebral arteries of man. *J. Path. & Bact.*, 1959, **78**, 179–185.
7. Schornagel, H. E. Intimal thickening in the coronary arteries in infants. *A.M.A. Arch. Path.*, 1956, **62**, 427–432.
8. Hass, G. M. Elastic tissue. *Arch. Path.*, 1939, **27**, 334–365 and 583–613.

9. STEHBENS, W. E. Turbulence of blood flow. *Quart. J. Exper. Physiol.*, 1959, 44, 110–117.

Thanks are due to Professors F. R. Magarey and D. A. Cameron for their advice and encouragement; to Drs. R. D. K. Reye and J. M. Moyes for the specimens; to Mr. T. Jones for his technical assistance; and to the Department of Medical Illustration, University of Sydney, for the illustrations.

[*Illustrations follow*]

Legends for Figures

Fig. 1. A tangential section of the internal elastic lamina. Note the fenestrae and the homogeneous appearance of the elastic tissue. Black dots are due to formalin pigment. Verhoeff's stain. × 500.

Fig. 2. An internal carotid artery, showing a facial pad (center) with prominent elastic tissue changes (center). Lateral pads are seen at L; that on the left is continuous with the facial pad. Verhoeff's stain. × 20.

Fig. 3. A lateral angle pad at branching of a middle cerebral artery in an infant. Note pallor of the elastic lamina beneath the pad. There is a defect of the media but no pad at the apex. Verhoeff's stain. × 35.

Fig. 4. An internal elastic lamina, pale and lacy, in tangential section. Endothelial cells and formalin pigment are manifest to the left. Compare with Figure 2. Verhoeff's stain. × 500.

Fig. 5. Slight intimal thickening associated with fragmentation of the elastic lamina at an apex. Verhoeff's stain. × 300.

Fig. 6. Slight intimal thickening but deficient elastic lamina at an apex. Verhoeff's stain. × 300.

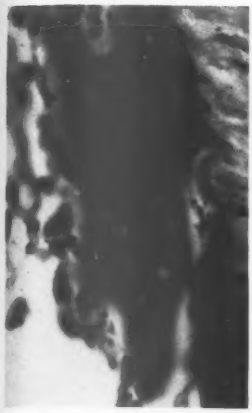

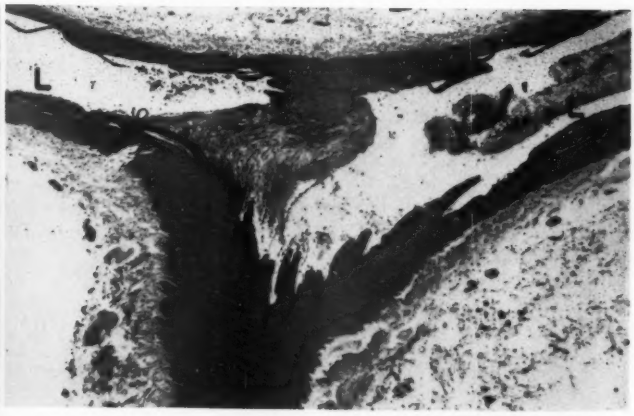

2

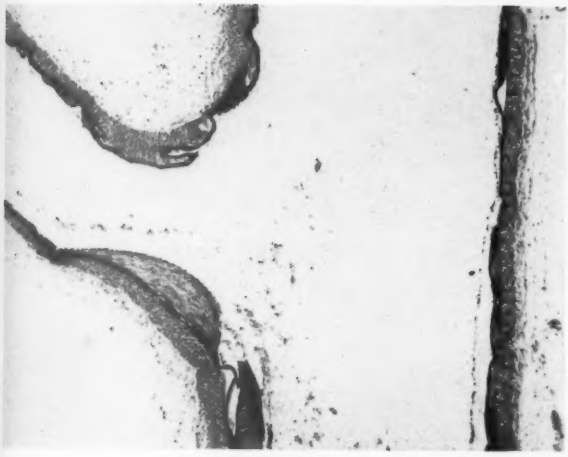

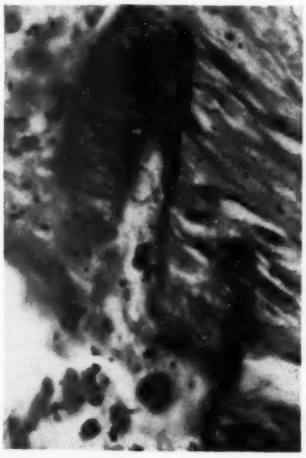

4

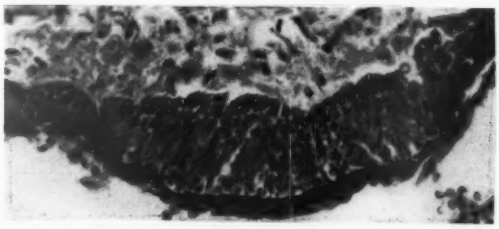

5

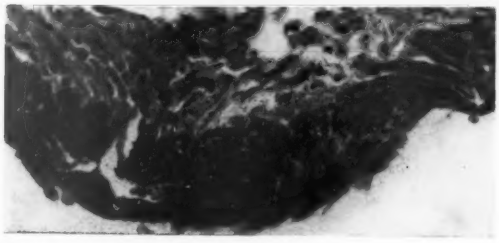

6

FIG. 7. A lateral angle pad containing muscle fibers more loosely arranged than in the media. Mallory's phosphotungstic acid-hematoxylin (PTAH) stain. × 300.

FIG. 8. A pad containing numerous elastic fibers. Verhoeff's stain. × 300.

FIG. 9. A larger pad than that shown in Figure 8. Numerous elastic fibers run longitudinally in the pad. Verhoeff's stain. × 300.

FIG. 10. A large pad with a palely staining elastic lamina. Newly formed laminas are seen at the edges of the pad (see arrows). Verhoeff's stain. × 75.

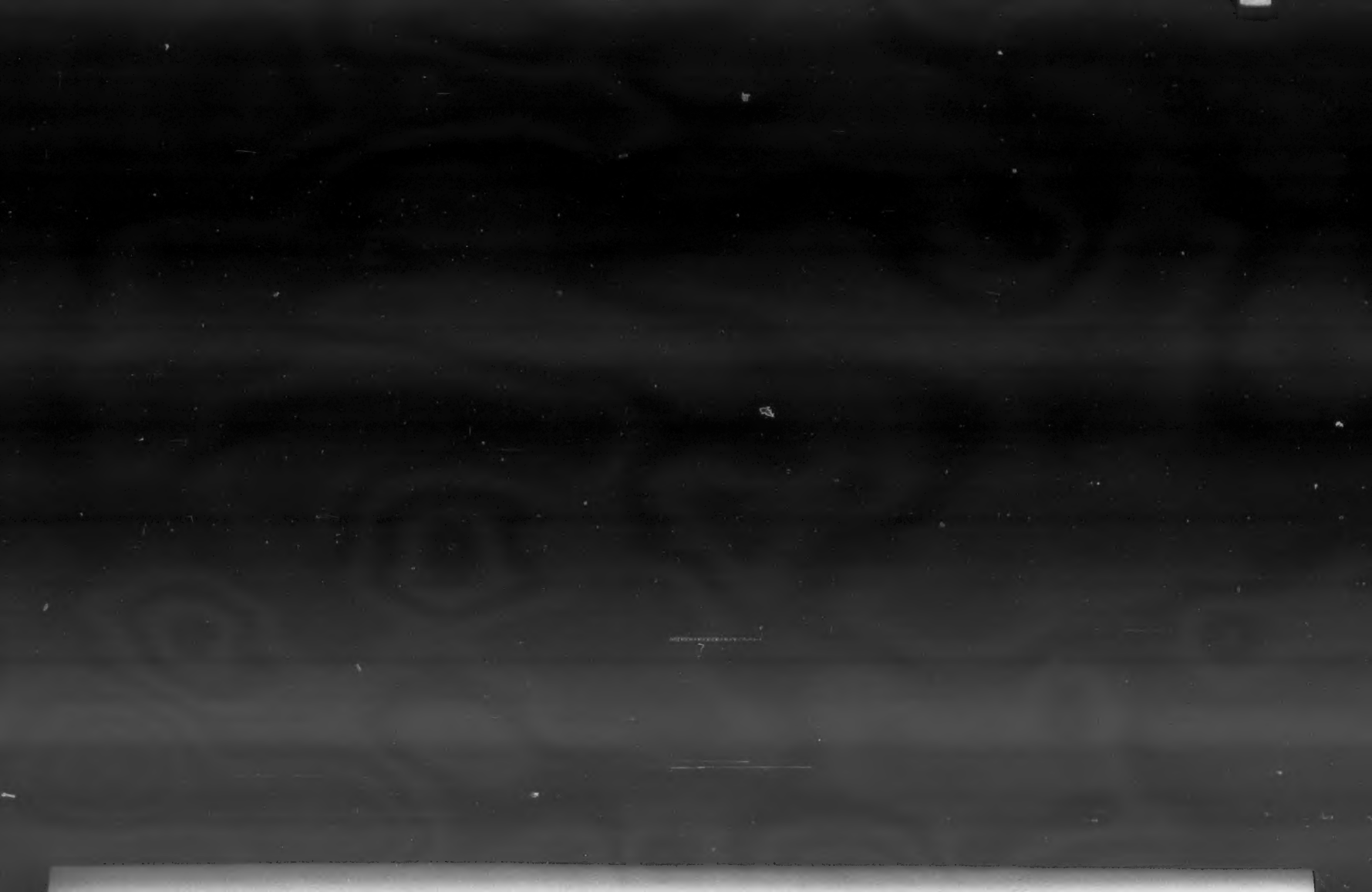

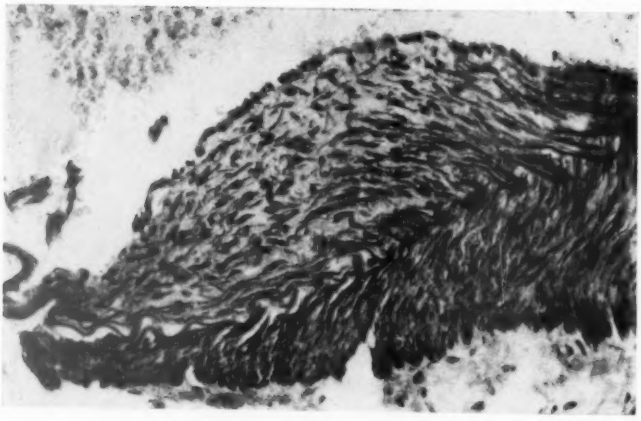

7

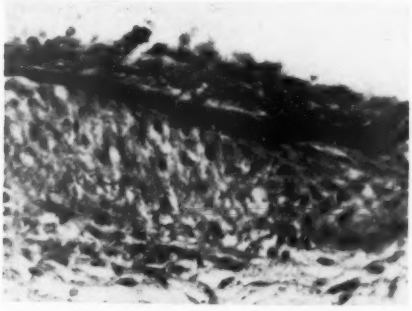

8

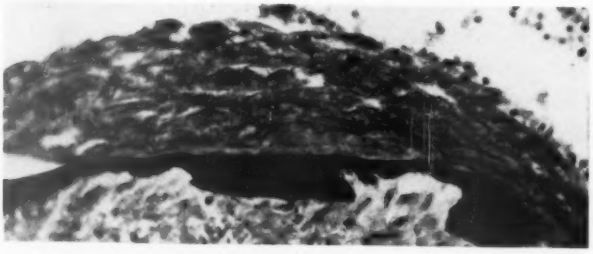

9

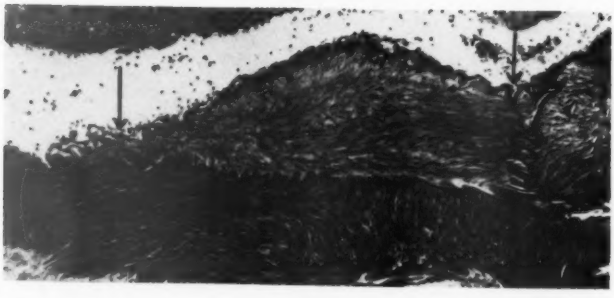

10

FIG. 11. A pale, lacy elastic lamina beneath the endothelium at the edge of a pad. The original elastic lamina is palely stained when seen in tangential section. Formalin pigment appears on the surface of the pad. Verhoeff's stain. × 300.

FIG. 12. Two thick elastic laminas in a facial pad, 6-months-old infant. The subendothelial lamina is beaded, though near the arrow it is palely stained and lacy. The original (deeper) lamina is also degenerated. Verhoeff's stain. × 150.

FIG. 13. The original elastic lamina is palely stained. A newly formed lamina in the middle of the pad is also pale and tends to divide the pad into two strata. Verhoeff's stain. × 75.

FIG. 14. Apparent splitting of the internal elastic lamina in an apical pad. Note the thinness of the original elastic lamina and subendothelial lamina at edges of the pad. Verhoeff's stain. × 300.

FIG. 15. An apical pad with gross degeneration of the internal elastic lamina, remnants of which separate the media from the intima. Verhoeff's stain. × 300.

FIG. 16. An apical pad with two elastic laminas. Note the gap in the deeper lamina and the irregularity of the superficial one. Verhoeff's stain. × 300.

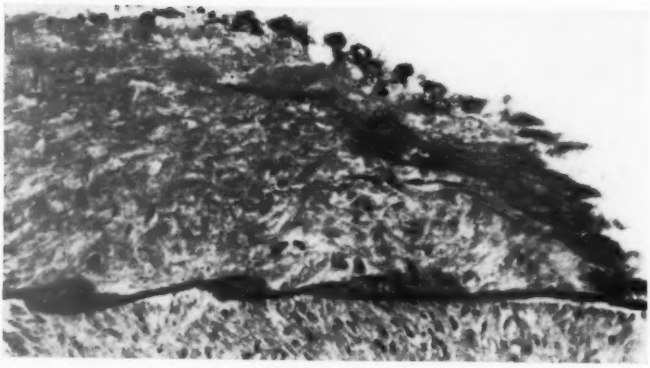

11

12

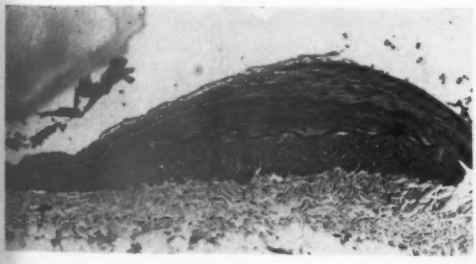

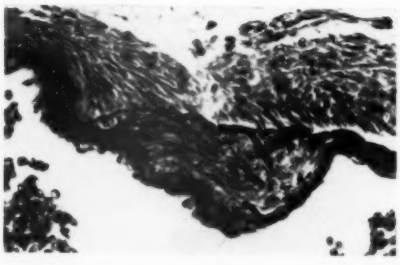

14

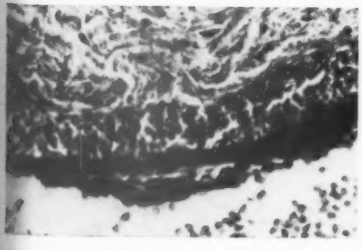

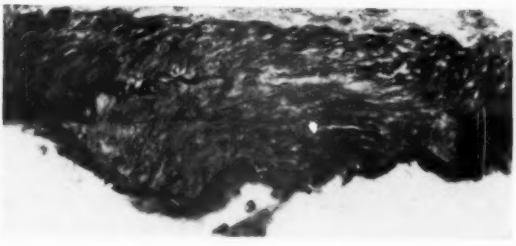

16

PATHOGENESIS OF EXPERIMENTAL NEPHROSIS
ELECTRON MICROSCOPIC OBSERVATIONS

JAMES C. HARKIN, M.D., AND LILLIAN RECANT, M.D.

From the Department of Pathology and the Nutrition Research Laboratory of the Department of Preventive Medicine, Washington University School of Medicine, St. Louis, Mo.

A nephrotic syndrome can be induced in rats by the administration of an aminonucleoside, 6-dimethylamino purine, 3-amino-*d*-ribose. During the early stages of the disorder, no detectable glomerular lesions are seen by light microscopy, although tubular alterations which parallel the progression of proteinuria, hypoalbuminemia, hyperlipemia and edema do occur. The microscopic changes resemble those of pure nephrosis in man.[1,2] Farquhar, Vernier, Good and Brunson[3-6] illustrated glomerular epithelial lesions in the nephrotic syndrome of man by electron microscopy where none were seen by light microscopy. Among the limitations imposed by biopsy in a study of disease are an inability to procure such specimens at the earliest stages of a disorder when clinical manifestations are not yet evident, and an insufficient number of specimens obtained consecutively to provide a sequence illustrating the changing morphologic features of the condition.

We feel that observations on the experimental model of aminonucleoside-induced nephrosis may help elucidate the sequential structural and functional changes in this form of renal injury.

METHODS

Male Sprague-Dawley rats, weighing 120 gm., were caged individually in metabolic units. Water and a diet of Purina Rat Chow were provided *ad libitum*. Eight rats received daily subcutaneous injections of 6-dimethylamino purine, 3-amino-*d*-ribose (supplied by the Lederle Laboratories), 0.3 ml. of a 0.5 per cent solution per 100 gm. of body weight. Tissues from these rats and from 4 untreated control animals were examined by electron microscopy. Experimental animals were sacrificed in pairs after 1, 5, 8, and 14 days of treatment. Twenty other rats received smaller daily doses, 0.3 ml. of a 0.25 per cent solution per 100 gm. of body weight for 60 days. Ten animals served as untreated controls

Supported in part by Grants C-2836 and A-587 from the United States Public Health Service.

Presented in part at the Fifty-fifth Annual Meeting of the American Association of Pathologists and Bacteriologists, Cleveland, Ohio, April 24, 1958.

Received for publication, June 30, 1959.

for this group. One experimental and one control rat from the 60-day group were examined by electron microscopy.

Animals were weighed daily. Daily urine specimens were collected for measurement of protein content. Total and fractional estimations of serum proteins, serum cholesterol, and nonprotein nitrogen were determined by methods previously described [7] from blood collected at the time of decapitation.

Tissue sections from all of the animals were examined by conventional light microscopic techniques. For this purpose, renal tissue was fixed in cobalt-formalin. Paraffin sections were stained with hematoxylin and eosin and by the periodic acid-Schiff (PAS) method. Frozen sections were stained with oil red O for lipid. For electron microscopy, fragments of kidney, 1 to 2 mm. in diameter, were selected from the cortex, corticomedullary junction, and medulla and promptly immersed in Dalton's 1 per cent osmic acid and bichromate solution buffered to pH 7.6. Tissues were fixed for 45 minutes to 1 hour at room temperature.[8] The methods of dehydration and embedding used were those previously described.[9] Polymerization was carried out at 60° C. Thin sections were cut with glass knives on a Servall Porter-Blum microtome, placed on collodion-covered copper grids, and examined, without removing the plastic, in an EMU-3B RCA electron microscope.

Results

Normal Kidney

The ultrastructure of adult mammalian kidney has been defined by a number of investigators.[10–25] In the glomerulus the thin endothelial cytoplasm is interrupted by numerous small spaces or pores. Between the plasma membrane of the endothelial cell and the limiting membrane of the glomerular epithelium lie 3 zones. The central zone is electron dense; although relatively distinct as an entity, this zone or membrane does not possess the distinct sharpness characteristic of plasma membranes or nuclear membranes. The electron-dense membrane varies somewhat in thickness; it has a granular character, and at times its granules are arranged in linear manner, thereby suggesting cross sections of platelike structures. On either side of the electron-dense membrane are zones of low density. The term basement membrane as used in electron microscopy is limited to the electron-dense structure. Each glomerular epithelial cell is plicated over the basement membrane with a number of relatively uniform foot processes. The tip of each foot process is characterized by an area that is granular and electron dense. No cells other than those of the capillary endothelium and the visceral and parietal glomerular epithelium were observed in the glomerulus.

The ultrastructural characteristics of the tubular epithelium have not been the cause of as much controversy as have the features of the glomerulus.[20,26–29] Rhodin has recently summarized the features of the different tubular cells.[29] Common to all of them is a complex infolding of the plasma membrane at the basilar part of the cell. This feature is most striking in the distal convoluted tubule. The proximal convoluted tubular epithelium has numerous projections of the apical part of the plasma membrane; these microvilli correspond to the brush border observed by light microscopy.

Kidney in Aminonucleoside-treated Rats

Appearance of the Kidney Prior to Proteinuria. With the electron microscope, normal glomerular epithelial foot processes were uniform in appearance. Only occasional processes were noted to be large or fused. After 24 hours of treatment with aminonucleoside, large and fused foot processes were seen in much larger numbers (Fig. 1). Four to 6 such abnormal processes were observed surrounding a capillary in cross section, whereas in the control animal enlarged processes of this nature were rarely encountered. Thus it seemed that this glomerular alteration was quantitative, in that the number of large processes was increased; it was not qualitative, in that the processes were similar to those seen occasionally in controls.

By the fifth day of aminonucleoside treatment, prior to proteinuria, glomerular lesions were dramatic as viewed by electron microscopy, in striking contrast to the absence of alterations detectable by conventional microscopy. Progressive merging of fused foot processes into cytoplasmic masses adjacent to the basement membrane constituted the principal change (Fig. 2). Not all foot processes were affected; approximately three fourths remained unfused. The main mass of the glomerular epithelial cytoplasm contained smooth-surfaced profiles outlining foci with approximately the same electron density as the remainder of the cytoplasm (Fig. 3). In some glomerular epithelium there were collections of granular electron-dense material arranged in irregular lines; these were of approximately the same size as mitochondria but did not have outlining membranes. In other epithelial cells there were increased numbers of membrane-lined vacuoles, some of which contained electron-dense structures.

Appearance of the Kidney Following the Development of Proteinuria. Specimens from rats that had received aminonucleoside for 8 days were characterized by rather dramatic electron microscopic changes in the glomeruli and tubules. This was in sharp contrast to the lack of demonstrable alteration in glomeruli and the equivocal lesions in the tubules as observed by conventional microscopy.

More of the glomerular foot processes were fused than at the fifth day stage. A prominent, granular, electron-dense zone was present within the glomerular epithelial cytoplasm, adjacent to the basement membrane, and there were cytoplasmic vacuoles. Within the epithelium, and free in Bowman's space were discrete, electron-dense bodies measuring approximately 1 μ in diameter. There was evidence that these bodies corresponded to PAS-positive granules identified by light microscopy. No alterations in the endothelium or basement membrane of the glomerulus were identified.

Electron-dense bodies, similar to those in the glomerulus, were found in the lumens of the proximal convoluted tubules and also in the cytoplasm of some of the proximal tubular epithelial cells (Fig. 5). These were accompanied by numerous altered and distorted mitochondria in both locations. Cytoplasmic vacuoles were also present in the epithelium of the distal convoluted tubules, but they were smaller and less frequent than those in the proximal segment.

Tubular lesions, as viewed by conventional means, became more prominent with continuing treatment, and during the second month glomerular alterations also became manifest. In the chronic phase of the disease, at 60 days, the glomeruli rather uniformly contained vacuolated epithelium in both the visceral and parietal layers, and there was formation of adhesions and epithelial crescents. It was thought that there was a thickening of the glomerular basement membrane.

Electron microscopy likewise demonstrated more advanced lesions (Figs. 6 to 9). These appeared principally in the visceral and parietal epithelium. In some areas the basement membrane was tortuous and irregular. Although on occasion the electron-dense zone appeared to be thickened, segments with this degree of thickness also were observed, though less frequently, in control animals at sites where the membrane was twisted or turned.

Such focal knobs or thickenings were almost always directed toward the endothelial side (Fig. 6). In one instance (Fig. 8) a subendothelial deposit of granular material, almost certainly lipid, was found between the endothelium and the basement membrane. The glomerular epithelium was practically devoid of foot processes. Dense deposits of electron-dense substance were found beneath the plasma membrane, both on the surface adjacent to the basement membrane and also on the side facing Bowman's space. Large cytoplasmic vacuoles were prominent. In some of the cells, accumulations of material arranged in irregular lamellas suggested the "myelin figures" [30, 31] identified in a variety of other tissues (Fig. 6). Parietal epithelium was also vacuolated, and there were adhesions between the visceral and parietal layers (Fig. 7).

All types of tubular epithelium were altered, even those in the collecting ducts. Occasional epithelial elements were considerably distorted whereas their neighbors were relatively undisturbed (Fig. 9). The tubular lesions described at 8 days of treatment were more severe after 14 days and had attained an advanced stage in the animals which had received aminonucleoside for 60 days.

Discussion

The nephrotic syndrome in man presents challenging questions concerning its cause, the site of injury, and the correlation of structural with physiologic abnormalities. Hence, the investigation of an experimental renal disease which mimics a human disorder provides a rare and important opportunity. In this paper, electron microscopic examination of the renal lesions induced in rats by 6-dimethylamino purine, 3-amino-*d*-ribose have been described. Initially, the aminonucleoside produced a nephrotic syndrome characterized by proteinuria and hyperlipemia. With continuation of treatment, edema and hyperlipemia, having reached a maximum, diminished after 30 days although proteinuria persisted. The disease subsequently became chronic in character, resembling the "dry" phase of chronic glomerulonephritis.[32] This clear-cut sequential division of the syndrome into pre-proteinuric, early post-proteinuric, and chronic phases permitted the definition of the primary lesion in nephrosis by electron microscopy. The experimental observations assume considerable significance in view of the remarkable histologic similarities between aminonucleoside injury and nephrosis in man.[3, 6]

When kidney sections from aminonucleoside-treated rats were examined by light microscopy, no glomerular lesions were identified in the early and reversible stages of injury. At this stage, swelling of tubular epithelium and intracellular lipid deposits in the proximal convoluted tubules were seen. These observations were identical to those described in "pure" or "lipoid" nephrosis in children.[1, 2]

In the advanced stage the light microscopic features of the experimental lesion were strikingly similar to those designated the Ellis type II glomerulonephritis.[33] The experimental lesions were characterized by involvement of all glomeruli, proliferation of glomerular epithelium, apparent thickening of the glomerular basement membrane, proliferation of glomerular parietal epithelium with the formation of crescents, dilatation of cast-filled renal tubules, and the intracytoplasmic deposition of lipid and "hyaline" droplets in the proximal convoluted tubules. A failure to demonstrate hyalinized glomeruli probably indicates that the experimental animals were not observed for a sufficient period of time.

The investigations of Oliver,[34] Davies,[35] and others [36] have suggested

that protein commonly escapes the blood stream at the glomerulus and passes into the lumen of the tubules. This occurs despite a failure to detect any alteration in the glomerulus by light microscopy. Part of the protein is believed to be resorbed in the proximal convoluted tubule where it may be identified as intracellular PAS-positive granules or "hyaline" droplets. These were thought by earlier microscopists to represent degeneration of tubular cells. Apparently cytoplasmic enzymes of the tubular epithelium undergo a form of alteration or "exhaustion" when continually "insulted" by protein and other products.[37] Obviously, that part of the protein in the glomerular filtrate that is not resorbed is lost in the urine.

Examination of the sequential changes in experimental nephrosis by electron microscopy indicates that the glomeruli are altered and leak protein although this is not demonstrable by conventional microscopy. The glomerular epithelial alteration was encountered not only at the time when proteinuria first occurred, but also during the period immediately preceding its development. These observations, along with those of other investigators, serve to redefine the morphologic parallel of the nephrotic syndrome in man and in the experimental animal; the entity is probably now better designated as a primary glomerulopathy.[3-6, 21, 38-46]

In a review of the observations of others and our own, two features are manifest: (1) In both clinical and experimental states in which proteinuria occurs, ultrastructural alteration of the glomerular epithelial cell has been found consistently. (2) Many if not all of the tubular epithelial lesions found in a number of different types of renal damage are similar. The latter appears to be the case by electron microscopy as well as by enzyme studies, at least in some instances,[37] and may well merely reflect accommodation to an abnormal glomerular filtrate.

Glomerular Lesions and Proteinuria

At the present stage of knowledge concerning ultrastructural pathologic alterations, observations are limited and frequently isolated. Proteinuria in the absence of overt renal abnormality occurs in the newborn animal.[47, 48] At birth the glomerular epithelial foot processes are poorly formed, and there is a prominent subendothelial space. We have been unable as yet to correlate a functional change with the prominent subendothelial space, although this space is thought to be the site of deposition of electron-dense material in lupus erythematosus and diabetic glomerulosclerosis in the adult.[3, 49, 50] In the newborn, the basement membrane is not thickened, and we have been unable to identify any discontinuities in it. Kurtz [51] examined the kidney of the human newborn by electron microscopy and also noted an absence of glomerular epithe-

lial foot processes. Since his specimens were obtained at necropsy and there was considerable autolysis, it might seem that delayed fixation had caused alteration of the processes. However, we have allowed pieces of renal tissue to be incubated at 37° C. for a period of one hour before fixation and have examined renal tissues removed at necropsy; the glomerular epithelial foot processes appear to be among the structures most resistant to change.

In pure nephrosis and in familial nephrosis,[3, 5, 43] fusion of the foot processes has been the only glomerular lesion reported. Similarly, in the experimental proteinuria produced by saccharated iron, the glomerular lesion appears to be confined to the epithelium.[52] In these conditions there appears to be a specific correlation of structure and function. In the electron microscopic studies of chronic glomerulonephritis, lupus erythematosus, and diabetic glomerulosclerosis, alterations have been reported in all of the glomerular components; viz., endothelium, basement membrane, and epithelium.

There has not yet been sufficient investigation of nephrotoxic nephritis, serum sickness, and acute glomerulonephritis to permit an appraisal of the various changes; it would appear, however, that these are similar, in that both glomerular endothelium and epithelium are altered, although the degree of change in the two cell types varies in the different diseases.[53–57] On the other hand, it appears that in amyloidosis the primary alteration is characterized by thickening of the basement membranes, not only in the glomeruli but in other sites as well.

Our own investigations[38, 47] and those of others[39, 41, 42, 45, 46, 52, 53] appear to indicate that fusion of glomerular epithelial foot processes and a loss of the spaces between them parallel the development of proteinuria. Conversely, when foot processes emerge from a solid cytoplasmic mass either in the course of normal maturation or during recovery from disease, then proteinuria ceases. Such observations warrant a re-evaluation of the hypothesis that the spaces between the foot processes represent the sites for the passage of the glomerular filtrate. However, assumptions regarding the passage of nonprotein substances into the glomerular filtrate cannot be made on the basis of the present data. It would appear likely that protein is able to pass through the basement membrane and enter the epithelial cytoplasm when the foot processes are fused. The protein then moves or is moved through the epithelium into the glomerular filtrate.

In aminonucleoside nephrosis, when proteinuria existed for 3 days or more, it was possible to demonstrate round or oval electron-dense structures within the cytoplasm of the glomerular epithelium (Fig. 4). By a comparison with sections examined by light microscopy, it appeared that these structures corresponded to PAS-positive droplets. Similar

structures were identified in some of the partly formed glomeruli of the newborn mouse with proteinuria and also in rats (Fig. 10) with elevated serum albumin and proteinuria for several days following the intraperitoneal injection of dilute bovine albumin.[59]

In aminonucleoside nephrosis, intracytoplasmic, electron-dense structures that appeared to correlate with PAS-positive droplets also were found, after the onset of proteinuria, in the proximal segment of the convoluted tubule. Such structures could not be distinguished by electron microscopy from similar bodies seen in proximal convoluted tubules of rats with proteinuria associated with rabbit anti-rat kidney serum nephritis (Fig. 11).[60]

Tubular Structural Alterations

The electron microscopic observations of renal tubular damage have been fewer than those of glomerular changes. Since the tubules of the newborn are not completely developed, they constitute a special case. Thus it is not surprising that their appearance differs somewhat from that found in experimental nephrosis, although in both situations proteinuria occurs.[61] The tubular injury induced by sucrose is also unlike that caused by aminonucleoside.[62] In preliminary observations in the nephrotoxic nephritis of rats, we observed electron-dense bodies, swollen mitochondria and distorted proximal convoluted tubular epithelium not unlike the lesion seen in the aminonucleoside nephrosis.[63] Fisher and Gruhn[37] compared the tubular lesions in the latter with nephrotoxic nephritis by histochemical methods and concluded that the tubular lesion was similar in the two conditions and that it seemed to increase in severity with progression of proteinuria.

Although we have not yet excluded the possibility of direct injury to the tubules in either aminonucleoside nephrosis or in nephrotoxic nephritis, we believe that the tubular damage is probably secondary to the abnormal glomerular filtrate. The chronologic sequence of the alterations following aminonucleoside injury tends to support this concept; i.e., first, glomerular epithelial cell injury; second, proteinuria; third, prompt evolution of the tubular lesion.

The exact site of action of aminonucleoside within the glomerular epithelium is still unknown. Since some of the abnormal organelles in these cells are similar in size and configuration to mitochondria but lack outlining membranes, it is suggested that an enzyme associated with these mitochondria might be the site of action of the drug.

Summary

Sequential electron microscopic observations of the kidneys were made in rats with the nephrotic syndrome induced by injections of an

aminonucleoside, 6-dimethylamino purine, 3-amino-*d*-ribose. The initial lesion, which developed prior to the occurrence of proteinuria, was characterized by alterations in glomerular epithelium, with fusion of foot processes, cytoplasmic vacuolation, and accumulations of granular electron-dense material. The latter was thought possibly to represent degenerating mitochondria.

At 8 days, shortly after the onset of proteinuria, glomerular lesions were more advanced although glomerular alterations were not demonstrable by conventional microscopy at this stage. With continuing proteinuria, the tubular epithelium, especially in the proximal segment, exhibited cytoplasmic vacuolation, swelling of mitochondria, and the appearance of electron-dense bodies. In the chronic stage of nephrosis, the lesions were more advanced in both the glomerular and tubular epithelium. In contrast, only minor abnormalities of the glomerular endothelium and basement membrane developed.

From the evidence it was tentatively concluded that the ultrastructural parallel of proteinuria appeared to be fusion of glomerular epithelial foot processes. Many of the tubular lesions encountered in the nephrotic syndrome were thought to be secondary to resorption of an abnormal glomerular filtrate. The term "primary glomerulopathy" was proposed to characterize the nephrotic syndrome.

References

1. Allen, A. C. The clinicopathologic meaning of the nephrotic syndrome. *Am. J. Med.*, 1955, **18**, 277–314.
2. Bell, E. T. Renal Diseases. Lea & Febiger, Philadelphia, 1950, ed. 2, 448 pp.
3. Farquhar, M. G.; Vernier, R. L., and Good, R. A. An electron microscope study of the glomerulus in nephrosis, glomerulonephritis, and lupus erythematosus. *J. Exper. Med.*, 1957, **106**, 649–660.
4. Farquhar, M. G.; Vernier, R. L., and Good, R. A. The application of electron microscopy in pathology; study of renal biopsy tissues. *Schweiz. med. Wchnschr.*, 1957, **87**, 501–510.
5. Farquhar, M. G.; Vernier, R. L., and Good, R. A. Studies of familial nephrosis. II. Glomerular changes observed with the electron microscope. *Am. J. Path.*, 1957, **33**, 791–817.
6. Vernier, R. L.; Farquhar, M. G.; Brunson, J. G., and Good, R. A. Chronic renal disease in children—the renal lesion by light and electron microscopy. (Abstract) *J. Lab. & Clin. Med.*, 1956, **48**, 951–952.
7. Fiegelson, E. B.; Drake, J. W., and Recant, L. Experimental aminonucleoside nephrosis in rats. *J. Lab. & Clin. Med.*, 1957, **50**, 437–446.
8. Dalton, A. J. A chrome-osmium fixative for electron microscopy. (Abstract) *Anat. Rec.*, 1955, **121**, 281.
9. Harkin, J. C. An electron microscopic study of the castration changes in the rat prostate. *Endocrinology*, 1957, **60**, 185–199.
10. Bergstrand, A. Electron microscopic investigations of the renal glomeruli. *Lab. Invest.*, 1957, **6**, 191–204.

11. HALL, B. V. Studies of Normal Glomerular Structure by Electron Microscopy. Proceedings, Fifth Annual Conference on the Nephrotic Syndrome, Philadelphia, November 5–7, 1953. National Nephrosis Foundation, 1954, pp. 1–39.

12. HALL, B. V. Further Studies of the Normal Structure of the Renal Glomerulus. Proceedings, Sixth Annual Conference on the Nephrotic Syndrome, Cleveland, November 5–6, 1954. National Nephrosis Foundation, Inc., 1955, pp. 1–39.

13. MUELLER, C. B.; MASON, A. D., JR., and STOUT, D. G. Anatomy of the glomerulus. *Am. J. Med.*, 1955, **18**, 267–276.

14. OBERLING, C.; GAUTIER, A., and BERNHARD, W. La structure des capillaires glomérulaires vue au microscope électronique. *Presse méd.*, 1951, **59**, 938–940.

15. PAK POY, R. K. F. Electron microscopy of the marsupial renal glomerulus. *Australian J. Exper. Biol. & M. Sc.*, 1957, **35**, 437–447.

16. PEASE, D. C. Fine structures of the kidney seen by electron microscopy. *J. Histochem.*, 1955, **3**, 295–308.

17. POLICARD, A.; COLLET, A., and GILTAIRE-RALYTE, L. Recherches au microscope électronique sur la structure du glomérule rénal des mammifères. *Arch. anat. micr. Paris*, 1955, **44**, 1–19.

18. REID, R. T. W. Observations on the structure of the renal glomerulus of the mouse revealed by the electron microscope. *Australian J. Exper. Biol. & M. Sc.*, 1954, **32**, 235–239.

19. RHODIN, J. Electron microscopy of the glomerular capillary wall. *Exper. Cell Res.*, 1955, **8**, 572–574.

20. RHODIN, J. Electron microscopy of the kidney. *Am. J. Med.*, 1958, **24**, 661–675.

21. RINEHART, J. F.; FARQUHAR, M. G.; JUNG, H. C., and ABUL-HAJ, S. K. The normal glomerulus and its basic reactions in disease. *Am. J. Path.*, 1953, **29**, 21–31.

22. RINEHART, J. F. Fine structure of renal glomerulus as revealed by electron microscopy. *A.M.A. Arch. Path.*, 1955, **59**, 439–448.

23. HARTROFT, P. M. A preliminary study of the electron microscopy of renal juxtaglomerular cells; correlation with light microscopy. (Abstract) *Anat. Rec.*, 1956, **124**, 458.

24. VAN BREEMEN, V. L.; REGER, J. F., and COOPER, W. G. Observations on the basement membranes in rat kidney. *J. Biophys. & Biochem. Cytol.*, 1956, **2**, Suppl. to No. 4, 283–286.

25. YAMADA, E. The fine structure of the renal glomerulus of the mouse. *J. Biophys. & Biochem. Cytol.*, 1955, **1**, 551–566.

26. DALTON, A. J. Structural details of some of the epithelial cell types in the kidney of the mouse as revealed by the electron microscope. *J. Nat. Cancer Inst.*, 1951, **11**, 1163–1185.

27. RUSKA, H.; MOORE, D. H., and WEINSTOCK, J. The base of the proximal convoluted tubule cells of rat kidney. *J. Biophys. & Biochem. Cytol.*, 1957, **3**, 249–254.

28. SJÖSTRAND, F. S., and RHODIN, J. The ultrastructure of the proximal convoluted tubules of the mouse kidney as revealed by high resolution electron microscopy. *Exper. Cell Res.*, 1953, **4**, 426–456.

29. RHODIN, J. Anatomy of Kidney Tubules. In: International Review of Cytology. Bourne, G. E., and Danielli, J. F. (eds.). Academic Press, New York, 1958, **7**, pp. 485–534.

30. REVEL, J. P.; ITO, S., and FAWCETT, D. W. Electron micrographs of myelin figures of phospholipide simulating intracellular membranes. *J. Biophys. & Biochem. Cytol.*, 1958, **4**, 495–498.

31. STOECKENIUS, W. An electron microscope study of myelin figures. *J. Biophys. & Biochem. Cytol.*, 1959, **5**, 491–500.

32. RECANT, L.; BOROWSKY, B. A., and KESSNER, D. M. Aminonucleoside glomerulonephritis: morphologic and metabolic studies. (Abstract) *J. Clin. Invest.*, 1958, **37**, 924.

33. ELLIS, A. Natural history of Bright's disease; clinical, histological and experimental observations. *Lancet*, 1942, **1**, 1–7; 34–36; and 72–76.

34. OLIVER, J., and MACDOWELL, M. Cellular mechanisms of protein metabolism in the nephron. VII. The characteristics and significance of the protein absorption droplets (hyaline droplets) in epidemic hemorrhagic fever and other renal diseases. *J. Exper. Med.*, 1958, **107**, 731–754.

35. DAVIES, J. Cytological evidence of protein absorption in fetal and adult mammalian kidneys. *Am. J. Anat.*, 1954, **94**, 45–71.

36. SELLERS, A. L.; GRIGGS, N.; MARMORTSON, J., and GOODMAN, H. C. Filtration and reabsorption of protein by the kidney. *J. Exper. Med.*, 1954, **100**, 1–10.

37. FISHER, E. R., and GRUHN, J. Aminonucleoside nephrosis in rats. *A.M.A. Arch. Path.*, 1958, **65**, 545–553.

38. HARKIN, J. C., and RECANT, L. The earliest lesion in aminonucleoside nephrosis; an electron microscopic study. (Abstract) *Am. J. Path.*, 1958, **34**, 559.

39. PIEL, C. F.; DONG, L.; WARDLOW, N.; MARTNER, G., and GOODMAN, J. Experimental renal disease as observed by electron microscopy. (Abstract) *Fed. Proc.*, 1958, **17**, 453.

40. PIEL, C. F.; DONG, L.; MODERN, F. W. S.; GOODMAN, J. R., and MOORE, R. The glomerulus in experimental renal disease in rats as observed by light and electron microscopy. *J. Exper. Med.*, 1955, **102**, 573–580.

41. VERNIER, R. L.; PAPERMASTER, B. W., and GOOD, R. A. Light and electron microscopic pathology of experimental aminonucleoside nephrosis; relation to nephrosis in man. (Abstract) *Fed. Proc.*, 1958, **17**, 463.

42. VERNIER, R. L.; PAPERMASTER, B. W., and GOOD, R. A. Aminonucleoside nephrosis. I. Electron microscopic study of the renal lesion in rats. *J. Exper. Med.*, 1959, **109**, 115–126.

43. VERNIER, R. L.; FARQUHAR, M. G.; BRUNSON, J. G., and GOOD, R. A. Chronic renal disease in children. Correlation of clinical findings with morphologic characteristics seen by electron microscopy. *A.M.A. Am. J. Dis. Child.*, 1958, **96**, 306–343.

44. SPIRO, D. The structural basis of proteinuria in man; electron microscopic studies of renal biopsy specimens from patients with lipid nephrosis, amyloidosis, and subacute and chronic glomerulonephritis. *Am. J. Path.*, 1959, **35**, 47–73.

45. FELDMAN, J. D., and FISHER, E. R. Renal lesions of aminonucleoside nephrosis as revealed by electron microscopy. *Lab. Invest.*, 1959, **8**, 371–385.

46. FOLLI, G.; POLLAK, V. E.; REID, R. T. W.; PIRANI, C. L., and KARK, R. M. Electronmicroscopic studies of reversible glomerular lesions in the adult nephrotic syndrome. *Ann. Int. Med.*, 1958, **49**, 775–795.

47. HARKIN, J. C. Electron microscopy of developing renal glomerular basement membranes of the newborn mouse. (Abstract) *Anat. Rec.*, 1959, **133**, 285.

48. HARKIN, J. C., and LADDA, R. S. Ultrastructural studies of glomerular differentiation in the newborn mouse. (In preparation.)

49. BERGSTRAND, A., and BUCHT, H. The glomerular lesions of diabetes mellitus and their electron-microscope appearances. *J. Path. & Bact.*, 1959, **77**, 231–242.

50. BERGSTRAND, A., and BUCHT, H. Electron microscopic investigations on the glomerular lesions in diabetes mellitus (diabetic glomerulosclerosis). *Lab. Invest.*, 1957, **6**, 293–300.

51. KURTZ, S. M. The electron microscopy of the developing human renal glomerulus. *Exper. Cell Res.*, 1958, **14**, 355–367.

52. ELLIS, J. T. Glomerular lesions in rabbits with experimentally induced proteinuria as disclosed by electron microscopy. (Abstract) *Am. J. Path.*, 1958, **34**, 559–560.

53. REID, R. T. W. Electron microscopy of glomeruli in nephrotoxic serum nephritis. *Australian J. Exper. Biol. & M. Sc.*, 1956, **34**, 143–150.

54. SAKAGUCHI, H.; SUZUKI, Y., and YAMAGUCHI, T. Electron microscopic study of Masugi nephritis. I. Glomerular changes. *Acta path. Japan*, 1957, **7**, 53–66.

55. SIMER, P. H. Electron microscopic studies of the glomerulus in nephritic mice of NH strain. (Abstract) *Anat. Rec.*, 1954, **118**, 409.

56. SIMER, P. H. Electron microscopic study of the glomerulus, especially its basement membrane in normal and nephritic rats. (Abstract) *Anat. Rec.*, 1955, **121**, 416.

57. FELDMAN, J. D. Electron microscopy of serum sickness nephritis. *J. Exper. Med.*, 1958, **108**, 957–962.

58. GEER, J. C.; STRONG, J. P.; MCGILL, H. C., JR., and MUSLOW, I. Electron microscopic observations on the localization of amyloid in the kidney in secondary amyloidosis. *Lab. Invest.*, 1958, **7**, 554–565.

59. BAXTER, J. H., and COTZIAS, C. G. Effects of proteinuria on the kidney. Proteinuria, renal enlargement, and renal injury consequent on protracted parenteral administration of protein solutions in rats. *J. Exper. Med.*, 1949, **89**, 643–668.

60. SMADEL, J. E., and SWIFT, H. F. Experimental nephritis in rats induced by injection of antikidney serum. V. Chronic nephritis of insidious development following apparent recovery from acute nephrotoxic nephritis. *J. Exper. Med.*, 1941, **74**, 345–358.

61. CLARK, S. L., JR. Cellular differentiation in the kidneys of newborn mice. Studies with the electron microscope. *J. Biophys. & Biochem. Cytol.*, 1957, **3**, 349–362.

62. ROUILLER, C., and MODJTABAI, A. La néphrose expérimentale du lapin. Comparaison entre la microscopie optique et électronique. I. Les modifications des cellules à bordure striée. *Ann. d'anat. path.*, 1958, **3**, 223–250.

63. HARKIN, J. C.; KESSNER, D. M., and RECANT, L. Correlated electron microscopic and laboratory findings in the development of nephrotoxic nephritis. (In preparation.)

[*Illustrations follow*]

Legends for Figures

FIG. 1. Electron micrograph of a rat glomerulus after one day of treatment with aminonucleoside. This resembles the glomerulus of the untreated rat. Although the majority of the epithelial foot processes are uniform in appearance, the 3 in the center of the illustration are slightly enlarged. After 24 hours of treatment, the number of enlarged foot processes is greater than in control animals. The glomerular epithelial nucleus is in the lower right corner. Approximately × 20,000.

FIG. 2. A rat glomerulus 5 days after the inception of daily treatment with aminonucleoside. The orientation of the structures is as in Figure 1. Several enlarged foot processes are seen. Within the glomerular epithelial cytoplasm are several mitochondria, measuring 0.5 to 1 cm. in diameter in the reproduction. In at least one of these an outlining membrane cannot be defined. × 25,000.

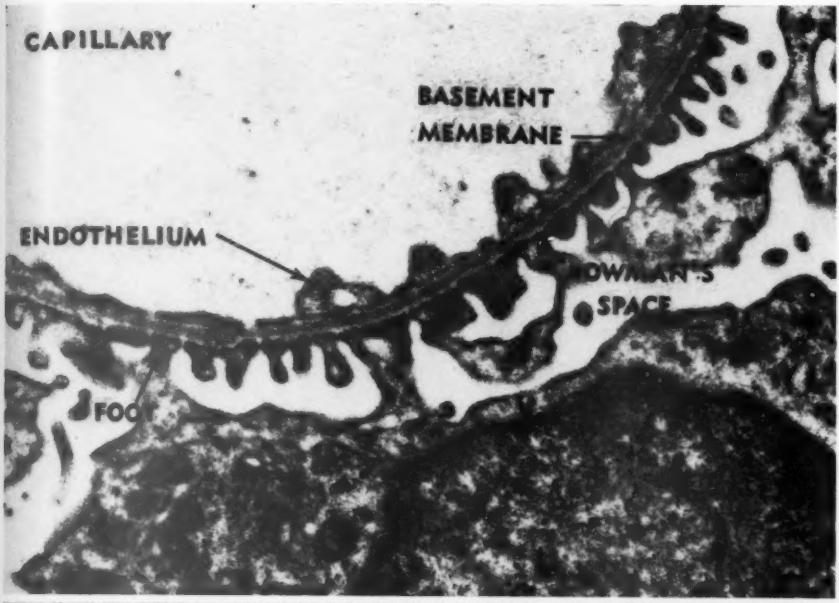
CAPILLARY
BASEMENT MEMBRANE
ENDOTHELIUM
SPACE
FOO

1

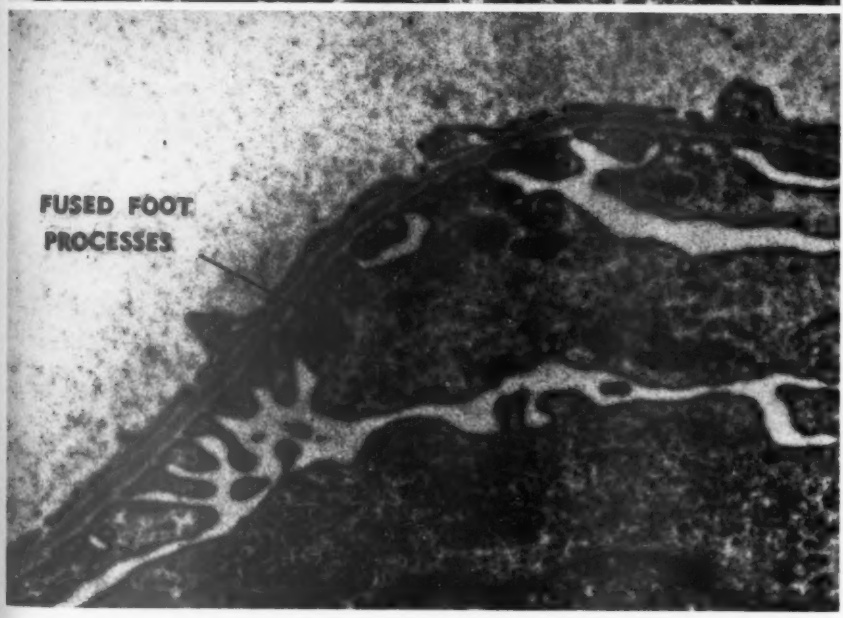
FUSED FOOT PROCESSES

2

FIG. 3. A portion of a rat glomerulus; treatment with aminonucleoside for 5 days. Two smooth-surfaced profiles lie adjacent to each other within the epithelial cytoplasm. The electron-dense material is manifest at the tips of the foot processes, both those of normal appearance and those that are fused. × 20,000.

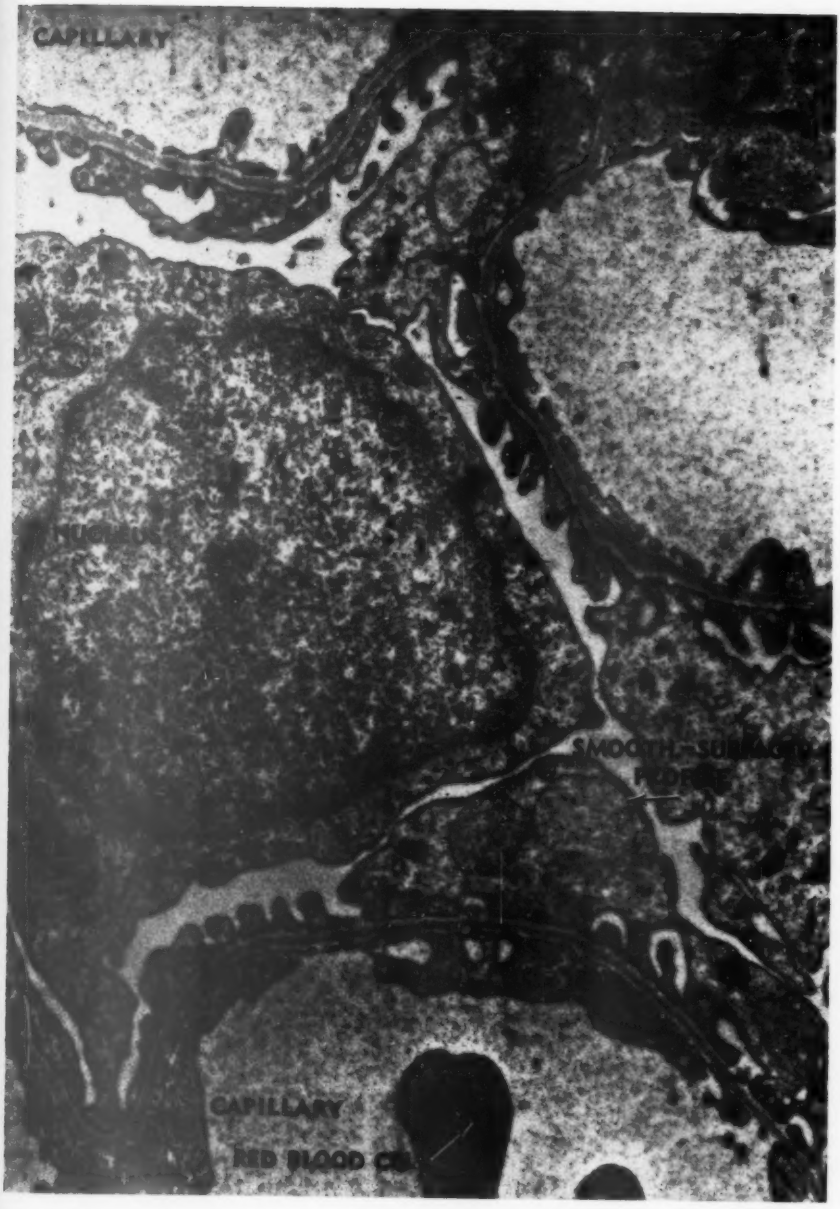

3

FIG. 4. Rat glomerulus; animal treated with aminonucleoside for 8 days. Proteinuria had been present for one day. No foot processes are present in this particular illustration. There is, however, a continuous mass of epithelial cytoplasm abutting against the basement membrane. Several electron-dense structures are shown. It was thought that these corresponded to PAS-positive granules identified by light microscopy. × 20,000.

FIG. 5. A cross section of the proximal convoluted tubule in a rat treated with aminonucleoside for 8 days. One of the electron-dense structures is labeled. These granules are thought to correspond to the PAS-positive granules identified by light microscopy. Mitochondria differ in size and structure from these granules. However, an internal lamellar structure can be seen in some of them. Many irregular bodies are present in the lumen. Some of these are thought to be altered mitochondria. × 9,000.

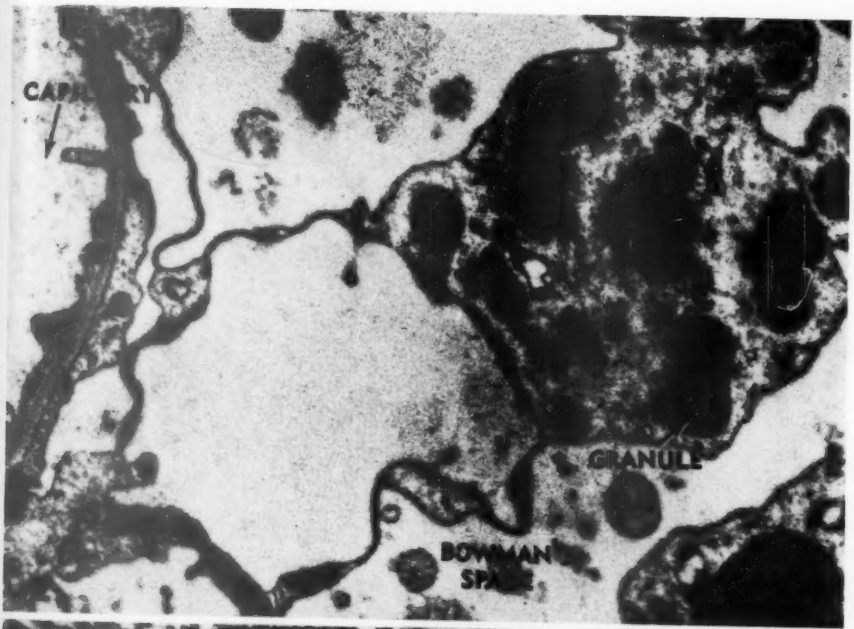

4

5

FIG. 6. Portion of a rat glomerulus; daily injections of aminonucleoside for 60 days. In many areas the endothelium and basement membrane appear unaltered. The epithelium is vacuolated, and few mitochondria are identified. A slight distortion of the basement membrane is labeled "knob." An irregular lamellar structure similar to some types of "myelin figures" is labeled "figure." × 12,000.

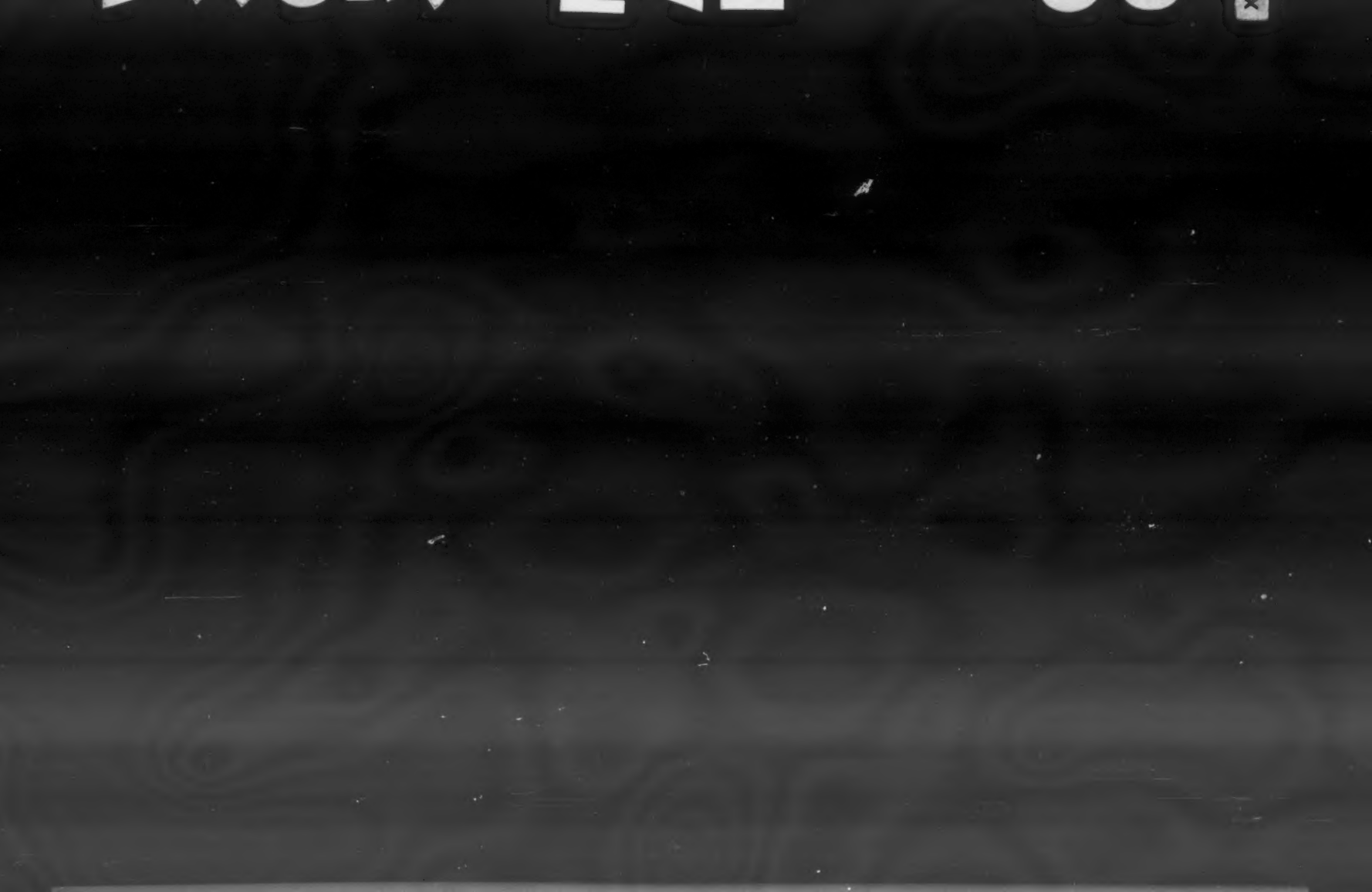

6

FIG. 7. Portion of the rat glomerulus and adjacent tubular epithelium; treated with aminonucleoside 60 days. Below a nucleus of the parietal glomerular epithelium is a laminated basement membrane that surrounds the glomerulus. At the bottom of the illustration is part of the tubular epithelial cell. Both the parietal and the adjacent visceral epithelium above it are vacuolated. By light microscopy the glomerulus was the seat of cellular proliferation, adhesions, and crescent formation. × 18,000.

FIG. 8. Portion of the wall of a glomerular capillary; rat treated 60 days with aminonucleoside. At the left the epithelial cell has no discrete foot processes. The basement membrane does not appear thickened. An endothelial cell projects into the capillary lumen and overlies numerous electron-dense structures, probably lipid. These lie in the zone between the electron-dense basement membrane and the plasma membrane of the endothelial cell. × 18,000.

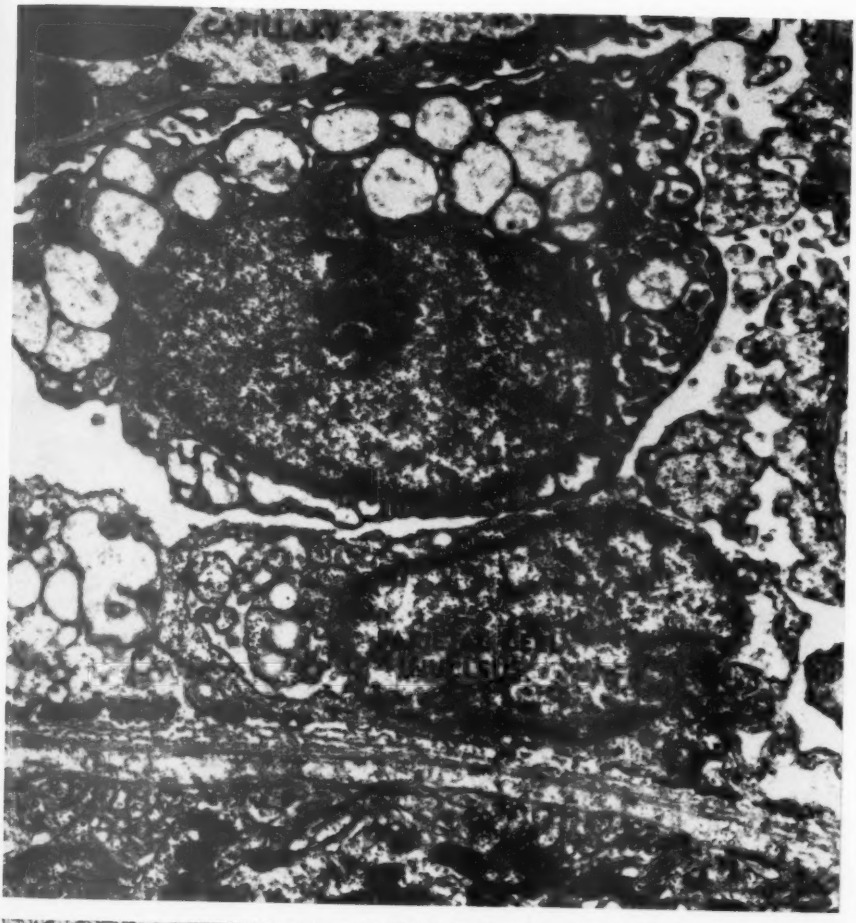

7

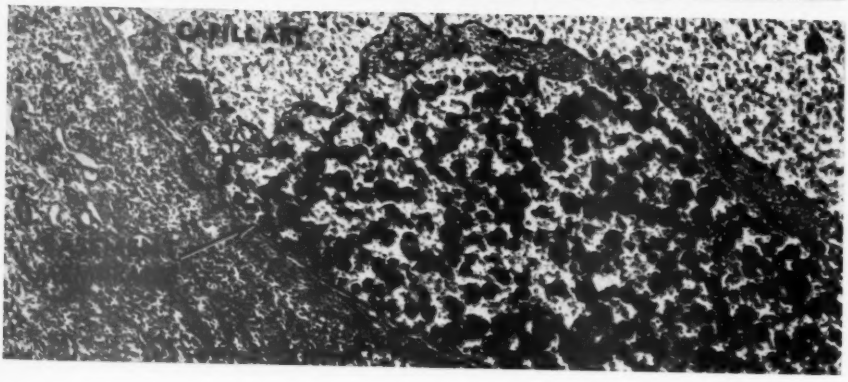

8

FIG. 9. Two cells in the proximal convoluted tubule of a rat treated 60 days with aminonucleoside. The microvilli, Palade's granules of the endoplasmic reticulum, and mitochondria in the cell to the left are more like those of control animals than are the distorted structures of the cell to the right and top of the photograph. A cytoplasmic lipid inclusion is labeled. × 12,000.

9

FIG. 10. Portion of a glomerulus in a rat with proteinuria; animal had received daily intraperitoneal injections of dilute bovine albumin. Some of the foot processes are apparently fused. Note particularly the electron-dense granules within the epithelial cytoplasm. Approximately × 14,000.

FIG. 11. Portion of a proximal convoluted tubular cell; rat with nephritis and proteinuria induced by injections of rabbit anti-rat-kidney serum. Within the cytoplasm are electron-dense structures that are not recognizable as mitochondria. These appear to correspond to PAS-positive droplets seen by light microscopy. Note the similarity between this illustration and Figure 5. Approximately × 18,000.

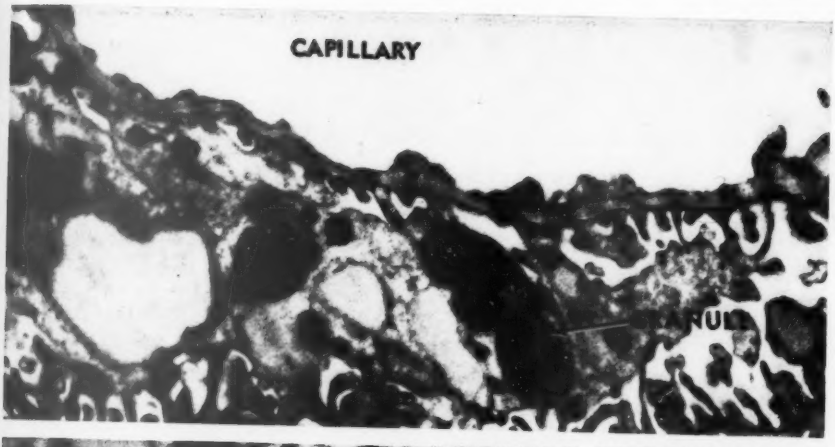

10

11

A COMPARATIVE CYTOCHEMICAL AND CYTOLOGIC STUDY OF VITAMIN D INDUCED NEPHROCALCINOSIS

DANTE G. SCARPELLI, M.D.; GILLES TREMBLAY, M.D.,* AND A. G. EVERSON PEARSE, M.D.

From the Departments of Pathology, The Ohio State University, Columbus, Ohio, and the Postgraduate Medical School of London, England

The renal lesions produced by hypervitaminosis D were first described simultaneously by Kreitmair and Moll[1] and Pfannenstiel[2] in 1928. Since then these lesions have been studied both experimentally and clinically by numerous investigators.[3-9] However, little is known about their pathogenesis. In fact, such basic questions as whether cell damage precedes the deposition of calcium or is caused by it remain unanswered at present. The results of this investigation show that the intracellular deposition of calcium is preceded by cell damage, as evidenced by cytochemical and cytologic alterations.

MATERIAL AND METHODS

Fifty-four male albino rats, weighing between 160 and 190 gm., were divided into 3 groups of 18 animals each. In each group 9 animals were given 50,000 units each of vitamin D_2 (Radiostol, British Drug Houses, Ltd.) daily by stomach tube. The remaining rats served as controls. An experimental and a control animal were sacrificed each day for 9 days. Groups 1 and 2 were used for cytochemical and cytologic investigations. The animals of group 3 were used in a second experiment to determine the morphologic stability of kidney mitochondria and the concentrations of calcium and citric acid in this tissue.

Cytochemical and Tinctorial Techniques

The kidneys were removed as rapidly as possible after death, mounted on metal chucks, and frozen within 20 seconds by dipping the base of the chuck in an acetone-solid CO_2 mixture. Fresh frozen sections of kidney were cut at 4 and 8 μ in a cryostat and mounted on cover slips. To demonstrate sites of diphosphopyridine nucleotide (DPN) diaphorase, triphosphopyridine nucleotide (TPN) diaphorase, isocitric dehydrogenase, alkaline phosphatase, and A type and B type indoxyl esterase

This investigation was supported by a Senior Research Fellowship (SF-104) from the United States Public Health Service.

Received for publication, July 6, 1959.

* Fellow of the Canadian Cancer Society.

activities, the following methods were employed: DPN diaphorase and TPN diaphorase by chelation of cobalt by the formazan of 3,5-diphenyl-2-(4,5 dimethyl-thiazol-2-yl) tetrazolium bromide with reduced DPN and TPN as substrates,[10] isocitric dehydrogenase by using Nitro-BT [2,2′-di-p-nitrophenyl-5,5′-diphenyl-3,3′-(3,3′-dimethoxy-4,4′-biphenylene)-ditetrazolium chloride] [11] with DL isocitric acid lactone as substrate and oxidized DPN as coenzyme [12] (these reactions were carried out in media containing 7.5 per cent polyvinylpyrrolidone to preserve mitochondrial structure [13]); alkaline phosphatase by the azo dye method described by Grogg and Pearse [14] with the diazotate of 4-benzoyl amino-2:5-dimethyoxyaniline as the coupling salt, and indoxyl esterase by using o-acetyl-5-bromoindoxyl as substrate, according to the method of Holt and Withers.[15] Diethyl-p-nitrophenyl phosphate (E-600) was used to inhibit carboxylic acid B type esterases.[16] Incubation at pH 5.0 in the presence of E-600 showed sites of A type cathepsinlike esterase activity.[17] To demonstrate the presence of neutral fat, duplicate sections were stained with oil red O. In addition, serial sections were fixed in Helly's fluid and stained with Heidenhain's iron hematoxylin for the demonstration of mitochondria. Duplicate paraffin sections were stained with hematoxylin and eosin in the conventional manner, the Hotchkiss periodic acid-Schiff (PAS) reaction for 1,2 glycol groups, using diastase and saliva controls, and the Millon and Sakaguchi reactions for tyrosine and arginine-containing proteins.[18]

Biochemical Techniques

Alterations of mitochondrial structure were determined by the light-scattering technique of Cleland [19] and Raaflaub.[20] The kidney was stripped of its capsule, placed on ice and the corticomedullary area dissected free under a dissecting microscope. The tissue from these areas was diced and forced through a precooled perforated plate with 1 mm. holes. This was homogenized in a Potter-Elvehjem homogenizer in 0.44 M sucrose containing 0.01 M disodium ethylenediamine tetraacetate (EDTA).[21] The resulting brei was centrifuged at 900 × g. The supernatant was then centrifuged at 7,000 × g, and the resulting mitochondrial pellet suspended in 0.3 M sucrose buffered at pH 7.3 with tris (hydroxymethyl) amino-methane (tris). Changes in optical density at 520 mμ were determined in a Beckman DU spectrophotometer at 10-minute intervals at 20° C. The serum and kidney tissue concentration of calcium was determined with a Beckman flame photometer according to the method described by Ballentine and Burford.[22] The citric acid concentration was determined colorimetrically by the method of Natelson, Pincus and Lugovoy.[23]

Results

Results Obtained by Cytochemical and Tinctorial Methods

DPN Diaphorase, TPN Diaphorase, and Isocitric Dehydrogenase. Sites of DPN diaphorase, TPN diaphorase and isocitric dehydrogenase activity in the epithelium of the proximal convoluted tubules of control rats were localized as fine cytoplasmic deposits of blue-black formazan (Fig. 1). Under oil immersion these were resolved as a series of discrete 0.2 to 0.35 μ cobalt-formazan deposits distributed in rod-shaped mitochondria. Forty-eight hours after the administration of vitamin D, there was a decrease in the number of rod-shaped mitochondria (Fig. 2). In addition, the rate and intensity of the reaction were increased. The formazan deposits measured 0.3 to 0.6 μ, and some were localized at the periphery of swollen globose mitochondria which measured 2 to 5 μ in diameter (Fig. 3). On the third day the number of swollen mitochondria was increased. On the fourth and fifth days the intensity of the reaction was decreased markedly, and rod-shaped mitochondria were absent (Fig. 4). This was most pronounced in the case of isocitric dehydrogenase. From the sixth through the ninth days the reaction was weak and diffuse, and fine intracellular localization of enzyme activity was no longer possible.

Alkaline Phosphatase. Strong activity was observed in the proximal and distal segments of the proximal convoluted tubules (Fig. 5). The reaction was strongest in the brush border, with a weaker, diffuse reaction in the remaining cytoplasm. No activity was seen in the tubules located in the medulla. After 5 days of vitamin D administration, a weaker reaction was noted. On the seventh day a very weak to negative reaction was observed around calcium deposits (Fig. 6). After 9 days of treatment, enzyme activity remained essentially unchanged, although the epithelium of dilated tubules frequently exhibited little or no activity. In no instance was a high alkaline phosphatase activity observed around calcific deposits.

Indoxyl Esterase. Nonspecific esterase activity was strongest in the proximal convoluted tubules (Fig. 7). The descending and ascending limbs of Henle's loop exhibited a weak activity, while the papilla contained only an occasional focus of weak activity. The enzyme was distributed diffusely throughout the tubular epithelial cytoplasm. On the fifth day of vitamin D administration, an increase in enzyme activity was seen in the proximal convoluted tubules and in the descending and ascending limbs. An occasional tubule exhibited an intense reaction which was localized both in the lining epithelium and in desquamated cells (Fig. 8). In many instances, intensely active amorphous material

corresponding to calcific casts was seen in the lumens of collecting ducts. Enzyme activity in the flattened epithelium lining dilated tubules was markedly decreased.

Treatment of renal sections with E-600 caused a striking inhibition of indoxyl esterase activity both in normal animals and in those receiving vitamin D. The proximal convoluted and distal tubules, the collecting ducts, and interstitial stromal cells of the cortex exhibited sites of resistant esterase activity. Following vitamin treatment, the activity of all these elements was increased. Desquamated cells showed the most intense E-600-resistant, cathepsinlike esterase activity.

Oil Red O. Neutral fat was demonstrable only in the renal papillas in normal rats. In one instance, positively stained droplets were observed in focal areas in the inner and middle zones of the cortex. Subsequent histologic examination showed these to represent sites of pyelonephritis. After 2 to 3 days of vitamin administration, oil red O-positive droplets, 2 to 5 μ in diameter, were observed in the proximal convoluted tubules; the formazan deposits were located at the periphery of the droplets (Fig. 9). From the fourth through the ninth days these droplets increased in size, often measuring 5 to 11 μ, and were found in larger numbers in most of the tubules.

Mitochondrial Staining. Mitochondria in the renal tubules of normal controls appeared as rodlets of varying lengths. They were most often oriented at right angles to the lumens (Fig. 10). Forty-eight to 96 hours after vitamin D administration, a diminution of rod-shaped mitochondria and the appearance of numerous spherical, swollen ones (1.5 to 2.7 μ in diameter) were noted (Fig. 11). Absolute counts of the number of damaged organelles per cell were not done. During the early stages of vitamin D treatment, these changes were present in small groups of proximal convoluted tubules, especially those in the inner cortex near the corticomedullary border. However, as treatment continued, more tubules were affected, including those in the middle and outer cortex.

Periodic Acid-Schiff Reaction (PAS). The proximal convoluted tubules were the most strongly PAS-positive structures observed in the normal kidney. The brush border exhibited an intense, diffuse staining, while the remaining cytoplasm contained moderate numbers of PAS-positive, diastase-resistant granules measuring 1 to 2 μ in diameter. After 4 days of vitamin D administration, staining of the brush border was reduced, and the PAS-positive cytoplasmic granules coalesced into 3 to 5 μ globules and rodlets. In many instances these appeared to be more numerous at the apical portion of the epithelium near the brush border. Many PAS-positive granules and globules were also noted in the lumens of these tubules (Fig. 12). From the fifth through the ninth days,

increasing numbers of cells in the descending and ascending limbs of Henle's loop exhibited an intense, diffuse, amorphous, nongranular, PAS-

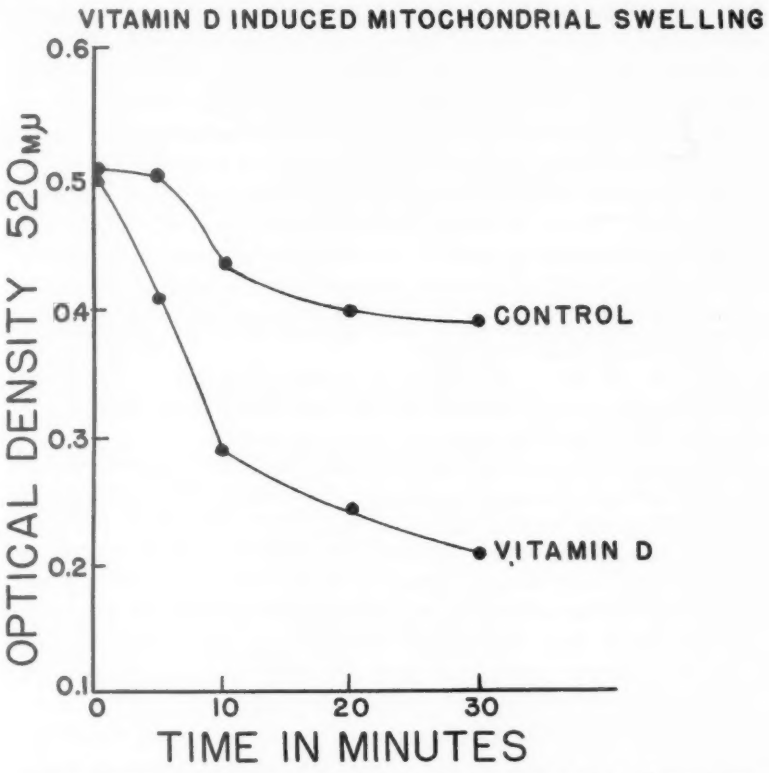

TEXT-FIGURE 1. A comparison of spontaneous swelling of mitochondria in normal control rats and vitamin D-treated rats.

positive cytoplasmic staining. In many instances an intense staining was observed in the adjacent basement membrane and stroma (Fig. 13). Many dilated tubules showed weakly stained brush borders and contained strongly PAS-positive, homogeneous casts (Fig. 14). Calcific deposits and the tissue adjacent to them were also intensely PAS-positive (Fig. 15).

Millon and Sakaguchi Reactions. Cytoplasmic granules in the proximal convoluted tubules in vitamin D-treated animals showed positive reactions for tyrosine and arginine-containing proteins. They were identical in size, shape, and intracellular location to the PAS-positive granules. Homogeneous casts in the lumens of the proximal convolutions on the fifth day also exhibited positive reactions.

Results Obtained by Biochemical Techniques

Mitochondrial Swelling. In Text-figure 1 are shown comparisons of the rates of spontaneous and vitamin D-induced swelling of mitochon-

TABLE I

SERUM AND KIDNEY CALCIUM CONCENTRATION IN CONTROL AND VITAMIN D-TREATED RATS

Animals*	Days of treatment	Serum calcium, mg. per 100 ml.	Kidney calcium, mg. per 100 gm. of dry weight
Control	0	9.8–12.3	36–52
Treated	3	10.5–16	80–300
	6	13.5–20	1400–3120
	9	12.2–22	1440–3960

* Each group consisted of 9 animals.

dria. The rate was considerably greater in mitochondria isolated from vitamin D-treated rats.

Serum and Kidney Calcium. Serum calcium levels in control animals ranged from 9.8 to 12.3 mg. per 100 ml. After 3 days of vitamin D treatment, serum levels ranged from 10.5 to 16 mg., on the sixth day from 11.5 to 20 mg., and on the ninth day from 11.2 to 22 mg. per 100 ml. Kidney calcium levels in normal controls ranged from 36 to 52 mg. per 100 gm. of dry, fat-free tissue. After 3 days of vitamin D treatment, kidney calcium levels ranged from 80 to 300 mg., on the sixth day from 1,400 to 3,120 mg., and on the ninth day from 1,440 to 3,960 mg. per 100 gm. These results are summarized in Table I.

Kidney Citrate. The concentration of citrate in control rat kidneys ranged from 2 to 4 μg. per mg. of protein nitrogen. After 3 days of vitamin D treatment, the range increased from 12.5 to 20 μg. On the sixth day of treatment, the highest values were observed; these ranged from 33 to 52 μg. By the ninth day the citrate levels had fallen; they ranged from 8 to 29 μg. The observations are summarized in Text-figure 2.

Cytopathologic Changes

Cytologic alterations in the tubular epithelium first became evident after 4 days of vitamin D administration. The lesion consisted of hydropic degeneration (Fig. 16) which was limited for the most part to the proximal convolutions. The distribution was patchy, involving groups of tubular cells at the corticomedullary junction and outer medulla. An occasional ascending limb of Henle's loop contained a finely granular basophilic substance in its lumen. On the fifth day numerous proximal convoluted tubules and both limbs of Henle's loop contained homo-

geneous eosinophilic casts with entrapped leukocytes and cellular detritus (Fig. 17). Some of the tubular cells showed an intense cytoplasmic basophilia, pyknotic nuclei, and contained a finely granular basophilic material (Fig. 18). In addition, several tubules contained amorphous, deeply basophilic, intracellular and intraluminal deposits, necrosis of tubular epithelium, and an occasional epithelial cell in mitosis. The basement membrane was extensively thickened and basophilic.

On the sixth and seventh days an increased number of tubules exhibited similar cytologic changes. The basement membranes of the proximal convolutions and Henle's loop showed even greater thickening and basophilia. In several instances large deposits of basophilic hyaline material were present between the basement membrane and the epithelial cells, displacing the latter into the lumen (Fig. 19); this was also seen in the calyces.

No new cytologic alterations were observed in the last two days of the experiment, although there was an increase in the number of affected tubules. Many tubules were dilated and exhibited atrophy of their lining cells (Fig. 20). The epithelium was flattened and contained a hyaline, eosinophilic cytoplasm. Some cells had desquamated into the lumen. A

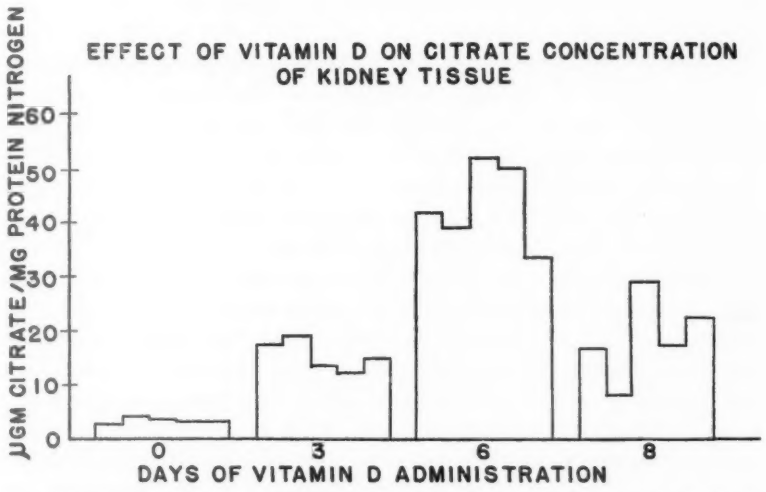

TEXT-FIGURE 2. The effect of vitamin D on the citrate concentration of rat kidney tissue.

mild inflammatory reaction consisting wholly of histiocytes was seen around large calcific deposits. In no instance were cytologic changes observed in blood vessels or glomeruli.

Discussion

The pathogenesis of metastatic calcification has remained obscure since Virchow's classic description[24] of the lesions in 1854. The inability of many investigators to demonstrate definite evidence of cellular damage prior to the deposition of calcium salts has been largely responsible for the firmly rooted concept that metastatic calcification occurs in essentially normal tissues.[25] The present study has clearly shown that extensive morphologic and cytochemical damage at the mitochondrial level precedes calcification by a considerable period of time. This corroborates previous reports which have shown that mitochondria were among the most sensitive indicators of cell function and damage.[26-28]

The striking resemblance of the renal lesions produced by hypervitaminosis D and hyperparathyroidism led Anderson[29] to suggest that the renal lesions were the result of hypercalcemia, the only factor which was common to both conditions. The deleterious effects of calcium ions on mitochondrial structure and function have been demonstrated by various investigators.[30, 31] However, hypercalcemia may not be the only mechanism by which large doses of vitamin D exert a toxic effect on kidney epithelium. Recently de Luca, Reiser and Steenbock[32] showed that vitamin D added to a suspension of renal mitochondria was capable of inhibiting their metabolism.

It is now generally agreed that certain oxidative enzymes are associated exclusively with the mitochondria.[33-35] In addition, biochemical data indicate that the mitochondria probably represent a link between the energy-producing system of the cell and the conversion of energy to forms capable of driving the various synthetic and functional activities of the cell.[36, 37] Thus, injury at this level would be expected to result in a serious disturbance of these processes.

The marked reduction of DPN and TPN diaphorase activity indicates that the activities of all the coenzyme I and II linked dehydrogenases are impaired early in vitamin D-induced nephrocalcinosis. The decrease in enzyme activity and the diffusion of DPN-linked isocitric dehydrogenase from swollen mitochondria are no doubt responsible for the accumulation of citrate observed in renal tissue. This is in keeping with current views that the adverse alterations in biochemical function accompanying mitochondrial damage are due to the loss of soluble enzymes, coenzymes and cofactors by passage across altered mitochondrial membranes.[38, 39] This initial change in cell metabolism precedes any microscopically visible alteration in the tubular epithelium and may represent a "biochemical lesion" as described by Gravilescu and Peters.[40] Inasmuch as citrate turnover is highest in the kidney,[41] ac-

cumulation of this metabolite may not be a specific vitamin D effect but simply the result of damage to renal epithelium.

Since citrate forms a soluble, non-ionized complex with calcium, the high citrate levels in kidney tissue probably influence the deposition of calcium to a considerable degree. Although high concentrations of citrate inhibit the calcification of rachitic rat bone slices *in vitro*,[42] Kuyper [43] showed that small amounts of citrate in solution are completely co-precipitated with calcium phosphate and carbonate upon the addition of these ions. Therefore, Hass's view [44] that diffusible, non-ionized, organic calcium compounds secondarily attract phosphate ions and result in metastatic calcification may be correct.

The hydropic changes in tubular epithelium which became evident two days after the onset of mitochondrial swelling and reduced diaphorase activity suggest a relation between the content of intracellular water and mitochondrial integrity. This is in accord with the observations of Macfarlane and Spencer [45] and Bartley, Davies and Krebs [46] that the active transport of water and electrolytes in cells is a function of the mitochondria. Tissue changes similar to hydropic degeneration were observed by Robinson [47] in kidney slices in which respiration was inhibited by cyanide or uncoupled by 2,4 dinitrophenol. Thus the water and electrolyte balance of tissues depends upon their metabolism in addition to the osmotic pressure of extracellular fluid.

The simultaneous appearance of intracellular neutral fat droplets and the disappearance of enzymatically active mitochondria suggest a relationship between the two. Although this has been suggested by histologists for some time, confirmatory evidence had only recently been obtained. Christie and Judah [48] have reported that 36 hours after carbon tetrachloride administration, numerous neutral, fat-positive globules were isolated from the mitochondrial fraction of rat liver. These exhibited succinoxidase activity and contained ribonucleic acid, two characteristics of mitochondria. According to Dixon,[49] the appearance of visible fat droplets may be due to the conversion of invisible micellar complex mitochondrial lipid following cell injury. However, this problem is by no means settled, as evidenced by the recent report of Recknagel and Anthony [50] that lipid accumulation may appear considerably earlier than mitochondrial degeneration. They suggest that the two processes may occur independently of each other.

During the early stages of swelling, many mitochondria resemble the so-called "target forms" described by Harman and Feigelson.[51] The eccentric peripheral localization of enzyme activity in the globose organelles is similar to the grouping and displacement of cristae observed with the electron microscope in swollen mitochondria by Hogeboom, Kuff and

Schneider.[52] However, their identity remains to be established with certainty.

Shortly after the onset of mitochondrial swelling, the PAS-positive, diastase-resistant granules in the cytoplasm of the proximal convoluted tubule cells increased in number and size. As damage progressed to the point of reduced enzyme activity, the number of granules increased, filling the cytoplasm and in some instances the tubule lumens. Although their origin is at present unknown, these PAS-positive protein granules may represent mucoprotein mobilized from the ground substance of bone by massive doses of vitamin D, as postulated by Eisenstein and Groff.[53] In addition, since the resorption of protein by the cells of the proximal convoluted tubules appears to be intimately associated with mitochondria,[54–57] and probably depends on their function, the droplets may also be the result of impaired protein resorption by the damaged organelles. The high intracellular concentration of mucoprotein in the various components of the nephron may determine in part the deposition of calcium in these sites. The affinity of various components of the ground substance for calcium has been shown repeatedly.[58–61]

Although the role of alkaline phosphatase in normal calcification has been defined, its relation to pathologic calcification is by no means settled.[62] Gomori [63] found that calcification in bone tumors and granulation tissue was always associated with alkaline phosphatase activity; however, he was not able to show such an association in calcification of the aorta. Our results indicate that calcification can occur at sites devoid of alkaline phosphatase activity. This is in agreement with Waldman [64] and McLean's [65] observations that calcification can occur in cartilage in which enzyme activity has been inhibited either by heat or heavy metal treatment.

Increased activity of nonspecific esterase and cathepsin was found in the proximal convoluted tubules shortly after the onset of hydropic degeneration. The highest activity was localized in desquamated epithelium and in amorphous necrotic material in tubular casts. These changes represent the augmented activity of proteolytic enzyme systems characteristic of cell death.

The nephropathy induced by hypervitaminosis D is characterized by a sequence of cytochemical and morphologic changes which eventuate in tubular necrosis and calcium deposition. Our results suggest the following mode of pathogenesis: Large doses of vitamin D result in a mobilization of both calcium and mucoprotein from the ground substance of bone. The hypercalcemia causes cell injury at the mitochondrial level and is identical with cellular sites of calcification seen in the later stages of this lesion. Mitochondrial swelling results in a loss of isocitric dehydrogenase

activity due to diffusion of the enzyme, which in turn causes an accumulation of citrate in the renal epithelium. The damaged cells of the proximal convolutions are unable to resorb proteins, and these substances accumulate in the kidney cells and eventually in the tubule lumens. The affinity of mucoproteins for calcium ions coupled with the increased tissue concentration of citrate capable of complexing calcium may provide a mechanism by which phosphate and carbonate ions are secondarily attracted to form calcific deposits.

References

1. Kreitmair, H., and Moll, T. Hypervitaminose durch grosse Dosen Vitamin D. *München med. Wchnschr.*, 1928, **75**, 637–639.
2. Pfannenstiel, W. A summary of recent work on vigantol (irradiated ergosterol). *Lancet*, 1928, **2**, 845–847.
3. Gough, J.; Duguid, J. B., and Davies, D. R. The renal lesions in hypervitaminosis D: observations on the urinary calcium and phosphorus excretion. *Brit. J. Exper. Path.*, 1933, **14**, 137–145.
4. Hueper, W. Metastatic calcifications in the organs of the dog after injections of parathyroid extract. *Arch. Path.*, 1927, **3**, 14–25.
5. Kreitmair, H., and Hintzelmann, U. Über sklerotische Organveränderungen, insonderheit der Arterien. *Arch. exper. Path. u. Pharmakol.*, 1928, **137**, 203–214.
6. Rabl, C. R. H. Organverkalkungen unter dem Einfluss von Vitamin D. *Deutsche med. Wchnschr.*, 1929, **55**, 63–64.
7. Shohl, A. T.; Goldblatt, H., and Brown, H. B. The pathological effects upon rats of excess irradiated ergosterol. *J. Clin. Invest.*, 1930, **8**, 505–531.
8. Smith, M. I., and Elvove, E. The action of irradiated ergosterol in the rabbit. *Pub. Health Rep.*, 1929, **44**, 1245–1256.
9. Spies, T. D., and Glover, E. C. Renal lesions with retention of nitrogenous products produced by massive doses of irradiated ergosterol. *Am. J. Path.*, 1930, **6**, 485–498.
10. Scarpelli, D. G.; Hess, R., and Pearse, A. G. E. The cytochemical localization of oxidative enzymes. I. Diphosphopyridine nucleotide diaphorase and triphosphopyridine nucleotide diaphorase. *J. Biophys. & Biochem. Cytol.*, 1958, **4**, 747–752.
11. Nachlas, M. M.; Walker, D. G., and Seligman, A. M. A histochemical method for the demonstration of diphosphopyridine nucleotide diaphorase. *J. Biophys. & Biochem. Cytol.*, 1958, **4**, 29–38.
12. Hess, R.; Scarpelli, D. G., and Pearse, A. G. E. The cytochemical localization of oxidative enzymes. II. Pyridine nucleotide-linked dehydrogenases. *J. Biophys. & Biochem. Cytol.*, 1958, **4**, 753–760.
13. Scarpelli, D. G., and Pearse, A. G. E. Physical and chemical protection of cell constituents and the precise localization of enzymes. *J. Histochem.*, 1958, **6**, 369–376.
14. Grogg, E., and Pearse, A. G. E. Coupling azo dye methods for histochemical demonstration of alkaline phosphatase. *Nature, London*, 1952, **170**, 578–579.
15. Holt, S. J., and Withers, R. F. J. Cytochemical localization of esterases using indoxyl derivatives. *Nature, London*, 1952, **170**, 1012–1014.
16. Aldridge, W. N. Some esterases of the rat. *Biochem. J.*, 1954, **57**, 692–702.

17. HESS, R., and PEARSE, A. G. E. The histochemistry of indoxyl-esterase of rat kidney with special reference to its cathepsin-like activity. *Brit. J. Exper. Path.*, 1958, **39**, 292–299.

18. PEARSE, A. G. E. Histochemistry, Theoretical and Applied. Little, Brown & Co., Boston, 1953, 530 pp.

19. CLELAND, K. W. Permeability of isolated rat heart sarcosomes. *Nature, London*, 1952, **170**, 497–499.

20. RAAFLAUB, J. Die Schwellung isolierter Leberzellmitochondrien und ihre physikalisch-chemische Beeinflussbarkeit. *Helvet. physiol. et. pharmacol. acta*, 1953, **11**, 142–156.

21. LEHNINGER, A. L. Physiology of Mitochondria. Relationship Between Mitochondrial Structure, Oxidative Phosphorylation, and the Action of Thyroxine. In: Enzymes: Units of Biological Structure and Function. Henry Ford Hospital International Symposium. Gaebler, O. H. (ed.). Academic Press, New York, 1956, pp. 217–233.

22. BALLENTINE, R., and BURFORD, D. D. Determination of Metals. (Na, K, Mg, Ca, Mn, Fe, Co, Cu, Zn). In: Methods in Enzymology. Vol. III, Section VII, Determination of Inorganic Compounds. Colowick, S. P., and Kaplan, N. O. (eds.). Academic Press, New York, 1957, pp. 1002–1035.

23. NATELSON, S.; PINCUS, J. B., and LUGOVOY, J. K. Microestimation of citric acid, a new colorimetric reaction for pentabromoacetone. *J. Biol. Chem.*, 1948, **175**, 745–750.

24. VIRCHOW, R. Kalk-Metastasen. *Virchows Arch. path. Anat.*, 1854, **8**, 103–113.

25. HASS, G. M.; TRUEHEART, R. E.; TAYLOR, C. B., and STUMPE, M. An experimental histologic study of hypervitaminosis D. *Am. J. Path.*, 1958, **34**, 395–431.

26. POLICARD, A. Sensibilité des chondriosomes aux élévations de température. *Compt. rend. Soc. de biol.*, 1912, **72**, 228–229.

27. NOËL, R., and PALLOT, G. Recherches sur le chondriome de la cellule hépatique des mammifères: le chondriome hépatique chez le rat. *Bull. histol. appliq. physiol.*, 1933, **10**, 169–186.

28. FAWCETT, D. W. Observations on the cytology and electron microscopy of hepatic cells. *J. Nat. Cancer Inst.*, 1955, **15**, 1475–1502.

29. ANDERSON, W. A. D. Hyperparathyroidism and renal disease. *Arch. Path.*, 1939, **27**, 753–778.

30. SLATER, E. C., and CLELAND, K. W. Stabilization of oxidative phosphorylation in heart muscle sarcosomes. *Nature, London*, 1952, **170**, 118–119.

31. HARMAN, J. W. The Cytochondria of Cardiac and Skeletal Muscle. In: International Review of Cytology. Bourne, G. H., and Danielli, J. F. (eds.). Academic Press, New York, 1956, **5**, pp. 89–146.

32. DELUCA, H. F.; REISER, S., and STEENBOCK, H. Vitamin D inhibition of citrate oxidation in kidney mitochondria. (Abstract) *Fed. Proc.*, 1958, **17**, 210.

33. HOGEBOOM, G. H.; CLAUDE, A., and HOTCHKISS, R. D. The distribution of cytochrome oxidase and succinoxidase in the cytoplasm of the mammalian liver cell. *J. Biol. Chem.*, 1946, **165**, 615–629.

34. KENNEDY, E. P., and LEHNINGER, A. C. Oxidation of fatty acids and tricarboxylic acid cycle intermediates by isolated rat liver mitochondria. *J. Biol. Chem.*, 1949, **179**, 957–972.

35. SCHNEIDER, W. C., and HOGEBOOM, G. H. Cytochemical studies of mammalian tissues: the isolation of cell components by differential centrifugation. A review. *Cancer Res.*, 1951, **11**, 1–22.

36. CHANCE, B., and HESS, B. On the control of metabolism in ascites tumor cell suspensions. *Ann. New York Acad. Sc.*, 1956, **63**, 1008–1016.

37. RACKER, E. Carbohydrate metabolism in ascites tumor cells. *Ann. New York Acad. Sc.*, 1956, **63**, 1017–1021.

38. RAAFLAUB, J. Die Metallpufferfunktion der Adenosinphosphate. *Helvet. physiol. et pharmacol. acta*, 1956, **14**, 304–318.

39. ERNSTER, L., and LÖW, H. Reconstruction of oxidative phosphorylation in aged mitochondrial systems. *Exper. Cell Res.*, 1955, Suppl. **3**, 133–153.

40. GRAVILESCU, N., and PETERS, R. A. On the function of torulin. An *in vitro* effect of antineuritic vitamin concentrates. *Biochem. J.*, 1931, **25**, 2150–2161.

41. BUFFA, P., and PETERS, R. A. The *in vivo* formation of citrate induced by fluoroacetate and its significance. *J. Physiol.*, 1949, **110**, 488–500.

42. SHIPLEY, P. G.; KRAMER, B., and HOWLAND, J. L. Studies upon calcification *in vitro*. *Biochem. J.*, 1926, **20**, 379–387.

43. KUYPER, A. C. The chemistry of bone formation. I. The composition of precipitates from salt solutions. *J. Biol. Chem.*, 1945, **159**, 411–416.

44. HASS, G. M. Pathological Calcification. In: The Biochemistry and Physiology of Bone. Bourne, G. H. (ed.). Academic Press, New York, 1956, Chapt. XXIV, pp. 767–810.

45. MACFARLANE, M. G., and SPENCER, A. G. Changes in the water, sodium and potassium content of rat-liver mitochondria during metabolism. *Biochem. J.*, 1953, **54**, 569–575.

46. BARTLEY, W.; DAVIES, R. E., and KREBS, H. A. Active transport in animal tissues and subcellular particles. *Proc. Roy. Soc. London s.B*, 1954, **142**, 187–196.

47. ROBINSON, J. R. Osmoregulation in surviving slices from the livers of adult rats. *Proc. Roy. Soc. London s.B*, 1952–1953, **140**, 135–144.

48. CHRISTIE, G. S., and JUDAH, J. D. Mechanism of action of carbon tetrachloride on liver cells. *Proc. Roy. Soc. London s.B*, 1954, **142**, 241–257.

49. DIXON, C. Fatty deposition: a disorder of the cell. *Quart. J. Exper. Physiol.*, 1958, **43**, 139–159.

50. RECKNAGEL, R. O., and ANTHONY, D. D. Biochemical changes in carbon tetrachloride fatty liver: separation of fatty changes from mitochondrial degeneration. *J. Biol. Chem.*, 1959, **234**, 1052–1059.

51. HARMAN, J. W., and FEIGELSON, M. Studies on mitochondria. *Exper. Cell Res.*, 1952, **3**, 47–58.

52. HOGEBOOM, G. H.; KUFF, E. L., and SCHNEIDER, W. C. Recent approaches to the cytochemical study of mammalian tissues. In: International Review of Cytology. Bourne, G. H., and Danielli, J. F. (eds.). Academic Press, New York, 1957, **6**, 425–467.

53. EISENSTEIN, R., and GROFF, W. A. Experimental hypervitaminosis D: hypercalcemia, hypermucoproteinemia, and metastatic calcification. *Proc. Soc. Exper. Biol. & Med.*, 1957, **94**, 441–444.

54. OLIVER, J.; MACDOWELL, M., and LEE, Y. C. Cellular mechanisms of protein metabolism in the nephron. I. The structural aspects of proteinuria; tubular absorption, droplet formation, and disposal of proteins. *J. Exper. Med.*, 1954, **99**, 589–604.

55. OLIVER, J.; MOSES, M. J.; MACDOWELL, M. C., and LEE, Y. C. Cellular mechanisms of protein metabolism in the nephron. II. The histochemical characteristics of protein absorption droplets. *J. Exper. Med.*, 1954, **99**, 605–620.

56. KRETCHMER, N., and DICKERMAN, H. W. Cellular mechanisms of protein metabolism in the nephron. IV. The partition of succinoxidase and cytochrome oxidase activities in the cells of the proximal convolutions of the rat after intraperitoneal injection of egg white. *J. Exper. Med.*, 1954, **99**, 629–635.

57. RHODIN, J. Correlation of Ultrastructural Organization and Function in Normal and Experimentally Changed Proximal Convoluted Cells of the Mouse Kidney. Karolinska Institutet, Stockholm, Aktiebolaget Godvil, 1954.

58. FREUDENBERG, E., and GYÖRGY, P. Über kalkbindung durch tierische Gewebe. III. *Biochem. Ztschr.*, 1921, **118**, 50–54.

59. RUBIN, P. S., and HOWARD, J. E. Histochemical Studies on the Role of Acid Muco-polysaccharides in Calcifiability and Calcification. In: Metabolic Interrelations. Transactions of the Second Conference, Josiah Macy, Jr., Foundation, New York, 1950, pp. 155–166.

60. NEUMAN, W. F.; BOYD, E. S., and FELDMAN, I. The Ion-binding Properties of Cartilage. In: Metabolic Interrelations. Transactions of the Fourth Conference, Josiah Macy, Jr., Foundation, New York, 1952, pp. 100–112.

61. ROBISON, R. The possible significance of hexosephosphoric esters in ossification. *Biochem. J.*, 1923, **17**, 286–293.

62. ARMSTRONG, W. D. Phosphorus Metabolism in the Skeleton. In: The Role of Phosphorus in the Metabolism of Plants and Animals. A Symposium on Phosphorus Metabolism. McElroy, W. D., and Glass, B. (eds.). Johns Hopkins Press, Baltimore, 1952, Vol. 2, pp. 698–727.

63. GOMORI, G. Calcification and phosphatase. *Am. J. Path.*, 1943, **19**, 197–209.

64. WALDMAN, J. Calcification of hypertrophic epiphyseal cartilage *in vitro* following inactivation of phosphatase and other enzymes. *Proc. Soc. Exper. Biol. & Med.*, 1948, **69**, 262–263.

65. MCLEAN, F. C. The role of enzymes in calcification. In discussion following: WALDMAN, J. Effect of Inactivation of Enzymes on Calcification of Cartilage *in vivo*. In: Metabolic Interrelations. Transactions of the Second Conference, Josiah Macy, Jr., Foundation, New York, 1950, pp. 211–212.

The authors wish to thank W. Brackenbury and G. R. Millard for the photography, and C. V. Sittler for technical assistance.

LEGENDS FOR FIGURES

FIG. 1. Normal rat kidney. Sites of DPN diaphorase activity appear in the proximal convoluted tubules. DPN diaphorase reaction. × 650.

FIG. 2. Rat sacrificed after 2 days of vitamin D treatment. There is variation in DPN diaphorase activity. Swollen mitochondria are present in the tubule in center of the photograph. Rod-shaped mitochondria are manifest in the surrounding tubules. DPN diaphorase reaction. × 650.

FIG. 3. A higher magnification of the damaged tubule shown in Figure 2. Formazan deposits are localized at the periphery of swollen mitochondria. DPN diaphorase reaction. × 1450.

FIG. 4. Rat sacrificed after 4 days of vitamin D treatment. There are numerous swollen mitochondria and a complete absence of rod-shaped mitochondria. The diffuse nature of the reaction is probably due to enzyme diffusion from damaged organelles. Isocitric dehydrogenase reaction. × 650.

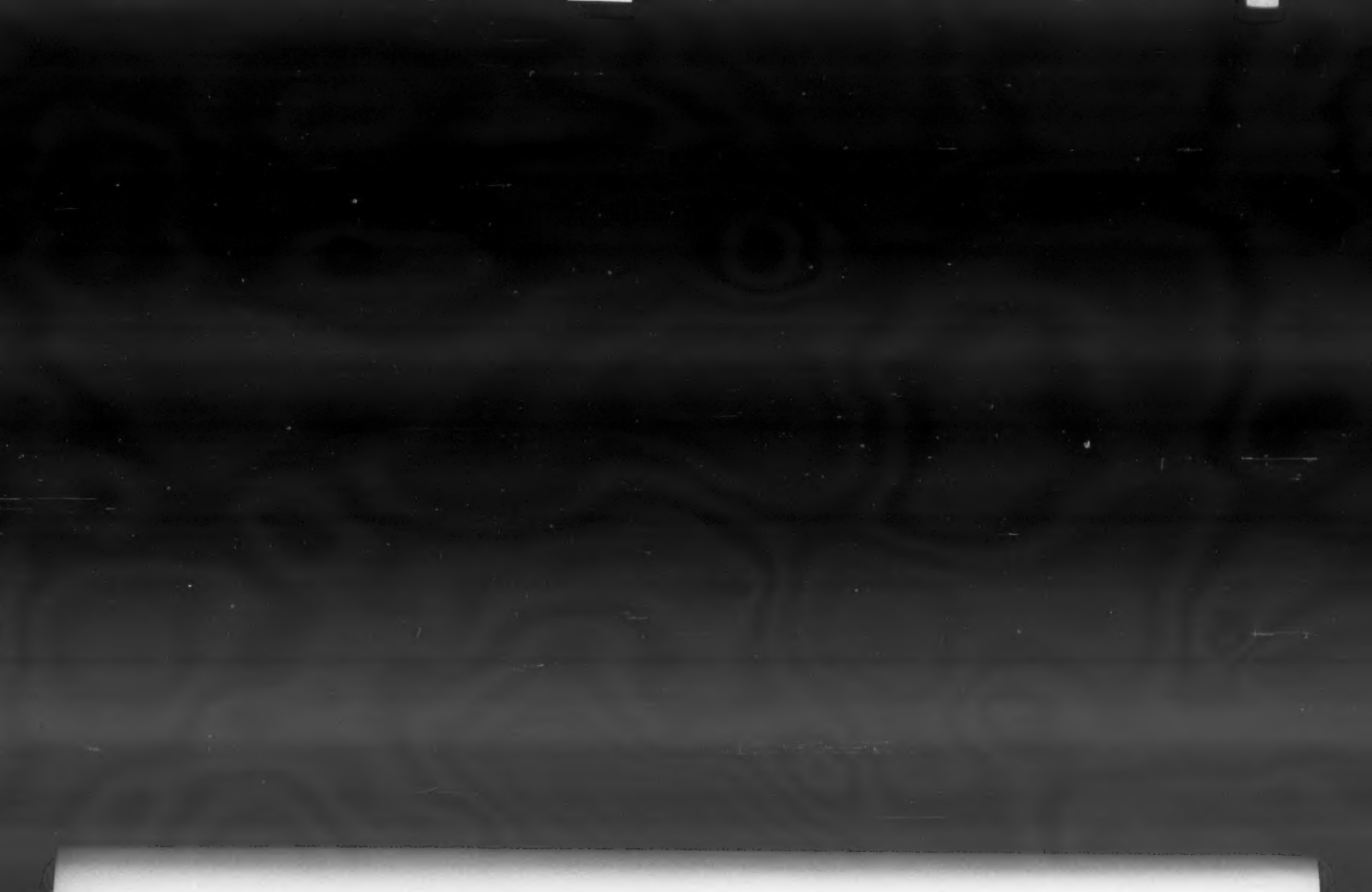

1

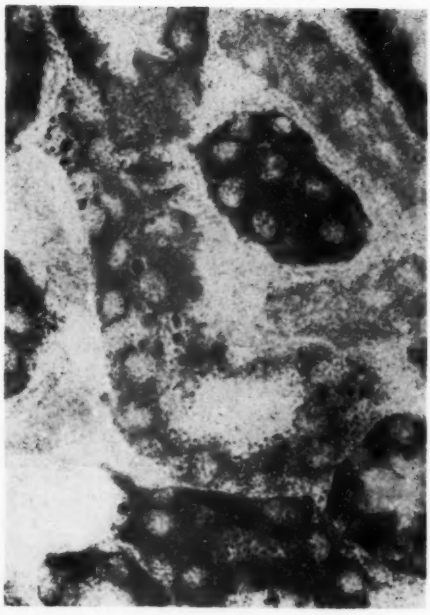

2

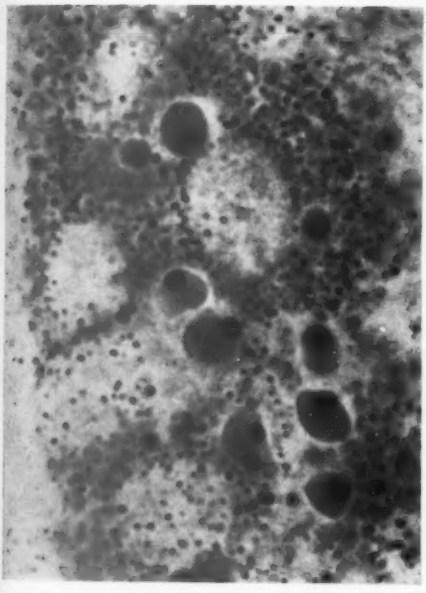

3

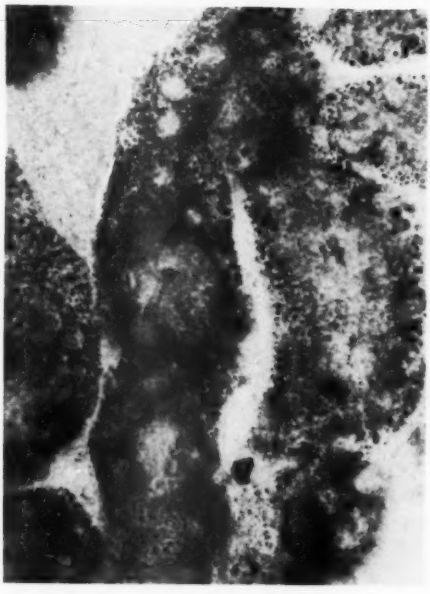

4

FIG. 5. Normal rat kidney. Alkaline phosphatase activity in the proximal convoluted tubules is localized in the brush border. Alkaline phosphatase reaction. × 650.

FIG. 6. Rat sacrificed after 7 days of vitamin D treatment. A very weak alkaline phosphatase activity is present around an intratubular calcific deposit. Alkaline phosphatase reaction. × 650.

FIG. 7. Normal rat kidney. Indoxyl esterase activity appears in the proximal convoluted tubules. Indoxyl esterase reaction. × 650.

FIG. 8. Rat sacrificed after 5 days of vitamin D treatment. Note the intense reaction in the desquamated cells and debris in the tubule lumens. Indoxyl esterase reaction. × 750.

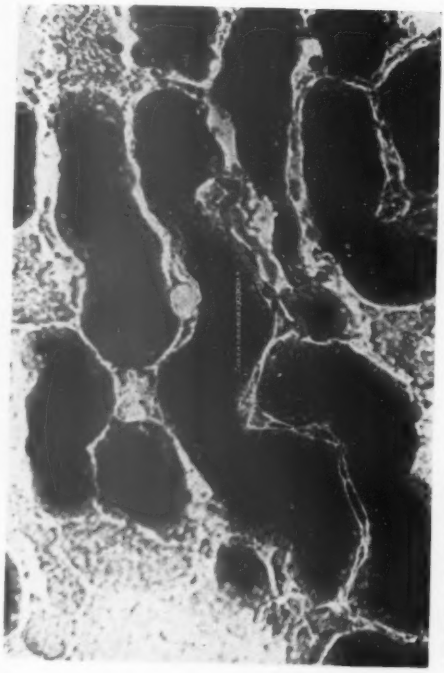

5

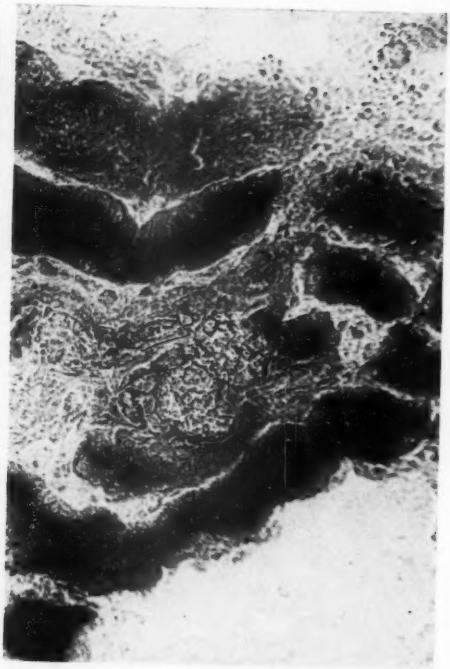

6

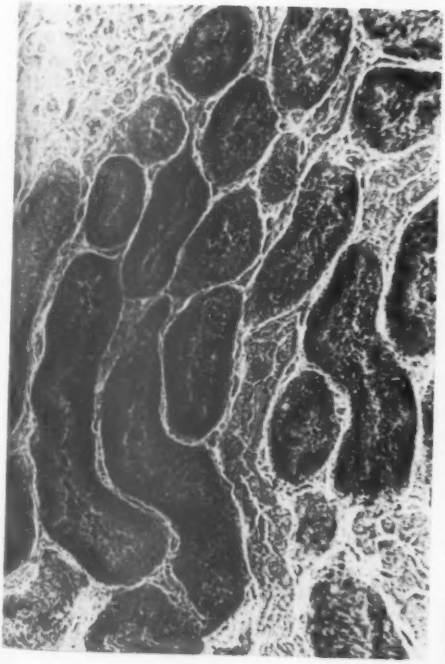

7

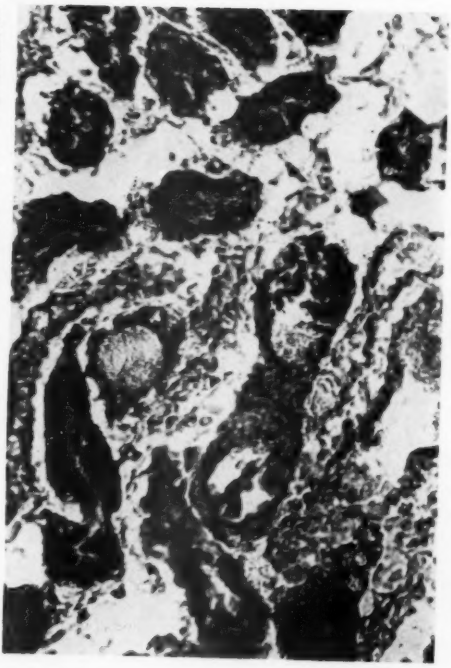

8

FIG. 9. Rat sacrificed after 3 days of vitamin D treatment. The swollen mitochondria exhibit an intense oil red O staining. DPN diaphorase reaction and oil red O stain. × 750.

FIG. 10. Normal rat kidney. Numerous rod-shaped mitochondria are oriented at right angles to the tubule lumens. Heidenhain's iron hematoxylin stain. × 600.

FIG. 11. Rat sacrificed after 3 days of vitamin D treatment. There are swollen spherical mitochondria and a few remaining rod-shaped forms. Heidenhain's iron hematoxylin stain. × 650.

FIG. 12. Rat sacrificed after 4 days of vitamin D treatment. Epithelium of the proximal convoluted tubules contains large numbers of PAS-positive granules which fill the cells and tubule lumens. Periodic acid-Schiff (PAS) reaction. × 650.

10

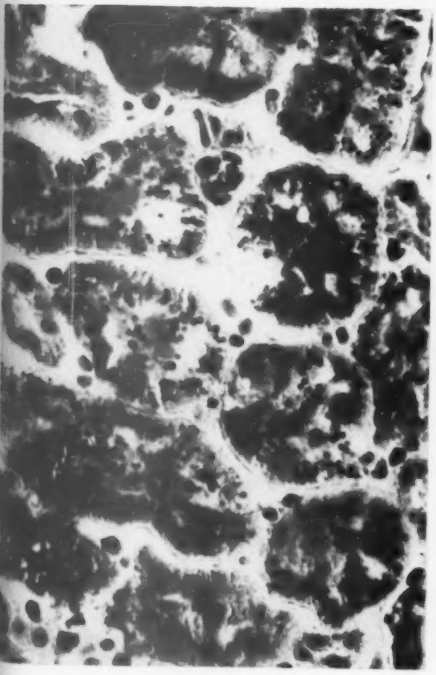

12

FIG. 13. Rat sacrificed after 5 days of vitamin D treatment. An intense PAS reaction is present in the basement membrane and adjacent stroma of a dilated proximal convoluted tubule. PAS reaction. × 300.

FIG. 14. Rat sacrificed after 6 days of vitamin D treatment. Intensely PAS-positive protein casts appear within the renal tubules. PAS reaction. × 260.

FIG. 15. Rat sacrificed after 7 days of vitamin treatment. Small, spherical, calcific deposits and the basement membrane are PAS-positive. PAS reaction. × 350.

FIG. 16. Rat sacrificed after 4 days of vitamin D treatment. A group of proximal convoluted tubular cells exhibit hydropic degeneration. Hematoxylin and eosin stain. × 600.

The sections illustrated in Figures 17 to 20 were stained with hematoxylin and eosin.

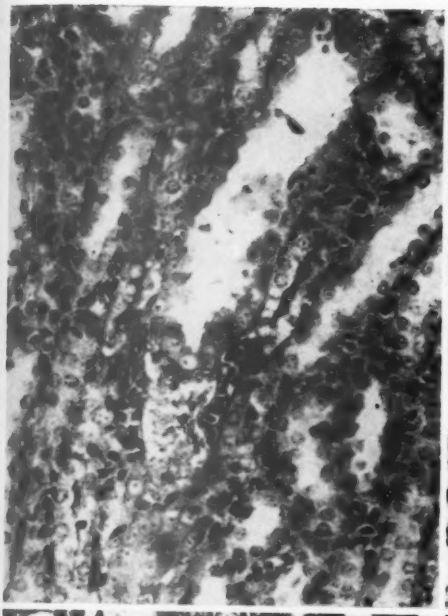

13

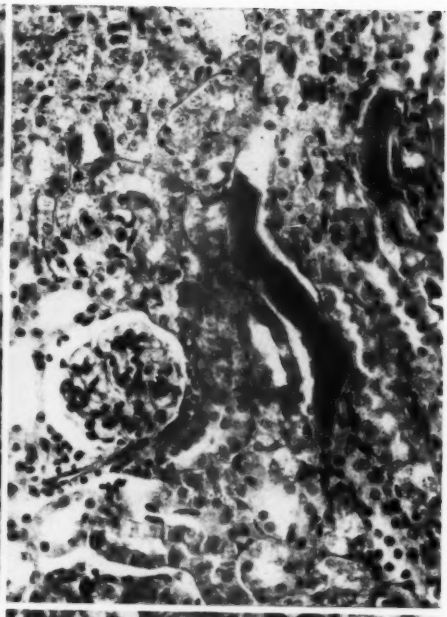

14

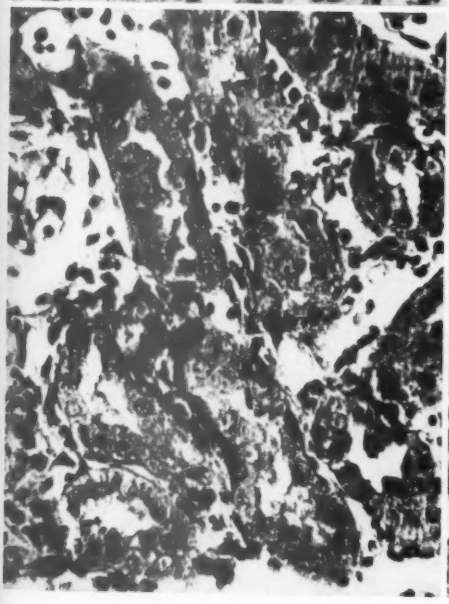

15

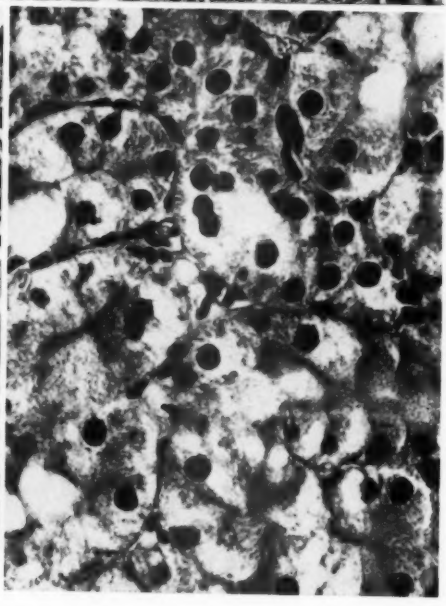

16

FIG. 17. Rat sacrificed after 5 days of vitamin D treatment. A protein cellular cast is manifest in the descending limb of Henle's loop. × 650.

FIG. 18. Rat sacrificed after 5 days of vitamin D treatment. Tubular epithelium exhibits intense cytoplasmic basophilia and focal necrosis. × 400.

FIG. 19. Rat sacrificed after 6 days of vitamin D treatment. There are degeneration and calcification of the basement membrane with displacement of the tubular epithelium into the lumen. × 400.

FIG. 20. Rat sacrificed after 8 days of vitamin D treatment. Many dilated tubules with pressure atrophy of the tubular epithelium are evident. Note the numerous protein casts. × 150.

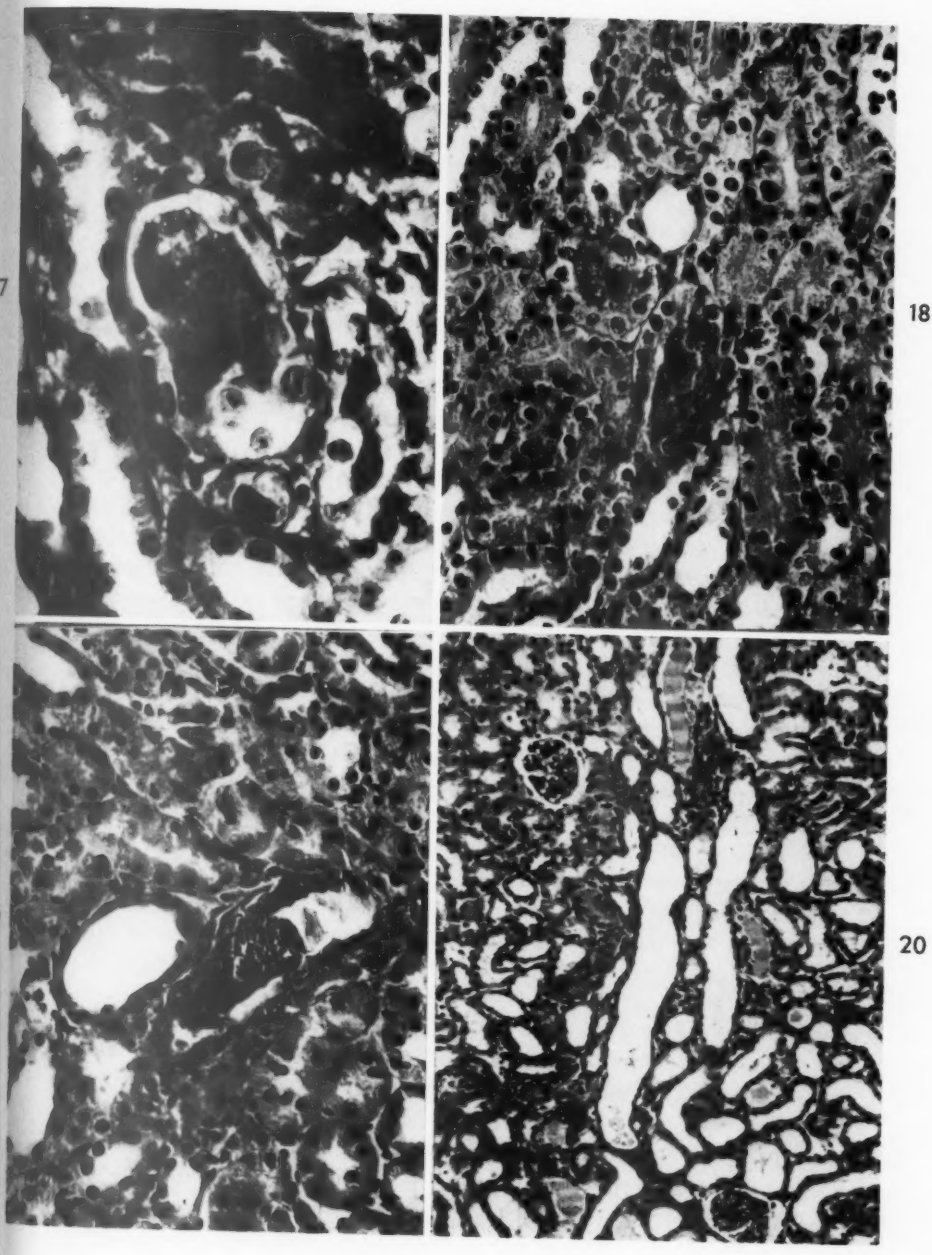

17

18

20

RESIDUAL PIGMENT ASSOCIATED WITH INTRAVENOUS FAT ALIMENTATION

SAMUEL W. THOMPSON II, D.V.M., M.S.*; MARY A. FOX, A.B., MT.; ALLAN L. FORBES, M.D.,† AND ROBERT W. THOMASSEN, B.S., D.V.M.‡

From the Pathology Branch, Research Support Division, and the Intravenous Alimentation Branch, Physiology Division, United States Army Medical Research and Nutrition Laboratory, Fitzsimons Army Hospital, Denver, Colo.

In 1957, Meyer, Fancher, Schurr and Webster [1] reported the observation of a brown pigment in the reticuloendothelial system of dogs and human beings receiving multiple infusions of an intravenous fat emulsion. In 1958, Thompson, Johnson and Forbes [2] described the staining characteristics of a pigment-lipoid complex which they designated "intravenous (i.v.) fat pigment." This pigment was deposited in the reticuloendothelial cells of the spleen and the Kupffer cells of the liver after multiple intravenous infusions of the fat emulsion. Recently, Thompson, Fox, Harrison and Forbes [3] reported the influence of fixatives, solvents and bleaches on the same pigment. They were able to demonstrate that i.v. fat pigment was an entity and not an artifact incident to methods of tissue processing and fixation.

The original investigators cited above dealt with the occurrence and the chemical and physical nature of i.v. fat pigment. The long-term effects of the presence of this pigment in the body have not been reported. To determine the fate and possible pathologic significance of the pigment, multiple infusions of the fat emulsion were administered to 25 adult albino rabbits. At periodic intervals subsequent to the last day of infusion, groups of animals were sacrificed and their tissues examined for histologic alterations. Since our previous experience had been chiefly with rabbits, this was the animal of our choice.

MATERIAL AND METHODS

Selected tissues were obtained at necropsy from the 25 rabbits. The intravenously administered fat emulsion was composed of a sterile aqueous preparation containing 15 gm. of cottonseed oil, 4 gm. of glucose, 1.2 gm. of soybean phosphatide, and 0.3 gm. of Pluronic F-68 (a polyoxyethylene-propylene polymer manufactured by Wyandotte Chemicals

* Major, Veterinary Corps, United States Army.
† Captain, Medical Corps, United States Army Reserve.
‡ First Lieutenant, Veterinary Corps, United States Army.
Received for publication, July 16, 1959.

Corporation, Wyandotte, Michigan) per 100 ml. The emulsion (15 ml. per kg. of body weight) was administered daily for 28 days. Rabbits were sacrificed at 1 and 25 days, and at 3, 6, 12 and 18 months after the last day of infusion. There were no spontaneous deaths and no evident clinical illnesses. The livers and spleens from the animals killed up to and including 6 months after infusion were harvested and fixed in 10 per cent formalin. The livers, spleens, mesenteric lymph nodes and femoral bone marrow were obtained from the animals sacrificed 6 months after infusion. Replicate tissue blocks from each location were fixed in 10 per cent neutral buffered formalin and in absolute alcohol.

In addition to the experimental animals, a control group of 10 rabbits of similar age was also examined. Each of these rabbits received daily intravenous infusions of a solution containing 5 per cent dextrose in water for 28 days; again, the dose was 15 ml. per kg. of body weight. Necropsies were performed on these animals 1, 25 and 62 days, and 3 and 8 months after the last day of infusion. Here, too, there were no spontaneous deaths and no evident clinical illnesses. Blocks of liver and spleen were procured from all animals and fixed in 10 per cent neutral buffered formalin and in absolute alcohol.

Replicate sections, 6 to 8 μ in thickness were prepared from paraffin-embedded tissues in all 35 rabbits. Sections from each specimen in the test animals were subjected to the same physical and histochemical tests originally used in the characterization of the i.v. fat pigment. These included fluorescent microscopy with the use of exciting light in the wave length range of 360 to 400 mμ.[5] In the control rabbits, sections were stained with Harris' hematoxylin and aqueous eosin,[4] and for iron by Gomori's method.

Results

In the Kupffer cells of the liver and in reticuloendothelial cells of the spleen of all rabbits killed one day after infusion, there were deposits of a brown granular pigment, surrounded by lipoid substances. This pigment-lipoid complex exhibited reactions to staining techniques and to histochemical and physical tests which were characteristic of the i.v. fat pigment.[2, 3]

In the spleens of all test rabbits sacrificed 25 days after the last infusion, numerous reticuloendothelial cells were heavily laden with the complex identifiable as i.v. fat pigment (Fig. 1). In the Kupffer cells of the livers of these rabbits, variable quantities of a similar substance were observed. In addition, focal accumulations of lymphocytes and monocytes were encountered within sinusoids and portal areas. In all but one of the rabbits, circumscribed collections of macrophages were observed

in sinusoids, most frequently in the zones adjacent to portal areas. These cells were invariably heavily laden with i.v. fat pigment, and in some instances they appeared to have fused to form giant cells of the Langhans type (Fig. 2).

In the rabbits sacrificed 3 months after the last infusion, considerable quantities of i.v. fat pigment were observed in the cytoplasm of many reticuloendothelial cells of the spleen. The pigment was not as diffusely distributed as in the groups of animals sacrificed earlier (Fig. 3), and there was a definite tendency toward clumping of the macrophages, thereby concentrating the pigment in focal areas of the pulp. In sections stained with osmium tetroxide, the pigment granules frequently stained more darkly than in the animals sacrificed at the termination of the infusion period. In sections stained by the acid-fast technique, the pigment and associated lipoid substances stained an intense violet rather than faint red. The complex was partially extracted on 24-hour exposure to hot methanol chloroform. This reaction differed decidedly from that experienced in the animals sacrificed 1 and 25 days after infusion. When treated with anhydrous pyridine (acetylation) and subsequently stained by the periodic acid-Schiff (PAS) method, considerable portions of the pigment-lipoid complex remained in the tissues as amorphous smudges of golden-brown, PAS-negative substance, whereas in rabbits killed 1 and 25 days after infusion, this material was completely extracted by similar procedures. On deacetylation and subsequent PAS staining, this substance regained a faint PAS positivity. Hemosiderin was plentiful in each spleen examined, and was frequently mixed with the i.v. fat pigment.

Most of the Kupffer cells in rabbits sacrificed 3 months after infusion contained no i.v. fat pigment. However, those Kupffer cells which did contain it were heavily laden. Circumscribed collections of macrophages, some forming giant cells of the Langhans type, were observed in the sinusoids adjacent to the portal tracts in every liver (Fig. 4). The pigment-lipoid complex in Kupffer cells, macrophages, and giant cells exhibited identical staining reactions. Hemosiderin was not observed in these cells. The staining characteristics of the complex were similar to those observed in the spleen, with the exception that there were more intense reactions to PAS and phosphomolybdic acid (PMA), and more pronounced acid-fast staining. The focal lymphocytic infiltration observed 25 days after infusion was not encountered at 3 months.

At 6 months, i.v. fat pigment was present regularly in the cytoplasm of aggregates of reticuloendothelial cells in the spleen. The pigment was similar in appearance, sites of deposition, and histochemical characteristics to that observed at 3 months (Fig. 5). In the livers of these animals, there was no i.v. fat pigment demonstrable in most of the Kupffer cells.

Some of these cells did contain considerable quantities of hemosiderin, however. In all of the livers, many clumps of macrophages and giant cells appeared in the sinusoids adjacent to portal tracts (Fig. 6). These were laden with the lipoid substance which was occasionally mixed with hemosiderin. The pigment-lipoid complex had histochemical characteristics similar to those encountered at 3 months.

In the spleens of rabbits sacrificed 12 and 18 months after the last infusion of fat emulsion, large quantities of hemosiderin were observed, but there was no i.v. fat pigment. In the livers the pigment was present in only a few Kupffer cells; however, many heavily laden macrophages and giant cells were observed in the sinusoids adjacent to portal tracts (Figs. 7 and 8). The granular portion of the pigment complex was very dark brown in color, and fewer of the particles were birefringent than in the cases examined earlier. Considerable quantities of hemosiderin were also mixed with the i.v. fat pigment in almost every cell in which the latter was observed. It was also evident that although the pigment was present in tissues fixed in both 10 per cent neutral buffered formalin and absolute alcohol, less of it was manifest in the alcohol-fixed sections.

The fat pigment was present in the cytoplasm of reticuloendothelial cells of the femoral bone marrow in the animals sacrificed 12 and 18 months after infusion (Fig. 9). A brown, smudgy substance was also observed in phagocytic elements in the mesenteric lymph nodes, appearing in clumps of cells in the cell-poor parenchyma. It was less granular than that observed in the liver or bone marrow, contained fewer birefringent particles, but was otherwise similar to the pigment-lipoid complex seen in the other tissues (Fig. 10).

Variable quantities of iron-positive pigment, considered to be hemosiderin, were present in the spleen, liver and mesenteric lymph nodes of the control animals. Neither i.v. fat pigment nor other significant lesions were observed in any of these rabbits.

Discussion

It is evident that the deposition of the pigment-lipoid complex in tissues of animals receiving intravenous infusions of a cottonseed fat emulsion was related to the emulsion, since a similar substance was not found in any of the control animals. The presence of the complex in the tissues of animals sacrificed 18 months after infusion would indicate that the substance was not readily eliminated from the body.

The disappearance of the complex from the spleen at some time between the sixth and twelfth month after infusion is of interest, since the quantity present in the mesenteric lymph nodes increased during this period. In some of our previous studies, negligible quantities of pigment

were observed in the mesenteric lymph nodes of animals sacrificed soon after termination of the infusions. In contrast, heavy depositions were noted in the spleen at such times. This would appear to indicate that the complex, as seen in the spleen, was being handled much as one might expect, by transport to the regional lymph nodes.

The formation of pigment-laden giant cells in the liver as early as 25 days after infusion is noteworthy. The persistence of the giant cells over a period of 18 months, with no other associated inflammatory reaction, is difficult to explain. However, it is felt that the phenomenon represents a host response to a foreign substance. The pigment-lipoid complex in the bone marrow was essentially unaltered during the period of the experiment. Its histochemical characteristics 18 months after infusion were identical to those observed at one day.

The changes noted in the histochemical characteristics of i.v. fat pigment during the period it remained in body tissues are thought to be correlated with its initial concentration in various types of cells. The apparent intensification of its acid-fast, PAS, PMA, osmium tetroxide and oil red O staining qualities could easily be related to an increasing concentration. Likewise, the alteration of its solubility in anhydrous pyridine and hot methanol chloroform probably have a similar relationship to its concentration in heavily laden cells. The increased solubility in absolute alcohol incident to alcohol fixation, a feature noted 12 and 18 months after infusion, is not unexpected. It was reported earlier [3] that prolonged storage of alcohol-fixed tissues in 70 per cent alcohol gradually removed the i.v. fat pigment content.

We have examined liver biopsy specimens from a few dogs which had received multiple intravenous infusions of various cottonseed oil emulsions. These specimens had been procured over a period of a year. I.v. fat pigment-laden giant cells were frequently observed in the specimens collected approximately one year after infusion. Thus, the phenomenon is not limited to rabbits alone, and it is not unlikely that a similar situation may occur in human beings. A pigment-lipoid complex with identical histochemical characteristics has been demonstrated in human subjects following fat infusion.[2, 3]

In order to determine the ultimate effect upon the host of such residual pigment, life-span animal studies are indicated. Our present data do not indicate the potential harm that the pigment might evoke.

Summary

The pathologic effect of i.v. fat pigment in animal tissues over prolonged periods of time has been investigated. Twenty-five rabbits were given daily intravenous infusions of a cottonseed oil emulsion for 28

days. Representative groups of these animals and suitable control animals were sacrificed at intervals up to 18 months after the infusions. Tissue sections prepared from these animals were examined by a variety of histochemical procedures for the identification of the fat pigment. The substance was observed in representative tissues throughout this 18 months' period. It was accompanied by the formation of giant cells in the livers of all rabbits from the 25th day after infusion to the termination of the experiment. The pigment remained in body tissues as a foreign substance which was not metabolized.

References

1. Meyer, C. E.; Fancher, J. A.; Schurr, P. E., and Webster, H. D. Composition, preparation and testing of an intravenous fat emulsion. *Metabolism*, 1957, **6**, 591–596.
2. Thompson, S. W.; Johnson, F. B., and Forbes, A. L. Staining characteristics of a pigment associated with intravenous fat alimentation. *Lab. Invest.*, 1958, **7**, 533–543.
3. Thompson, S. W.; Fox, M.; Harrison, M., and Forbes, A. L. Influence of fixatives, solvents, and bleaches on intravenous fat pigment. *Lab. Invest.* (In press)
4. Gridley, M. F. Manual of Histologic and Special Staining Technics. Armed Forces Institute of Pathology, Washington, D.C., 1957, p. 30.
5. Mallory, F. B. Pathological Technique. W. B. Saunders, Philadelphia, 1938, p. 137.

All illustrations are U.S. Army photographs taken by Mr. William Hummel of the Pathology Service, Fitzsimons Army Hospital, Denver, Colo. The authors appreciate the technical assistance of Sergeant First Class Harry Hoey, United States Army.

Legends for Figures

Photomicrographs were prepared from sections stained with hematoxylin and eosin.

Fig. 1. I.v. fat pigment in the reticuloendothelial cells of the spleen. Rabbit, 25 days after termination of intravenous fat infusions. × 850.

Fig. 2. An i.v. fat pigment-laden giant cell in the liver of the same rabbit photographed in Figure 1. × 850.

Fig. 3. I.v. fat pigment in the reticuloendothelial cells of the spleen. Rabbit, 3 months after termination of intravenous fat infusions. × 850.

Fig. 4. Pigment-laden giant cell in the liver. Rabbit, 3 months after termination of intravenous fat infusions. × 850.

Fig. 5. I.v. fat pigment mixed with hemosiderin in the reticuloendothelial cells of the spleen. Rabbit, 6 months after termination of intravenous fat infusions. × 850.

Fig. 6. I.v. fat pigment-laden giant cells in the liver. Rabbit, 6 months after termination of intravenous fat infusions. × 1000.

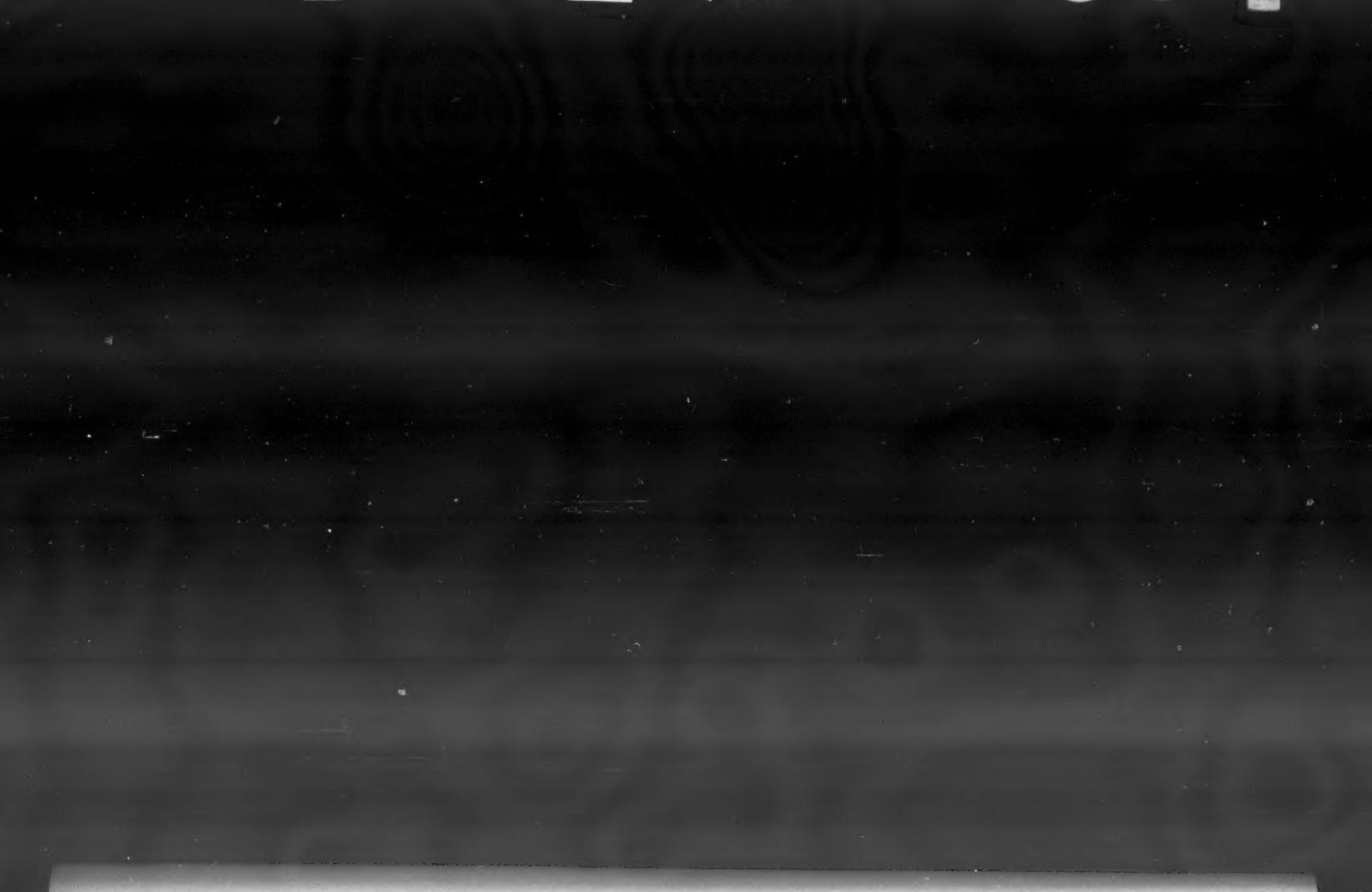

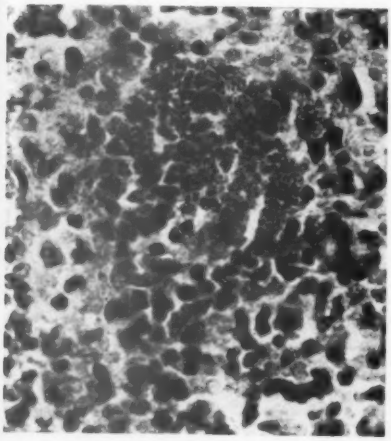

1

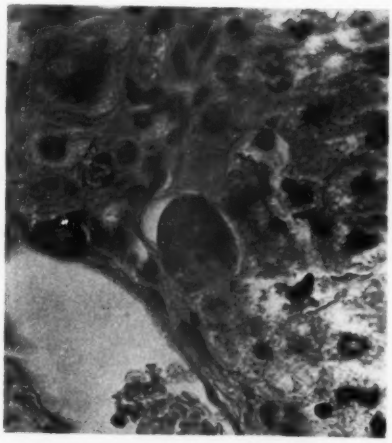

2

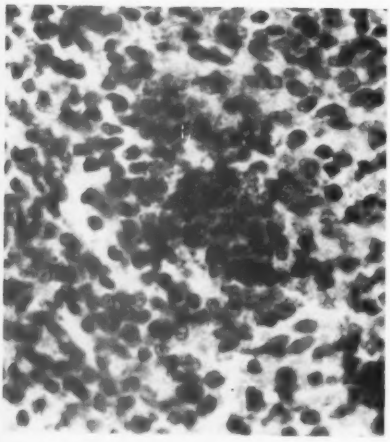

3

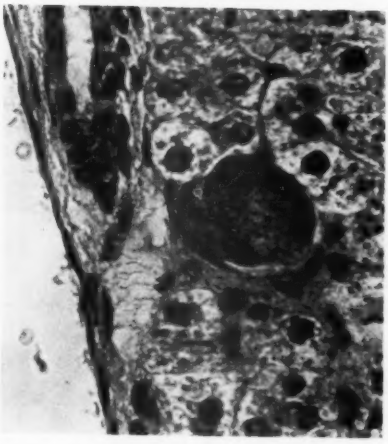

4

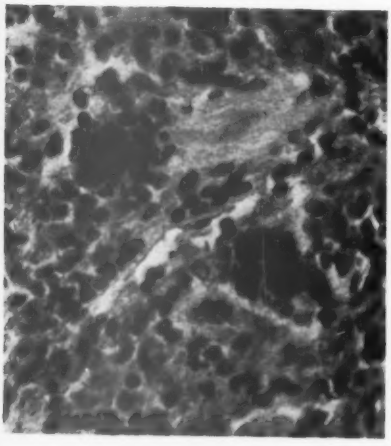

5

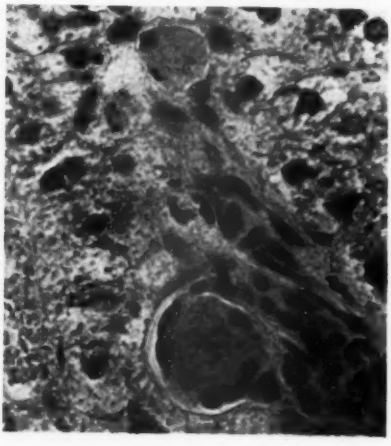

6

FIG. 7. Pigment-laden giant cell in the liver. Rabbit, 12 months after termination of intravenous fat infusions. × 850.

FIG. 8. I.v. fat pigment mixed with hemosiderin in a giant cell in the liver. Rabbit, 18 months after termination of intravenous fat infusions. × 850.

FIG. 9. I.v. fat pigment in the femoral bone marrow. Rabbit, 12 months after termination of intravenous fat infusions. × 1000.

FIG. 10. Pigment in the mesenteric lymph node. Rabbit, 18 months after termination of intravenous fat infusions. × 850.

7

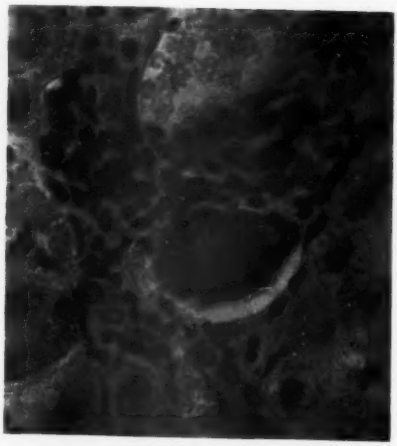

8

9

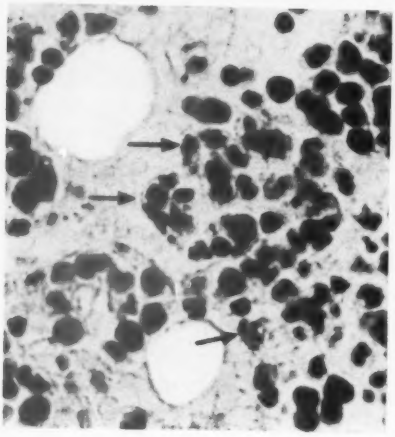

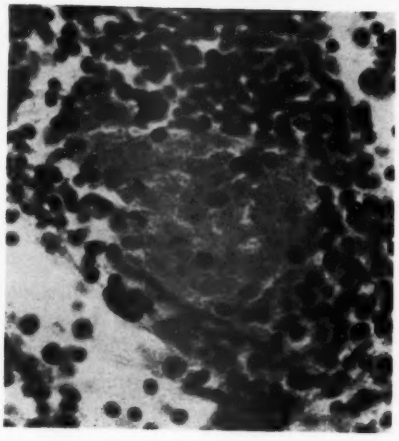
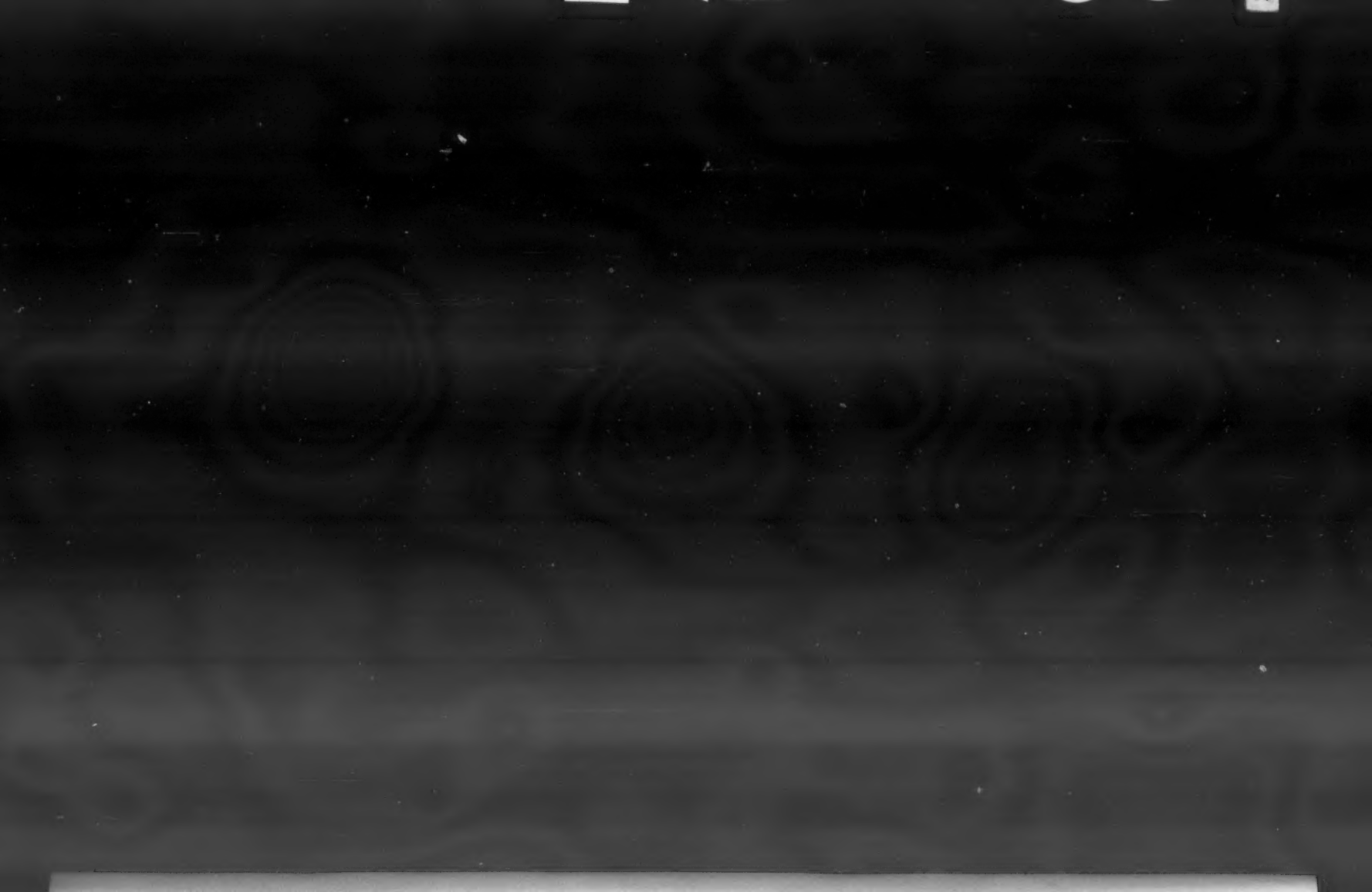
10